Hadrons In Dense Nuclear Matter

Thesis submitted for the Degree of
Doctor of Philosophy in Science (Physics)
Jadavpur University, Kolkata - 700 032, India
2 0 1 3

By
Subhrajyoti Biswas
Saha Institute of Nuclear Physics
1/AF Bidhannagar, Kolkata 700 064

CERTIFICATE FROM THE SUPERVISOR(S)

This is to certify that the thesis entitled **"HADRONS IN DENSE NUCLEAR MATTER"** submitted by **Sri SUBHRAJYOTI BISWAS** who got his name registered on 23**rd September,** 2008 for the award of Ph. D. (Science) degree of Jadavpur University, is absolutely based upon his own work under the supervision of **Prof. ABHEE KANTI DUTT-MAZUMDER** and that neither this thesis nor any part of it has been submitted for either any degree/diploma or any other academic award anywhere before.

Abhee Kanti Dutt-Mazumder 25/02/13

Signature of the Supervisor(s)
date with official seal

Dr. Abhee Kanti Dutt Mazumder
Professor
Saha Institute of Nuclear Physics
1/AF, Bidhannagar,
Kolkata-700 064

To
My parents
and My beloved wife.

Acknowledgement

There are many people who have helped me directly or indirectly to my research work. This thesis would be incomplete without their names being mentioned. At first I would like to express my sincere gratitude to my supervisor, Prof. Abhee K. Dutt-Mazumder, High Energy Nuclear and Particle Physics Division, Saha Institute of Nuclear Physics (HENPP Division, SINP). Without his constant and sincere supervision, it would have never been possible for me to finish the thesis. His expertise and deep understandings into the field made my work easier. His enthusiastic academic discussions helped me to find my elusive grounding into the research problem. Besides academic discussions, we often discussed various non-academic topics. From those non-academic discussions, I have learnt many things and found ingredients for future life. I always cherish those times!

Once again, I would like to thank him for sharing all the academic and non-academic problems during my research work at SINP. Truly speaking, without his enormous help and encouragement, I could hardly overcome those problems.

Next I would like to express my deep respect to Prof. Pradip Roy of HENPP Division. His valuable advice and academic discussion always motivated me into the research. I like to thank Prof. R. Shyam of Theory division, Prof. Sukalyan Chattopadhyay and all the office staff of HENPP Division. I am grateful to Dr. Sandip Sarkar, Applied Nuclear Physics Division, for his sincere guidance during my review work.

I am thankful to my juniors Kausik Pal, Lusaka Bhattacharya, Sreemoyee Sarkar, Mahatsab Mandal and Souvik Pryam Adhya for creating a cordial and homely atmosphere in the division. Specially I would like to mention Mahatsab Mandal. I am really indebted to him for providing me the hospitality at the Meghnad Saha Hostel during the preparation of my thesis.

I must thank the whole Post M.Sc batch, which includes Sanjoy Dutt, Sayan Chakroborty, Subhajit Karmakar, Ayan Chakroborty, Tapas Samanta, Rajib Sarkar, Md. Nurujjaman, Shubhrangshu Mukharjee, Partha Roy Chowdhury, Pulak Ranjan Giri, Anirnban Bose, Ritesh Khetri, and Sourav Ganguly, for making my days as a research fellow extremely enjoyable. I am grateful to my friends Subhajit and Sayan as they introduced me with my Supervisor at the right time.

I also like to thank Dr. Sanjib Kumar Saha, Principal of our college (Rishi Bankim Chandra College) and gratefully acknowledge my departmental colleagues

Mahadev Chattopadhyay and Dr. Susanta Kumar Nandi for their enormous help and encouragement. They made me free from most of the departmental jobs and official duties during the preparation of my thesis.

Now I would like to thank those people who may not be involved directly during my research work but it is hard to neglect their influence. The first name in that list should be of Gourpada Kashyapi, teacher of Bongaon Kavi Keshablal Vidyapith, who taught me Physics and Mathematics during my Madhyamik and Higher Secondary days. It would be injustice if I do not mention Dr. Dipak Kumar Nath, City College (Amharst Street) who helped me to keep my passion for physics alive. I could not forget one person for his help during M. Sc. at Rajabazar Science College, University of Calcutta. He is my friend Dr. Kuladeep Roy Chowdhury.

I cannot find suitable words to thank my friend Debashis Biswas. I feel fortunate to be his friend. I am really indebted to him for what he had done for me and my family during my M. Sc. and Ph. D. period. He has become more than a friend!

I would like to thank my brother Dibyajyoti Biswas, his wife Monalisa Pal, and my nephew Sushobhan Roy, and all my relatives for their love and support. I am grateful to my wife Sanchari Mitra for the amount of adjustments she made to accommodate my extreme working schedule. Without her sacrifice and constant inspiration it would have been hard to complete my Ph. D. thesis. She lifted my spirit whenever I felt low on my confidence. I like to mention someone, who does not even understand it but has helped rejuvenating my life once again. She is my seven month old daughter, Ritaja.

Finally I want to thank my parents, Dinabandhu Biswas and Aparna Biswas for all the love they have given to me from the childhood. It would have been extremely difficult for me to walk this distance without their support and inspiration. There must be many other people whose name I failed to mention here. I convey my sincere apology for this.

Subhrajyoti Biswas
25/04/13

Subhrajyoti Biswas

List of Publications

Refereed Journal:

1. **Isospin mode splitting and mixing in asymmetric nuclear matter.**
   Subhrajyoti Biswas and Abhee K. Dutt-Mazumder.
   Phys. Rev. C **74**, 065205 (2006).

2. **Effects of the Dirac sea on pion propagation in asymmetric nuclear matter.**
   Subhrajyoti Biswas and Abhee K. Dutt-Mazumder.
   Phys. Rev. C**77**, 045201 (2008).

3. ρ-ω **mixing and spin dependent CSV potential.**
   Subhrajyoti Biswas, Pradip Roy and Abhee K. Dutt-Mazumder.
   Phys.Rev.C**78**, 045207 (2008).

4. **Spin-dependent Fermi liquid parameters and properties of polarized quark matter.**
   Kausik Pal, Subhrajyoti Biswas and Abhee K. Dutt-Mazumder.
   Phys. Rev. C79, 015205 (2009).

5. **Ground state energy of spin polarized quark matter with correlation.**
   Kausik Pal, Subhrajyoti Biswas and Abhee K. Dutt-Mazumder.
   Phys. Rev. C**80**, 024903 (2009).

6. **Matter-induced charge-symmetry-violating** NN **potential.**
   Subhrajyoti Biswas, Pradip Roy and Abhee K. Dutt-Mazumder.
   Phys. Rev. C**81**, 014006 (2010).

7. π-η **mixing and charge symmetry violating** NN **potential in matter.**
   Subhrajyoti Biswas, Pradip Roy and Abhee K. Dutt-Mazumder.
   Phys. Rev. C**81**, 064002 (2010).

8. ρ-ω **mixing and density dependent CSV potential.**
   Subhrajyoti Biswas, Pradip Roy and Abhee K. Dutt-Mazumder
   Indian J. Phys. **Vol. 85** No. 7, pp. 1185-1189, July, 2011.

Conference Proceedings:

1. **CSV potential in matter.**
   Subhrajyoti Biswas, Pradip Roy and Abhee K. Dutt-Mazumder.
   DAE (Nuclear) Proceedings, Vol.**52**, Page:568, (2007)

2. **Pion dispersions in asymmetric nuclear matter**.
   Subhrajyoti Biswas and Abhee K. Dutt-Mazumder.
   DAE (Nuclear) Proceedings, Vol.**52**, Page:572, (2007)

3. **Density driven π-η mixing and mass modification.**
   Subhrajyoti Biswas and Abhee K. Dutt-Mazumder.
   DAE (Nuclear) Proceedings, Vol.*53*, Page:579 (2008)

4. **Off-shell ρ-ω mixing and CSV potential.**
   Subhrajyoti Biswas and Abhee K. Dutt-Mazumder.
   DAE (Nuclear) Proceedings, Vol.**53**, Page:509 (2008)

5. **New source of charge symmetry breaking.**
   Subhrajyoti Biswas, Pradip Roy and Abhee K. Dutt-Mazumder.
   DAE (Nuclear) Proceedings, Vol.**54**, Page:502 (2009)

Abstract

The subject matter of the present thesis has been the investigation of the hadronic properties in dense nuclear matter (DNM) with neutron-proton (n-p) density asymmetry. As a result we find many interesting and amusing phenomenon in the characteristic behavior of the mesons, particularly in the isovector sector, giving rise to phenomena like mode splitting of the different charge states of mesons like pion and ρ-meson or the mixing of different isospin states etc. which is not observed in symmetric nuclear matter.

In particular, the present work deals mostly with pion propagation in asymmetric nuclear matter (ANM) at high density within the framework of Quantum Hadrodynamics (QHD). We expose how such asymmetry in neutron-proton density can induce mixing of mesons having different isospins. Such matter driven phenomena are akin to spontaneous symmetry breaking where the Hamiltonian respects the symmetry, it is broken by the ground state. We estimate mixing amplitudes of π-η and ρ-ω mixing with this additional contribution in ANM which actually win over the corresponding vacuum mixing amplitudes. With this mixing amplitudes, in this thesis, various charge symmetry violating (CSV) potentials have been constructed. In this case, apart from the density dependent effects, new sources of vacuum symmetry breaking phenomena has been identified which also modifies previously known free space charge symmetry violating nucleon-nucleon potential. In addition, calculation determining the effect of medium on hadron masses in nuclear matter have also been performed including the effect of nuclear asymmetry on the effective masses of various mesons.

Notations

μ, ν	Space-time index of four vector
$g_{\mu\nu}$	Metric tensor, diag$(1, -1, -1, -1)$
N	Nucleon index, ($N = n$ for neutron, & p for proton)
M_N^*	Effective nucleon mass
$\tilde{m}_i$	Mixing modified meson mass
$\mathbf{k}_N$	Fermi momentum of nucleon
$E_N(E_N^*)$	Fermi energy with nucleon mass $M_N(M_N^*)$
Γ_i	Vertex factor
α	Asymmetry parameter
ρ_n (ρ_p)	Neutron (proton) density
Δ_i	Scalar meson propagator in momentum space
$\Delta_i^{\mu\nu}$	Vector meson propagator in momentum space
G_N	Nucleon propagator in medium with M_N
G_N^*	Nucleon propagator in medium with M_N^*
Π_{ij}	Mixing self-energy
Π_{ij}^T	Transverse component of mixing polarization
Π_{ij}^L	Longitudinal component of mixing polarization

Contents

List of Tables

List of Figures

Chapter 1

Introduction

The properties of hadrons in dense nuclear matter has been at the core of high energy nuclear physics research for quite some time now [1–4]. Such investigations are important to provide answers to some of the pertinent queries involving nuclei, nuclear matter, astrophysical objects like neutron stars, their evolution, structure, supernovae explosion [5, 6] and several other issues related to the laboratory based heavy ion collisions [7,8]. In astrophysical context, particularly many of the neutron star properties are sensitive to the underlying nuclear the equation of state (EOS) at densities much higher than those observed in ordinary nuclei [9]. Many models have been proposed over time to calculate the nuclear EOS at high densities starting from basic nuleon-nucleon interactions [10, 11]. The EOS is an essential ingradient for calculating the balance between the gravitational pull and nuclear pressure in neutron stars. Construction of such models are guided by the various observed phenomena of ordinary nuclei, nuclear saturation properties, incompressibility etc. [10–14].

Extrapolations of these models to higher densities can be tested against astrophysical data or in the laboratory based measurements involving heavy ion collisions where nuclear matter can be produced temporarily at densities few times higher than that of the ordinary nuclei. This also includes the possibility of forming quark gluon plasma (QGP) state of matter at extremely high temperature and/or densities. The experiments at relativistic heavy ion collider (RHIC) and large hadron collider (LHC) have provided further impetus in this context where mainly the high temperature effects have been the main focus [15]. The proposed experiments at GSI, on the other hand, are geared to uncover the properties of compressed baryonic matter (CBM) where the baryonic chemical potential is likely to be much higher compared to the temperature [16].

The nucleon-nucleus (N-A) and nucleus-nucleus (A-A) collisions also offer opportunities to measure various hadronic spectral functions both at normal and higher nuclear matter densities. Such measurements allow one to study the effective masses and the widths of the various hadronic resonances like σ, ω, π etc. In particular, the dilepton invariant mass spectra, provide penetrating probe to pin-down the properties of the light vector mesons *i. e.* ρ, ω and ϕ in nuclear medium. Several theoretical models have been advanced to study the in-medium properties of these mesons [17,18]. Many experiments have also measured the vector meson mass shifts in dense nuclear matter [19–22]. These apart, pion sprectral function in nuclear matter has also been a subject of intense research for quite some time [23].

The basic input of all these studies are the two body nucleon-nucleon interaction both in vacuum and in medium. Several investigatons have addressed these issues using both non-relativistic [24–31] and relativistic models [32–37]. In particular, the non-relativistic investigations like Brueckner-Hartree-Fock and Bathe-Salpeter formalisms have been very successful to describe the properties of dense nuclear matter [38–44].

To deal with nuclear matter at very high density such as what is found in neutron stars, one must describe hydrodynamic flow of nuclear matter at velocity that approaches to the speed of light and requires transport properties under extreme conditions. It is more appropriate to use the relativistic nuclear many body formalism in this regime [32–37].

The usual argument which is given in favour of using the non-relativistic model has been that the nuclear binding energy is small compared to the nucleon mass. But this small nuclear binding energy is a consequence of the cancellation between two large Lorentz scalar and four-vector potentials, each of which is approximately several hundred MeV even at ordinary densities [45]. In view of the above mentioned points, it has been argued by several authors to use relativistic formalism in order to study even ordinary nuclear systems. The evidence of such strong potentials came from the one boson exchange potential (OBEP) analysis of nucleon-nucleon scattering [46,47]. Furthermore, at high density nucleon mass reduces than its value in free space which makes the lower component of the Dirac spinor larger. This provides additional support in favour of using the relativistic models.

1.1 Nucleon-Nucleon interaction

Yukawa, in 1935 proposed that the nucleon-nucleon interaction is generated by the exchange of a massive particle, called meson [48]. He derived two body nuclear force considering a charged scalar meson exchanged between proton and neutron [48–52]. In 1937 muon was discovered in the cosmic ray and it was thought as the Yukawa's particle. But, Pancini and Piccioni showed that muon does not interact strongly with nuclei and therefore was not the proposed meson [53]. Later, a meson of mass about 140 MeV was discovered in the cosmic ray which interacts strongly with nucleon. This was the Yukawa's particle and it was named 'pion'.

Proca extended Yukawa's original idea of scalar meson exchange to the vector meson exchange [54] which provided a tensor force leading to the quadrupole moment of the deuteron with wrong sign. The correct sign of the quadrupole moment can be obtained by the exchange of the isovector and pseudoscalar mesons [55, 56]. The nucleon-nucleon interaction mediated by different mesons operate at different distance scale. In view of this Taketani, Nakamura and Sasaki proposed to subdivide the range of nuclear force into three regions [57]:

1. **Classical (or long-range) region:** Distance between the centers of two nucleons, r $\gtrsim$ 2 fm. In this region one-pion exchange (OPE) plays the dominant role.

2. **Dynamical (or intermediate) region:** 1 fm $\lesssim$ r $\lesssim$ 2 fm. Two-pion exchange (TPE) becomes important in the intermediate region.

3. **Phenomenological (or core) region:** r $\lesssim$ 1 fm. In this region multi-pion exchange, heavy mesons of various kinds and the quark-gluon exchange contribute.

This kind of subdivision may be helpful for developing the theory of nucleon-nucleon interaction stepwise, that means it permits one different derivation for the different regions of nuclear force.

It was well-established that the one-pion exchange accounts for the long-range part of the nuclear force [58–64]. But serious problems appeared in the case of two-pion exchange [65–70]. The discovery of heavy meson, specially the vector meson, rescued from that problem leading to the construction of the one-boson exchange (OBE) models for nucleon-nucleon interactions [71]. The basic assumption

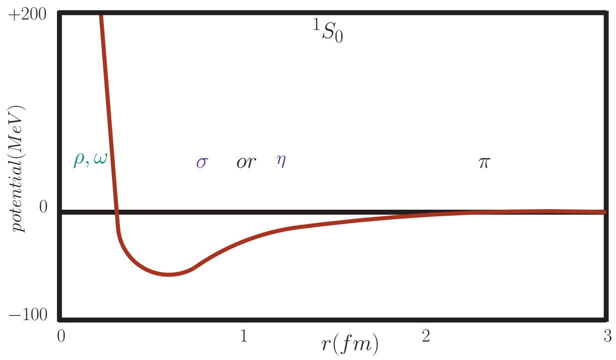

Figure 1.1: *Mesons in NN interaction.*

of these models are that the multi-pion exchange could be replaced by the appropriate multi-pion resonances as if they form a single particle with definite mass and definite intrinsic quantum numbers. For instance, the correlated two-pion S-wave contribution can be well approximated as the exchange of scalar meson of mass is about 500 MeV [72–79]. The ρ meson is a two-pion resonance in the P-state and the ω meson is a three-pion resonance. In the OBE models isoscalar scalar mesons like sigma (σ) meson or eta (η) meson dominate in the intermediate range of nuclear force. On the other hand, rho (ρ) and omega (ω) mesons had been included for the core region. Inclusion of other mesons were found to give negligible contribution. The various meson parameters given in Table.1.1 have been borrowed from Ref. [80]:

Table 1.1: *Meson parameters.*

Meson	J^P	T	$\frac{g^2}{4\pi}$	Mass (MeV)	Λ (MeV)
π	0^-	1	14.6	138.6	1300
η	0^-	0	5.0	548.0	1500
ρ	1^-	1	0.95	769.0	1400
ω	1^-	0	20.0	782.6	1500

J = total spin, P = Parity, T = isospin and g = coupling constant.

1.2 Classification of nuclear forces

For the construction of nucleon-nucleon potential one usually neglects the isospin dependence. In general the nucleon-nucleon forces can have isospin dependence also. According to the isospin dependence Henley and Miller listed four classes of NN forces [81–84]. One of which is isospin neutral and others break this symmetry. Before listing these four classes of nucleon-nucleon forces, we first discuss two main issues viz. the charge independence and charge symmetry of the interacting Hamiltonian.

Charge independence (CI) implies the equality between the neutron-neutron (nn), proton-proton (pp) and neutron-proton (np) interactions. The charge symmetry (CS) implies that the interaction between two neutrons or two protons are equal. The violation of CS automatically violates the charge independence (CI), however, the converse might not be always true [85–87]. It is possible to have CS even if the CI is violated which actually is a higher symmetry. In nature, both the symmetries are broken.

The CI requires that the Hamiltonian (H) of the system will be invariant under any rotation in isospin space *i. e.*

$$[\mathcal{H}, \mathbf{T}] = 0 \, , \tag{1.1}$$

where, $\mathbf{T}$ is the isospin operator. Actually, the above relation implies isospin independence of the system. But, the term "charge independence" is often used to indicate "isospin invariance" (II). The CS operator may be defined as

$$\mathbf{P}_{CS} = e^{i\pi T_2} \, , \tag{1.2}$$

if the third (or z) component of $\mathbf{T}$ is considered to be associated with the charge of the particle. This definition of the CS operator was first introduced in Ref. [88] in the context of CS of the up (u) and down (d) quarks. Since isospin is an additive quantum number and for hadrons it is expressed equivalently from the quark content, allows one to apply the quark based definition of CS to the hadronic systems. The CS is expressed as

$$[\mathcal{H}, \mathbf{P}_{CS}] = 0 \, . \tag{1.3}$$

Thus CS implies the invariance of the system under 180^0 rotation about the T_2 axis in the isospin space, that means the charge-reflected system must be identical to the original one under reflection on the T_1-T_2 (or T_x-T_y) plane in isospin space.

- **Class (I):** Class (I) forces are isospin or charge independent and the general form is

$$V_I^{NN} = a + b\tau(1) \cdot \tau(2), \tag{1.4}$$

where a and b are isospin independent operators and τ is the Pauli's isospin operator. This force obeys $[V_I^{NN}, \mathbf{T}] = 0$.

- **Class (II):** This type of forces are charge symmetric but violate charge independence:

$$V_{II}^{NN} = c\left[\tau_3(1)\tau_3(2) - \frac{1}{3}\tau(1) \cdot \tau(2)\right] \ . \tag{1.5}$$

- **Class (III):** This force breaks both charge independence and charge symmetry:

$$V_{III}^{NN} = d\ \ [\tau_3(1) + \tau_3(2)]\ \ . \tag{1.6}$$

where c and d are Hermitian operators. Since, $[V_{III}^{NN}, \mathbf{T}^2] = 0$, it does not causes isospin mixing in the two-body system. A class III interaction distinguishes nn and pp systems, but vanishes in the np system. An example of charge symmetry violating class III interaction is the Coulomb force which also contains class I and class II forces.

- **Class (IV):** The general form the Class IV NN force is

$$V_{IV}^{NN} = e[\tau_3(1) - \tau_3(2)][\sigma(1) - \sigma(2)] \cdot \mathbf{L} \textbf{ or } f[\tau(1) \times \tau(2)]_3[\sigma(1) \times \sigma(2)] \cdot \mathbf{L}, \tag{1.7}$$

where e, f are scalar operators and $\sigma(1)$, $\sigma(2)$ are the spin operators for nucleons. This type of forces break charge symmetry and therefore charge independence. The class IV forces have no effect on the nn and pp systems, but causes spin-dependent isospin mixing effects in the np system. The magnetic interaction between two nucleons is an example of class IV force.

1.3 Outline of the thesis

The thesis is structured into seven chapters. A short introduction into the field and important topics related to our study have been presented in Chapter 1. In chapter 2, we discuss about quantum hadrodynamic (QHD) models and consequently present the Walecka model which is based on mean field (MF) approximation. This model was the first of its kind where the field theoretic approach to describe the bulk properties of nuclear matter had been formulated [10]. Here we also present a derivation of in-medium nucleon propagator.

Chapter 3 has been devoted to the study of pion propagation in asymmetric nuclear matter (ANM). Pions in nuclear physics assume a special status. It is responsible for the spin-isospin dependent long range part of the nuclear force as mentioned before. In addition, there are variety of physical phenomena related to the pion propagation in nuclear matter. One of the fascinating ideas in relation to the pion-nucleon dynamics in nuclear matter is the pion condensation [89]. This might happen if there exists space like zero energy excitation of pionic modes. The short-range correlation, on the other hand, removes such a possibility at least upto densities near the saturation densities. In relativistic heavy ion collision, the importance of medium modified pion spectrum was discussed by Mishustin, [90] where it was shown that due to the lowering of energy, pion, in nuclear matter, might carry a bulk amount of entropy. Subsequently, Gyulassy and Greiner studied pionic instability in great detail in the context of RHIC [91]. The production of pionic modes in nuclear collisions was also discussed in [92].

In experiments, medium dependent pion dispersion relation can also be probed via the measurements of dilepton invariant mass spectrum. The lepton pairs produced with invariant mass near the ρ pole are sensitive to the slope of the pion dispersion relation in matter [7]. Particularly the softening of momentum dependence of the pion dispersion relation in matter leads to higher yield of dileptons. Gale and Kapusta were first to realize that the in-medium pion dynamics can be studied by measuring lepton pair productions [93]. Most of the earlier studies of in-medium pion properties were performed in the non-relativistic frame work [94–96]. A quasi-relativistic approach was taken in [97–99] where the calculations were extended to finite temperature. In particular, [99] discusses various non-collective modes with the possibility of pion condensation. In [7], on the other hand, the dilepton production rates were calculated using non-relativistic pion dispersion relations. Ref. [100]

treated the problem relativistically but free Fermi gas model was used, while in [101] pion propagation was studied by extending the Walecka model [10] including delta baryon.

In recent years, there has been significant progress to calculate dilepton production rates involving pionic properties in a more realistic framework [7,93,99,102–104]. The importance of relativistic corrections and density dependent pion mass splitting in ANM in the context of deriving pion-nucleus optical potential was discussed in [105]. The formalism adopted in [105] was that of chiral perturbation theory. Recently, in the context of astrophysics, pionic properties in ANM has also been studied by involving Nambu-Jona-Lasinio model [106, 107].

The other aspect which we address in chapter 4 is the mixing of various meson states due to symmetry violation. For example, it is known that, in nature, isospin is not an exact symmetry and this leads to the mixing of isoscalar ω and isovector ρ meson in vacuum. At the quark level this is driven by the mass splitting of the up and down quark. At the hadronic level such mixing can be attributed to the neutron and proton mass difference. Other well known example is the mixing of the π and η meson.

The nuclear medium can permit even another class of mixing which does not happen in vacuum. Matter induced σ-ω meson can here be cited as one of the classic examples [108–110]. Such a scalar (σ)-vector (ω) mixing cannot take place in vacuum because of Lorentz symmetry, which in medium is lost. There could be additional sources of mixing in ANM driven by the asymmetric neutron and proton density difference. This is akin to the spontaneous symmetry breaking where the Hamiltonian respects the symmetry but the ground state does not. In this case, as we shall see, even when $M_n = M_p$, various isospin states can mix. Here M_n and M_p denote the neutron and proton masses respectively. The physical consequence of this phenomenon constitutes a major part of the present thesis.

Physically, in dense hadronic system, intermediate mesons might be absorbed and re-emitted from the Fermi spheres. In symmetric nuclear matter (SNM) the emission and absorption involving different isospin states like π and η or ρ and ω cancel when the contributions of both the proton and neutron Fermi spheres are added provided the nucleon masses are taken to be equal. In ANM, on the other hand, the unbalanced contributions coming from the scattering of neutron and proton Fermi spheres, lead to the mixing which depends both on the baryon density (ρ_b) and the asymmetry parameter, $\alpha = (\rho_n - \rho_p)/\rho_b$, where ρ_n and ρ_p denote neutron and proton densities. This density driven mixing of π-η or ρ-ω and their importance in nuclear physics will be elucidated further in chapter 4.

In chapter 5 we construct various charge symmetry violating (CSV) potentials clearly delineating the difference between vacuum induced mixing due to the n-p mass difference and density dependent modification of such mixing in ANM. We include here few corrections to the existing two-body CSV potentials in vacuum. It is to be noted that the mixing amplitudes calculated in chapter 4 are required to construct such potentials which we accomplish in chapter 5.

In chapter 6, we present how the mixing further modifies the effective π and η meson masses in ANM. Here we also present relevant pion dispersion relations. Finally we summarize and conclude in chapter 7.

Chapter 2

Dense Nuclear Matter

Nuclear matter is a hypothetical uniform system with infinite number of nucleons (A) in absence of Coulomb interaction. In the past several years, many theoretical models have been proposed to study the bulk properties of nuclear matter [24–31]. Such studies find main applications in astrophysical contexts, particularly to study the neutron star properties as mentioned already in the introduction. For finite nuclei, the material at the center of ^{208}Pb-nucleus may be considered as nuclear matter.

For basic theoretical understanding of the bulk properties of nuclear matter, one takes equal densities of neutron and proton *i.e.* $\rho_n = \rho_p$. This is known as symmetric nuclear matter (SNM) where the neutron and proton Fermi momenta which determine the density are the same *i.e.* $k_n = k_p$. In many cases, however, one can deal with the asymmetric nuclear matter (ANM) *i.e.* when $\rho_n \neq \rho_p$. We shall here first outline the formalism for the SNM and then in the next chapter issues related particularly to ANM will be addressed.

A proper framework to describe nuclear matter at high densities and temperatures is relativistic quantum field theory based on a local Lagrangian density. Among these theories, the ones considering hadronic degrees of freedom are represented by a generic name: quantum hadrodynamics (QHD). In this framework, the mean field theory, or the Walecka model [10], was first introduced in the early seventies to study dense nuclear matter in the context of neutron stars [11]. This model explains the bulk nuclear matter such as the experimentally accessible observables: density and binding energy [111], the strong spin-orbit splitting in finite nuclei [10, 45, 112, 113]. In this approach, one also obtains the well-known feature of nucleon-nucleon interaction known from nucleon-nucleon scattering experiments: a short range repulsion and a long range attraction [46, 114]. We will explain these features gradually as we review the formalism of the Walecka model.

2.1 Walecka model

We start with the Lagrangian of QHD-I model, where nucleons interact via the exchange of σ and ω mesons as shown in Fig.2.1:

$$\begin{aligned}\mathcal{L} &= \bar{\psi}\left[\gamma_\mu\left(i\partial^\mu - \mathrm{g}_v V^\mu\right) - \left(M_N - \mathrm{g}_s\phi\right)\right]\psi + \frac{1}{2}\left(\partial_\mu\phi\partial^\mu\phi - m_s^2\phi^2\right) \\ &- F_{\mu\nu}F^{\mu\nu} + \frac{1}{2}m_v^2 V_\mu V^\mu + \delta\mathcal{L}, \end{aligned} \tag{2.1}$$

where ψ represents the baryon field with mass M_N, ϕ and V^μ are the neutral scalar and vector meson fields with masses m_s and m_v, respectively. $F^{\mu\nu} = \partial^\mu V^\nu - \partial^\nu V^\mu$ is the field tensor for spin-1 particle and $\delta\mathcal{L}$ contains the counter terms required for renormalization of the model. In Eq.(2.1), the scalar meson couples to the scalar density of baryon $\mathrm{g}_s\bar{\Psi}\Psi\phi$ and vector meson couples to the conserved baryon current through $\mathrm{g}_s\bar{\Psi}\gamma_\mu\Psi V^\mu$. This was motivated by the large Lorentz scalar and four-vector components observed in the nucleon-nucleon interaction [46, 47].

The Feynman amplitude for nucleon-nucleon interaction as shown in Fig.2.1 is given by

$$\mathcal{M}_i(q^2) = \left[\bar{u}_N(p_3)\Gamma_i(q)u_N(p_1)\right]\,\Delta_i(q^2)\,\left[\bar{u}_N(p_4)\Gamma_j(-q)u_N(p_2)\right], \tag{2.2}$$

where, u_N, $\Gamma_i(q^2)$ and $\Delta_i(q^2)$ denote the Dirac spinor, vertex factor and meson propagator, respectively. The non-relativistic limit of Eq.(2.2) yields the one boson

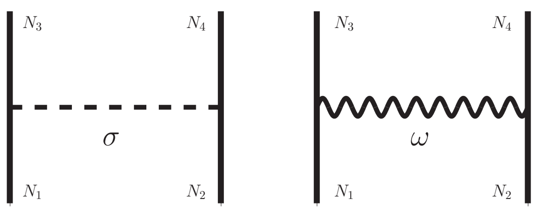

Figure 2.1: *NN interaction is generated via the exchange of a scalar meson (σ) and a vector meson (ω) in QHD-I.*

exchange potential in momentum space. The coordinate space potential can be obtained by Fourier transformation of the momentum space potential. Thus one obtains the following nucleon-nucleon interaction potential:

$$V_{eff}(r) = \left(\frac{g_v^2}{4\pi}\right) \frac{e^{-m_v r}}{r} - \left(\frac{g_s^2}{4\pi}\right) \frac{e^{-m_s r}}{r} . \tag{2.3}$$

The well-known feature of nucleon-nucleon interaction as found from nucleon-nucleon scattering experiment *i.e.* a short range repulsion and long range attraction [46, 47, 114] is clearly understood from the above expression of $V_{eff}(r)$. The short range repulsion between nucleons comes from vector meson (ω) exchange and scalar meson (σ) exchange generates the long range attraction. With an appropriate choice of the values of coupling constants g_v and g_s can give quantitative description of nuclear matter which will be discussed later. First we focus on the field equations.

2.1.1 Field equations

The field equations of motion can be found from the following Lagrange's equation of motion:

$$\frac{\partial}{\partial x^\mu}\left[\frac{\partial \mathcal{L}}{\partial\left(\frac{\partial q}{\partial x^\mu}\right)}\right] - \frac{\partial \mathcal{L}}{\partial q} = 0, \tag{2.4}$$

One obtains the field equations of motion replacing the generalized coordinate q by the fields ϕ, V^μ and $\bar{\psi}$.

$$\left[\partial^\mu\partial_\mu + m_s^2\right]\phi = g_s\bar{\psi}\psi \tag{2.5a}$$

$$\partial^\mu F_{\mu\nu} + m_v^2 V^\mu = g_v\bar{\psi}\gamma_\mu\psi \tag{2.5b}$$

$$\left[i\gamma^\mu\partial_\mu - M_N\right]\psi = \left[g_v\gamma^\mu V_\mu - g_s\phi\right]\psi \tag{2.5c}$$

Eq.(2.5a) and Eq.(2.5b) represent the Klein-Gordon equation with the $\bar{\psi}\psi$ as the source and equation for the spin-1 particle with $\bar{\psi}\gamma_\mu\psi$ as the current source. Eq.(2.5c) is the Dirac equation for baryon interacting with mesons.

2.1.2 MF approximation

It is clear from Eqs.(2.5a)-(2.5c), the exact solutions are very complicated and the perturbative approaches can not be applied because of the large value of the coupling constants, g_s and g_v. One may solve these equations considering the mean field approximation. In this approach the meson fields are replaced by their ground state expectation values.

$$\phi \longrightarrow <\phi>= \phi_0 \tag{2.6a}$$
$$V_\mu \longrightarrow <V_\mu>= \delta_{\mu 0} V_0 \tag{2.6b}$$

Now derivative of the meson field vanishes and the field equations (2.5a)-(2.5c) read as

$$\phi_0 = \frac{g_s}{m_s^2} <\bar{\psi}\psi>= \frac{g_s}{m_s^2}\rho_s, \tag{2.7a}$$
$$V_0 = \frac{g_v}{m_v^2} <\psi^\dagger\psi>= \frac{g_v}{m_v^2}\rho_b, \tag{2.7b}$$
$$[i\gamma_\mu\partial^\mu - M_N^*]\,\psi = g_v V_0 \psi. \tag{2.7c}$$

where, ρ_s and ρ_b are the scalar density and baryon density, respectively. M_N^* is the effective nuclear mass given by

$$M_N^* = M_N - g_s\phi_0 \tag{2.8}$$

Now the field equations (2.7a)-(2.7c) become exactly solvable and in the mean field approximation the Lagrangian given in Eq.(2.1) and the Hamiltonian reduces to

$$\mathcal{L}_{MF} = \bar{\psi}\left[i\gamma_\mu\partial^\mu - M_N^* - g_v\gamma^0 V_0\right]\psi + \frac{1}{2}m_v^2 V_0^2 - \frac{1}{2}m_s^2\phi_0^2\;, \tag{2.9}$$

$$\begin{aligned}\mathcal{H}_{MF} &= \frac{\partial\mathcal{L}_{MF}}{\partial\,\dot{q}_i}\,\dot{q}_i - \mathcal{L}_{MF}\\ &= -\frac{1}{2}m_v^2\,V_0^2 + \frac{1}{2}m_s^2\,\phi_0^2 - \bar{\psi}\left[-i\gamma^i\partial_i + g_v\gamma_0\,V_0 + M_N^*\right]\psi\;.\end{aligned} \tag{2.10}$$

2.1.3 Solution of Dirac equation

To solve Eq.(2.7c) one may consider the solution of the form $\psi = \Phi(\mathbf{k},\mathbf{s})e^{-\,ik\cdot x}$, where $k\cdot x = k_\mu x^\mu = k_0 x^0 - \mathbf{k}\cdot\mathbf{x} = \varepsilon(\mathbf{k})t - \mathbf{k}\cdot\mathbf{x}$ and $\mathbf{s}$ denotes the spin index.

$$(\alpha\cdot\mathbf{k} + \beta M_N^*)\,\Phi(\mathbf{k},\mathbf{s}) = (\varepsilon(\mathbf{k}) - g_v V_0)\,\Phi(\mathbf{k},\mathbf{s})\;, \tag{2.11}$$

where $\alpha^i = \gamma^0\gamma^i$, $\beta = \gamma^0$ and γ^μs are the Dirac's gamma matrices. Multiplying β to the both sides of Eq.(2.11) one obtains

$$(\gamma^\mu k_\mu - M_N^*)\,\Phi(\mathbf{k},\mathbf{s}) = 0, \tag{2.12}$$

where $k_0 = \varepsilon(\mathbf{k}) - \mathrm{g}_v V_0$. Multiplying Eq.(2.12) by $(\gamma^\mu k_\mu + M_N^*)$ yields,

$$\varepsilon(\mathbf{k}) = \mathrm{g}_v V_0 \;\pm\; \sqrt{\mathbf{k}^2 + M_N^{*2}} = \mathrm{g}_v V_0 \;\pm\; E_N^*(\mathbf{k}) \quad \equiv \varepsilon_\pm(\mathbf{k})\ . \tag{2.13}$$

Thus, for positive and negative energies *i.e.* for $\varepsilon_\pm(\mathbf{k})$, Eq.(2.11) reduces to

$$\begin{aligned} (\alpha\cdot\mathbf{k} + \beta M_N^*)\,\mathcal{U}(\mathbf{k},\mathbf{s}) &= (\varepsilon_+(\mathbf{k}) - \mathrm{g}_v V_0)\,\mathcal{U}(\mathbf{k},\mathbf{s}) \\ &= E_N^*(\mathbf{k})\ \mathcal{U}(\mathbf{k},\mathbf{s})\ , \qquad (2.14\text{a}) \\ (\alpha\cdot\mathbf{k} - \beta M_N^*)\ \mathcal{V}(\mathbf{k},\mathbf{s}) &= -\,(\varepsilon_-(\mathbf{k}) - \mathrm{g}_v V_0)\,\mathcal{V}(\mathbf{k},\mathbf{s}) \\ &= E_N^*(\mathbf{k})\ \mathcal{V}(\mathbf{k},\mathbf{s})\ , \qquad (2.14\text{b}) \end{aligned}$$

where $\mathcal{U}(\mathbf{k},\mathbf{s})$ and $\mathcal{V}(\mathbf{k},\mathbf{s})$ represent the corresponding Dirac spinors with the following normalization condition:

$$\sum_{\mathbf{s},\ \mathbf{s}'} \mathcal{U}(\mathbf{k},\mathbf{s})^\dagger \mathcal{U}(\mathbf{k},\mathbf{s}') = \sum_{\mathbf{s},\ \mathbf{s}'} \mathcal{V}(\mathbf{k},\mathbf{s})^\dagger \mathcal{V}(\mathbf{k},\mathbf{s}') = 2E_N^*(\mathbf{k})\ \delta_{\mathbf{s}\mathbf{s}'}\ . \tag{2.15}$$

The general solution is the superposition of the positive energy and negative energy solutions:

$$\psi(x) = \sum_{\mathbf{k},\mathbf{s}} \frac{1}{\sqrt{V\ 2E_N^*(\mathbf{k})}} \left[a_{\mathbf{k},\mathbf{s}}\ \mathcal{U}(\mathbf{k},\mathbf{s})\ e^{-\ i(\varepsilon_+(\mathbf{k})t - \mathbf{k}\cdot\mathbf{x})} + b^\dagger_{\mathbf{k},\mathbf{s}}\ \mathcal{V}(\mathbf{k},\mathbf{s})\ e^{-i(\varepsilon_-(\mathbf{k})t + \mathbf{k}\cdot\mathbf{x})} \right]. \tag{2.16}$$

Here $a^\dagger_{\mathbf{k},\mathbf{s}}$ and $a_{\mathbf{k},\mathbf{s}}$ are creation and annihilation operators for particles and likewise $b^\dagger_{\mathbf{k},\mathbf{s}}$ and $b_{\mathbf{k},\mathbf{s}}$ are the creation and annihilation operators for antiparticles. The only non-vanishing anticommutation relations are

$$\left\{ a_{\mathbf{k},\mathbf{s}}, a^\dagger_{\mathbf{k}',\mathbf{s}'} \right\} = \left\{ b_{\mathbf{k},\mathbf{s}}, b^\dagger_{\mathbf{k}',\mathbf{s}'} \right\} = \delta^3(\mathbf{k} - \mathbf{k}')\ \delta_{\mathbf{s},\mathbf{s}'}\ . \tag{2.17}$$

The scalar and baryonic density operators may be written as

$$\begin{aligned} \hat{\rho}_b &= \psi^\dagger\psi = \frac{1}{V}\sum_{\mathbf{k},\mathbf{s}} \left(a^\dagger_{\mathbf{k},\mathbf{s}} a_{\mathbf{k},\mathbf{s}} - b^\dagger_{\mathbf{k},\mathbf{s}} b_{\mathbf{k},\mathbf{s}} \right)\ , \qquad (2.18\text{a}) \\ \hat{\rho}_s &= \bar{\psi}\psi = \frac{1}{V}\sum_{\mathbf{k},\mathbf{s}} \frac{M_N^*}{E_N^*(\mathbf{k})} \left(a^\dagger_{\mathbf{k},\mathbf{s}} a_{\mathbf{k},\mathbf{s}} + b^\dagger_{\mathbf{k},\mathbf{s}} b_{\mathbf{k},\mathbf{s}} \right)\ , \qquad (2.18\text{b}) \end{aligned}$$

Thus the Eq.(2.10) reduces to

$$\hat{\mathcal{H}}_{MF} = -\frac{1}{2}m_v^2\, V_0^2 + \frac{1}{2}m_s^2\, \phi_0^2 + \mathrm{g}_v V_0\, \hat{\rho}_b + \frac{1}{V}\sum_{\mathbf{k},\mathbf{s}} E_N^*(\mathbf{k}) \left(a^\dagger_{\mathbf{k},\mathbf{s}} a_{\mathbf{k},\mathbf{s}} + b^\dagger_{\mathbf{k},\mathbf{s}} b_{\mathbf{k},\mathbf{s}}\right) \,. \tag{2.19}$$

In medium, the vacuum $|0\rangle$ is replaced by the ground state $|\Psi_0\rangle$ which contains positive-energy particles with same Fermi momentum k_N and no antiparticles. Since $|\Psi_0\rangle$ contains only positive-energy particles, the operators follow that

$$b_{\mathbf{k},\mathbf{s}}|\psi_0\rangle = 0 \quad \text{for all } |\mathbf{k}|, \tag{2.20a}$$

$$a_{\mathbf{k},\mathbf{s}}|\psi_0\rangle = 0 \quad \text{for } |\mathbf{k}| > k_N, \tag{2.20b}$$

$$a^\dagger_{\mathbf{k},\mathbf{s}}|\psi_0\rangle = 0 \quad \text{for } |\mathbf{k}| < k_N, \tag{2.20c}$$

$$a_{\mathbf{k},\mathbf{s}} a^\dagger_{\mathbf{k},\mathbf{s}}|\Psi_0\rangle = n(\mathbf{k})|\Psi_0\rangle \,. \tag{2.20d}$$

The value of $n(\mathbf{k})$ is either 0 or 1 depending upon $|\mathbf{k}|$ is greater than or less than k_N. This can be accomplished with the step function $\theta(k_N - |\mathbf{k}|)$.

2.1.4 Scalar and Baryon densities

The ground state of nuclear matter is obtained by filling up momentum space states up to Fermi momentum k_N and spin-isospin degeneracy γ. In nuclear matter $\gamma = 4$ and $\gamma = 2$ in pure neutron matter. For infinitely large volume V,

$$\frac{1}{V}\sum_{\mathbf{k}} \longrightarrow \int \frac{d^3\mathbf{k}}{(2\pi)^3} \,. \tag{2.21}$$

Therefore, the ground state expectation values of $\hat{\rho}_s$, $\hat{\rho}_b$ and $\mathcal{E}$ yield the scalar density, baryon density and energy density, respectively:

$$\begin{aligned} \rho_s = <\psi_0|\hat{\rho}_s|\psi_0> &= \frac{\gamma}{(2\pi)^3}\int \frac{M_N^*}{E_N^*(\mathbf{k})} d^3\mathbf{k}\ \theta(k_N - |\mathbf{k}|), \\ &= \frac{\gamma M_N^*}{4\pi^2}\left[k_N E_N^* - M_N^{*2}\ln\left(\frac{k_N + E_N^*}{M_N^*}\right)\right], \end{aligned} \tag{2.22}$$

$$\begin{aligned} \rho_b = <\psi_0|\hat{\rho}_b|\psi_0> &= \frac{\gamma}{(2\pi)^3}\int d^3\mathbf{k}\ \theta(k_N - |\mathbf{k}|), \\ &= \frac{\gamma}{6\pi^2}k_N^3, \end{aligned} \tag{2.23}$$

$$\mathcal{E} \;=\; \frac{g_v^2}{2\ m_v^2}(\rho_b)^2 + \frac{m_s^2}{2\ g_s^2}(M_N - M_N^*)^2 + \gamma \int \frac{d^3\mathbf{k}}{(2\pi)^3} E_N^*(\mathbf{k})\ \theta(k_N - |\mathbf{k}|)\ . \quad (2.24)$$

Note that $E_N^* = \sqrt{k_N^2 + M_N^{*2}}$ denotes the Fermi energy of nucleon. From Eqs.(2.7a) and (2.22) one obtains the self-consistency condition for the effective nucleon mass:

$$M_N^* = M_N - \frac{g_s^2}{m_s^2}\frac{\gamma M_N^*}{4\pi^2}\left[k_N E_N^* - M_N^{*2}\ln\left(\frac{k_N + E_N^*}{M_N^*}\right)\right]. \quad (2.25)$$

It is clear from Eq.(2.25) and (2.22) that $\Delta M^* = M_n^* - M_p^* = M_n - M_p = \Delta M$ as the nucleon masses are modified by the scalar mean field, which does not distinguish between neutron and proton. The Eq.2.25 can also be obtained by minimizing the energy density $\mathcal{E}$ at fixed baryon density *i.e.*

$$\left(\frac{\partial\mathcal{E}}{\partial M_N^*}\right)_{\rho_b} = 0\ . \quad (2.26)$$

2.1.5 Coupling constants

The coupling constants g_s and g_v are chosen in such a manner to reproduce the saturation properties of uniform nuclear matter. We use the values from Ref. [45],

$$C_s^2 = g_s^2\frac{M_N^2}{m_s^2} = 267.1\ , \qquad C_v^2 = g_v^2\frac{M_N^2}{m_v^2} = 195.9\ , \quad (2.27)$$

which provide a binding energy,

$$\frac{\mathcal{E}}{\rho_b} - M_N = -15.75\ MeV. \quad (2.28)$$

for a Fermi momentum $k_N = 1.42$ fm^{-1} corresponds to the baryonic density $\rho_b = 0.1934$ fm^{-3}. This small nuclear binding energy arises from the cancellation between large attractive and repulsive contribution of scalar and vector fields, respectively. We present the saturation curve in Fig.2.2. With this choice of coupling constants, $M_N^*/M_N = 0.56$ at the saturation density.

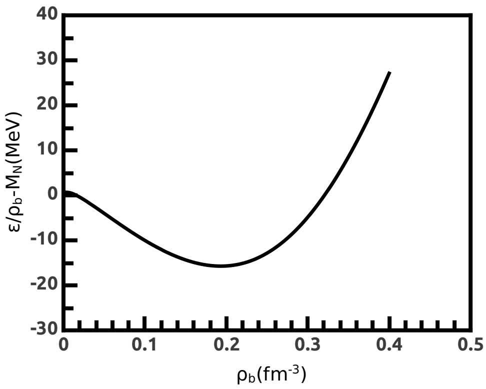

Figure 2.2: *Saturation curve for symmetric nuclear matter.*

2.2 Nucleon propagator in medium

The in-medium nucleon propagator which is one of the basic ingredient of our calculation, is different from the usual nucleon propagator. Here we present a derivation of in-medium nucleon propagator. The position space nucleon propagator in vacuum is given by the vacuum expectation value of the time ordered product of Fermion fields.

$$iG_N(x-x') = \langle\, 0|\ \mathcal{T}[\psi(x)\bar{\psi}(x')]\ |0\,\rangle\ . \tag{2.29}$$

In medium, $|0\,\rangle$ is to be replaced by $|\psi_0\,\rangle$ and we denote the nucleon propagator in medium, G^*_N to distinguish it from that in vacuum, G_N. Thus,

$$\begin{aligned} iG^*_N(x-x') &= \langle\, \Psi_0|\psi(x)\bar{\psi}(x')|\Psi_0\,\rangle\,\theta(t-t') \\ &- \langle\, \Psi_0|\bar{\psi}(x')\psi(x)|\Psi_0\,\rangle\,\theta(t'-t)\ . \end{aligned} \tag{2.30}$$

Note that the time-ordered product in Eq.(2.30) involves negative sign for Fermions (nucleons). To derive the nucleon propagator in medium we neglect the modification due to vector mean field (V_0) [2, 45] implies that $\varepsilon_\pm(\mathbf{k}) = \pm E^*_N(\mathbf{k})$. Therefore, Eq.(2.16) reduces to

$$\psi(x) = \int \frac{d^3\mathbf{k}}{\sqrt{(2\pi)^3\ 2E^*_N(\mathbf{k})}} \sum_{\mathbf{s}} \Big[a_{\mathbf{k},\mathbf{s}}\ \mathcal{U}(\mathbf{k},\mathbf{s})\ e^{-ik\cdot x} + b^\dagger_{\mathbf{k},\mathbf{s}}\ \mathcal{V}(\mathbf{k},\mathbf{s})\ e^{ik\cdot x}\Big]\ . \tag{2.31}$$

Now the ground state expectation values reads

$$\begin{aligned}
\langle\, \Psi_0|\psi(x)\bar{\psi}(x')|\Psi_0\,\rangle &= \int \frac{d^3\mathbf{k}}{\sqrt{(2\pi)^3 2E_N^*(\mathbf{k})}} \int \frac{d^3\mathbf{k}'}{\sqrt{(2\pi)^3 2E_N^*(\mathbf{k}')}} \\
&\times \sum_{\mathbf{s},\mathbf{s}'} \langle\, \Psi_0|a_{\mathbf{k},\mathbf{s}} a^\dagger_{\mathbf{k}',\mathbf{s}'}|\Psi_0\,\rangle\, \mathcal{U}(\mathbf{k},\mathbf{s})\bar{\mathcal{U}}(\mathbf{k}',\mathbf{s}') e^{-i(k\cdot x - k'\cdot x')} \\
&= \int \frac{d^3\mathbf{k}}{(2\pi)^3 2E_N^*(\mathbf{k})} (\not{k} + M_N^*) e^{-ik\cdot(x-x')} [1-\theta(k_N - |\mathbf{k}|)] \;,
\end{aligned} \tag{2.32}$$

$$\begin{aligned}
\langle\, \Psi_0|\bar{\psi}(x')\psi(x)|\Psi_0\,\rangle &= \int \frac{d^3\mathbf{k}}{\sqrt{(2\pi)^3 2E_N^*(\mathbf{k})}} \int \frac{d^3\mathbf{k}'}{\sqrt{(2\pi)^3 2E_N^*(\mathbf{k}')}} \\
&\times \sum_{\mathbf{s},\mathbf{s}'} \Big[\langle\, \Psi_0|a^\dagger_{\mathbf{k}',\mathbf{s}'} a_{\mathbf{k},\mathbf{s}}|\Psi_0\,\rangle\, \bar{\mathcal{U}}(\mathbf{k}',\mathbf{s}')\mathcal{U}(\mathbf{k},\mathbf{s}) e^{-i(k\cdot x - k'\cdot x')} \\
&+ \langle\, \Psi_0|b_{\mathbf{k}',\mathbf{s}'} b^\dagger_{\mathbf{k},\mathbf{s}}|\Psi_0\,\rangle\, \bar{\mathcal{V}}(\mathbf{k}',\mathbf{s}')\mathcal{V}(\mathbf{k},\mathbf{s})) e^{-i(k\cdot x - k'\cdot x')} \Big] \\
&= \int \frac{d^3\mathbf{k}}{(2\pi)^3 2E_N^*(\mathbf{k})} \Big[(\not{k} + M_N^*) e^{-ik\cdot(x-x')} \theta(k_N - |\mathbf{k}|) \\
&+ (\not{k} - M_N^*) e^{ik\cdot(x-x')} \Big] \,.
\end{aligned} \tag{2.33}$$

The theta functions can be written as

$$\begin{aligned}
\theta(t-t')e^{-ik\cdot(x-x')} &= e^{-ik\cdot(x-x')}\, i \int \frac{dk_0'}{2\pi} \left[\frac{e^{-ik_0'(t-t')}}{k_0' + i\epsilon} \right] \\
&= i e^{i\mathbf{k}\cdot(\mathbf{x}-\mathbf{x}')} \int \frac{dk_0'}{2\pi} \left[\frac{e^{-i(k_0' + E_N^*(\mathbf{k})(t-t')}}{k_0' + i\epsilon} \right] \\
&= i e^{i\mathbf{k}\cdot(\mathbf{x}-\mathbf{x}')} \int \frac{dk_0}{2\pi} \left[\frac{e^{-ik_0(t-t')}}{k_0 - E_N^*(\mathbf{k}) + i\epsilon} \right] \\
&= i \int \frac{dk_0}{2\pi} \left[\frac{e^{-ik\cdot(x-x')}}{k_0 - E_N^*(\mathbf{k}) + i\epsilon} \right] \,.
\end{aligned} \tag{2.34}$$

Similarly,

$$\theta(t'-t)e^{-ik\cdot(x-x')} = -i \int \frac{dk_0}{2\pi} \left[\frac{e^{-ik\cdot(x-x')}}{k_0 - E_N^*(\mathbf{k}) - i\epsilon} \right] \,, \tag{2.35}$$

$$\theta(t'-t)e^{ik\cdot(x-x')} = i \int \frac{dk_0}{2\pi} \left[\frac{e^{ik\cdot(x-x')}}{k_0 - E_N^*(\mathbf{k}) + i\epsilon} \right] \,. \tag{2.36}$$

Eqs.(2.33), (2.35) and (2.36) yields

$$\begin{aligned}
\langle\, \Psi_0|\bar{\psi}(x')\psi(x)|\Psi_0\,\rangle\, \theta(t'-t) &= -i\int \frac{d^4k}{(2\pi)^4 2E_N^*(\mathbf{k})} \\
&\times \left[(\not{k}+M_N^*)\frac{e^{-ik\cdot(x-x')}}{k_0-E_N^*(\mathbf{k})-i\epsilon}\theta(k_N-|\mathbf{k}|)\right] \\
&+ i\int \frac{d^4k}{(2\pi)^4 2E_N^*(\mathbf{k})}\left[(\not{k}-M_N^*)\frac{e^{ik\cdot(x-x')}}{k_0-E_N^*(\mathbf{k})+i\epsilon}\right] \\
&= -i\int \frac{d^4k}{(2\pi)^4 2E_N^*(\mathbf{k})}e^{-ik\cdot(x-x')}(\not{k}+M_N^*) \\
&\times \left[\frac{\theta(k_N-|\mathbf{k}|)}{k_0-E_N^*(\mathbf{k})-i\epsilon}-\frac{1}{k_0+E_N^*(\mathbf{k})-i\epsilon}\right]\,. \qquad (2.37)
\end{aligned}$$

To arrive at the last line of Eq.(2.37) we have changed $k \to -k$ in the last integral of the second line of that equation. Similarly, from Eqs.(2.32) and (2.34) we obtain

$$\begin{aligned}
\langle\, \Psi_0|\psi(x)\bar{\psi}(x')|\Psi_0\,\rangle\, \theta(t-t') &= i\int \frac{d^4k}{(2\pi)^4 2E_N^*(\mathbf{k})}e^{-ik\cdot(x-x')}(\not{k}+M_N^*) \\
&\times \left[\frac{1-\theta(k_N-|\mathbf{k}|)}{k_0-E_N^*(\mathbf{k})+i\epsilon}\right]\,. \qquad (2.38)
\end{aligned}$$

Substituting Eq.(2.37) and (2.38) in Eq.(2.30) one obtains

$$\begin{aligned}
iG_N^*(x-x') &= i\int \frac{d^4k}{(2\pi)^4 2E_k}e^{-ik\cdot(x-x')}(\not{k}+M_N^*) \\
&\times \left[\frac{1-\theta(k_N-|\mathbf{k}|)}{k_0-E_N^*(\mathbf{k})+\epsilon}+\frac{\theta(k_N-|\mathbf{k}|)}{k_0-E_N^*(\mathbf{k})-i\epsilon}-\frac{1}{k_0+E_N^*(\mathbf{k})-i\epsilon}\right]. \quad (2.39)
\end{aligned}$$

The first term of Eq.(2.39) represents particle propagation above the Fermi sea and the second term indicates the propagation of holes inside the Fermi sea. The last term shows the propagation of holes in the infinite Dirac sea. Here,

$$\frac{1}{k_0-E_N^*(\mathbf{k})+i\epsilon}-\frac{1}{k_0+E_N^*(\mathbf{k})-i\epsilon} = \frac{2E_N^*(\mathbf{k})}{k^2-M_N^{*2}+i\zeta}\,, \qquad (2.40)$$

$$\frac{1}{k_0-E_N^*(\mathbf{k})-i\epsilon}-\frac{1}{k_0-E_N^*(\mathbf{k})+i\epsilon} = 2i\pi\delta(k_0-E_N^*(\mathbf{k}))\,. \qquad (2.41)$$

From Eqs.(2.39)-(2.41),

$$iG_N^*(x-x') = i\int \frac{d^4k}{(2\pi)^4} e^{-ik\cdot(x-x')} G_N^*(k), \tag{2.42}$$

where $G_N^*(k)$ represents the in-medium nucleon propagator in momentum space which consists of

$$G_N^*(k) = G_N^{*F}(k) + G_N^{*D}(k) \ , \tag{2.43}$$

Explicitly,

$$G_N^{*F}(k) = \frac{\not{k} + M_N^*}{k^2 - M_N^* + i\zeta} \ , \tag{2.44a}$$

$$G_N^{*D}(k) = \frac{i\pi}{E_N^*(\mathbf{k})}(\not{k} + M_N^*) \ \delta(k_0 - E_N^*(\mathbf{k})) \ \theta(k_N - |\mathbf{k}|) \ . \tag{2.44b}$$

The superscript F and D denotes the free and dense parts, respectively. Note that delta function in Eq.(2.44b) indicates the nucleons are on-shell while $\theta(k_N - |\mathbf{k}|)$ ensures that propagating nucleons have momentum less than k_N.

Chapter 3

Pions in Asymmetric Nuclear Matter

In this chapter we investigate the pion propagation in asymmetric nuclear matter (ANM) using relativistic models [10, 45]. The importance of relativistic corrections and density dependent pion mass splitting in ANM in the context of deriving pion-nucleus optical potential was discussed in [105]. The formalism adopted in [105] was that of chiral perturbation theory. Such investigations are important to understand the pion-nucleon dynamics at finite density. Medium modifies the pion masses. Such mass shifts in nuclear matter can be used to calculate the pion-nucleus optical potential [20,21,105,115–120] which are different for different charged states. Recently, in the context of astrophysics, pionic properties in ANM has also been studied by involving Nambu-Jona-Lasinio model [106, 107]. Furthermore, in-medium pion dispersion relations also determine the low mass dilepton yields in relativistic heavy ion collisions which has been mentioned in the introduction [99, 102].

With this motivation, here we focus on the propagating modes of various charged states of pions which are non degenerate in ANM. This is in sharp contrast with most of the previous calculations which mostly deal with symmetric nuclear matter (SNM) [98, 100].

3.1 Pion-Nucleon interaction

Pion is the least massive meson which is responsible for the long range nucleon-nucleon interaction. The pion-nucleon interaction is strongly spin and isospin dependent. To study the pion dispersion in ANM, we consider both the pseudoscalar and pseudovector couplings of pion with nucleon.

3.1.1 Pseudoscalar πN interaction

Historically, pion (π) and rho (ρ) mesons were first included by Serot [121] into the original Walecka model for the realistic description of dense nuclear matter (DNM). However, the calculation was restricted to the mean field (MF) level. The renormalizibility of the theory was preserved by considering the pseudoscalar (PS) πN interaction. Our starting point is the following Lagrangian [122]:

$$
\begin{aligned}
\mathcal{L} &= \bar{\Psi}(i\gamma_\mu\partial^\mu - M)\Psi - ig_\pi\bar{\Psi}\gamma_5(\vec{\tau}\cdot\vec{\Phi}_\pi)\Psi - \frac{1}{2}g_\rho\bar{\Psi}\gamma_\mu(\vec{\tau}\cdot\vec{\Phi}^\mu_\rho)\Psi - g_\omega\bar{\Psi}\gamma_\mu\Phi^\mu_\omega\Psi \\
&+ \frac{1}{2}(\partial_\mu\Phi_s\partial^\mu\Phi_s - m_s^2\Phi_s^2) + g_s\bar{\Psi}\Phi_s\Psi - \frac{1}{2}m_\pi^2\vec{\Phi}_\pi^2 + \frac{1}{2}m_\omega^2\Phi_{\omega\mu}\Phi^\mu_\omega + \frac{1}{2}g_{\phi\pi}m_s\Phi_s\vec{\Phi}_\pi^2 \\
&+ \frac{1}{2}(\partial_\mu\vec{\Phi}_\pi - g_\rho\vec{\Phi}_{\rho\mu}\times\vec{\Phi}_\pi)\cdot(\partial^\mu\vec{\Phi}_\pi - g_\rho\vec{\Phi}^\mu_\rho\times\vec{\Phi}_\pi) + \frac{1}{2}m_\rho^2\vec{\Phi}_{\rho\mu}\cdot\vec{\Phi}^\mu_\rho \\
&- \frac{1}{4}G_{\mu\nu}G^{\mu\nu} - \frac{1}{4}\vec{B}_{\mu\nu}\cdot\vec{B}^{\mu\nu},
\end{aligned}
\tag{3.1}
$$

where,

$$
G_{\mu\nu} = \partial_\mu\Phi_{\omega\nu} - \partial_\nu\Phi_{\omega\mu} \tag{3.2a}
$$

$$
\vec{B}_{\mu\nu} = \partial_\mu\vec{\Phi}_{\rho\nu} - \partial_\nu\vec{\Phi}_{\rho\mu} - g_\rho\vec{\Phi}_{\rho\mu}\times\vec{\Phi}_{\rho\nu}. \tag{3.2b}
$$

Here, Ψ, $\vec{\Phi}_\pi$, Φ_s, $\vec{\Phi}_\rho$ and Φ_ω represents the nucleon, pion, sigma, rho and omega fields respectively and their masses are denoted by M, m_π, m_s, m_ρ and m_ω. In the present chapter we neglect the explicit symmetry breaking *i.e.* $M_n = M_p = M$ and $M_n^* = M_p^* = M^*$. In Eq.(3.1), the pion-nucleon dynamics is described by

$$
\mathcal{L}^{PS}_{\pi NN} = -ig_\pi\bar{\Psi}\gamma_5\left(\vec{\tau}\cdot\vec{\Phi}_\pi\right)\Psi, \tag{3.3}
$$

where, g_π is the pion-nucleon coupling constant [123].

This model successfully reproduces the saturation properties of nuclear matter and yields accurate results for closed shell nuclei in the Dirac-Hartree approximation [112]. But, the appearance of tachyonic mode for pions even at density as low as $0.1\rho_0$, (ρ_0 denotes normal nuclear matter density) poses a serious problem [124]. Such a non-propagating mode for the pions can be removed by extending the calculation beyond the MF level as showed by Kapusta [124].

This model has an added advantage because of the presence of π-σ coupling in addition to the usual PS coupling of the pion with the nucleons which is responsible for the generation of small s-wave pion nucleon interaction in vacuum. This is consistent with the observed characteristics of the pion-nucleon interaction which is dominated by the p-wave scattering while the s-wave scattering length is almost zero. In matter, however, as argued in [122, 124], such subtle cancellation does not occur and pion gets unrealistically large mass in matter. To circumvent this problem it was suggested in [124] to use the pseudovector coupling even though it makes the theory non-renormalizable.

3.1.2 Pseudovector πN interaction

The theoretical challenge, therefore, is to construct a model with πN pseudovector (PV) interaction which preserves the renormalizibility of the theory. This was accomplished in Ref. [122] following the technique developed by Weinberg [125–127] and Schwinger [128]. Here one starts with the PS coupling and subsequently invokes non-linear field transformations to obtain PV representation. Unlike straight forward inclusion of PV interaction in this method one requires only finite number of counter terms which makes the theory renormalizable.

We, here, start with this model developed by Matsui and Serot [122] to study the pion propagation in ANM. Clearly, the model adopted here is different from what we had invoked in our previous work [129]. Furthermore, in [129], for the determination of pion self-energy in matter only the scattering from the Fermi sphere was considered and the vacuum part was completely ignored. The latter gives rise to a large contribution to the pion self-energy in presence of strong scalar density (ρ_s).

To obtain the PV representation of πN interaction we start from the Lagrangian given in Eq.(3.1) and perform the following nonlinear chiral transformation [122]:

$$\Psi = \left[\frac{1 - i\gamma_5 \vec{\tau}\cdot\vec{\xi}}{\sqrt{1+\vec{\xi}^2}}\right]\Psi' \,, \tag{3.4a}$$

$$\vec{\xi} = \left(\frac{f_\pi}{m_\pi}\right)\vec{\Phi}'_\pi = \mathrm{g}_\pi\vec{\Phi}_\pi / \left[M - \mathrm{g}_s\Phi_s + \sqrt{(M-\mathrm{g}_s\Phi_s)^2 + \mathrm{g}_\pi^2\vec{\Phi}_\pi^2}\right] \,, \tag{3.4b}$$

$$\mathrm{g}_s\Phi'_s = M - \sqrt{(M-\mathrm{g}_s\Phi_s)^2 + \mathrm{g}_\pi^2\vec{\Phi}_\pi^2} \,. \tag{3.4c}$$

The last two equations (3.4b) and (3.4c) are used to express the old fields Φ_s and $\vec{\Phi}_\pi$ in terms of new fields Φ'_s and $\vec{\Phi}'_\pi$.

$$\vec{\Phi}_\pi = \left[\frac{1-2(f_\pi/m_\pi)\Phi'_s}{1+(f_\pi/m_\pi)^2\vec{\Phi}'^2_\pi}\right]\vec{\Phi}'_\pi, \tag{3.5a}$$

$$\Phi_s = \frac{(1-(f_\pi/m_\pi)^2\vec{\Phi}'^2_\pi)\Phi'_s + (\mathrm{g}_\pi/\mathrm{g}_s)(f_\pi/m_\pi)\vec{\Phi}'^2_\pi}{1+(f_\pi/m_\pi)^2\vec{\Phi}'^2_\pi}. \tag{3.5b}$$

After the above transformations the Lagrangian Eq.(3.1) reduces to

$$\begin{aligned}\mathcal{L}' &= \bar{\Psi}'(i\gamma_\mu\partial^\mu - M)\Psi' - \frac{1}{2}\mathrm{g}_\rho\bar{\Psi}'\gamma_\mu(\vec{\tau}\cdot\vec{\Phi}^\mu_\rho)\Psi' + \mathrm{g}_s\bar{\Psi}'\Phi'_s\Psi' - \mathrm{g}_\omega\bar{\Psi}'\gamma_\mu\Phi^\mu_\rho\Psi' \\ &+ \frac{1}{2}(\partial_\mu\Phi_s\partial^\mu\Phi_s - m_s^2\Phi_s^2) + \frac{1}{2}(\partial_\mu\vec{\Phi}_\pi - \mathrm{g}_\rho\vec{\Phi}_{\rho\mu}\times\vec{\Phi}_\pi)\cdot(\partial^\mu\vec{\Phi}_\pi - \mathrm{g}_\rho\vec{\Phi}^\mu_\rho\times\vec{\Phi}_\pi) \\ &- \frac{1}{2}m_\pi^2\vec{\Phi}_\pi^2 + \frac{1}{2}\mathrm{g}_{\phi\pi}m_s\Phi_s\vec{\Phi}^2_\pi + \frac{1}{2}m_\omega^2\Phi_{\omega\mu}\Phi^\mu_\omega + \frac{1}{2}m_\rho^2\vec{\Phi}_{\rho\mu}\cdot\vec{\Phi}^\mu_\rho \\ &- \frac{(f_\pi/m_\pi)^2}{1+(f_\pi/m_\pi)^2\vec{\Phi}'^2_\pi}\bar{\Psi}'\gamma_\mu(\vec{\tau}\cdot\vec{\Phi}'_\pi)\times(\partial^\mu\vec{\Phi}'_\pi - \mathrm{g}_\rho\vec{\Phi}^\mu_\rho\times\vec{\Phi}'_\pi)\Psi' \\ &- \frac{(f_\pi/m_\pi)}{1+(f_\pi/m_\pi)^2\vec{\Phi}'^2_\pi}\bar{\Psi}'\gamma_5\gamma_\mu\vec{\tau}\cdot(\partial^\mu\vec{\Phi}'_\pi - \mathrm{g}_\rho\vec{\Phi}^\mu_\rho\times\vec{\Phi}'_\pi)\Psi' \\ &- \frac{1}{4}G_{\mu\nu}G^{\mu\nu} - \frac{1}{4}\vec{B}_{\mu\nu}\cdot\vec{B}^{\mu\nu}\end{aligned} \tag{3.6}$$

It is seen from the Eq.3.6 that the πN PS coupling has disappeared and instead the pion-nucleon dynamics is now governed by the last term of the above mentioned equation. At the leading order one obtains the usual PV coupling represented by,

$$\mathcal{L}^{PV}_{\pi NN} = -\frac{f_\pi}{m_\pi}\bar{\Psi}'\gamma_5\gamma^\mu\partial_\mu\left(\vec{\tau}\cdot\vec{\Phi}'_\pi\right)\Psi' \tag{3.7}$$

Here f_π is the pseudo vector coupling constant and $\frac{f_\pi^2}{4\pi} = 0.08$ [23]. The factor f_π is related to g_π with

$$\frac{f_\pi}{m_\pi} = \frac{\mathrm{g}_\pi}{2M_N} \tag{3.8}$$

The above mentioned model has various shortcomings too. In fact, the Ref. [122] itself discusses its limitations in describing many body πN dynamics. For example, the successful description of the saturation properties of nuclear matter in this scheme requires higher scalar mass which gives rise to larger in-medium nucleon mass compared to the MFT. In addition, it also fails to account for the observed pion-nucleus scattering length at finite density [122]. In the same work, chiral π-σ model has also been discussed to which we shall come later. In the end, we present results calculated using this non-chiral model together with what we obtain from a chirally invariant Lagrangian.

3.2 Pion self-energy

It is well known that the particle dispersion changes in matter because of scattering with the medium constituents. This is characterized by the density dependent self-energy of the particle. At low density, this can be calculated by multiplying the forward scattering amplitude with the density, which, however fails at higher density where multiple scattering becomes important. To incorporate the higher order effects one needs to calculate the full self-energy by evaluating loops at various orders. The real and imaginary parts of the self-energy determine the in-medium mass and decay width of the particle.

The the one-loop contribution as shown in Fig.3.1, to the pion self-energy reads

$$\Pi^{*(N)}_{\pi\pi}(q^2) = \int \frac{d^4k}{(2\pi)^4} \mathrm{Tr}\,[\,\Gamma_\pi(q)G^*_N(k)\Gamma_\pi(-q)G^*_N(k+q)\,]\,, \tag{3.9}$$

where the subscript N stands for nucleon index (*i.e.* $N = p$ or n), $k = (k_0, \mathbf{k})$ denotes the four momentum of the nucleon in the loop and $q = (q_0, \mathbf{q})$ is the four momentum of the meson. Γ_π is the vertex factor. For PS coupling $\Gamma_\pi = -ig_\pi\gamma_5$ and $\Gamma_\pi = i\gamma_5\gamma^\mu q_\mu \frac{f_\pi}{m_\pi}$ for PV coupling.

The essential ingredient to calculate in-medium pion self-energy is the in-medium nucleon propagator G^*_N which consists of free (or vacuum) part,G^{*F}_N and a density

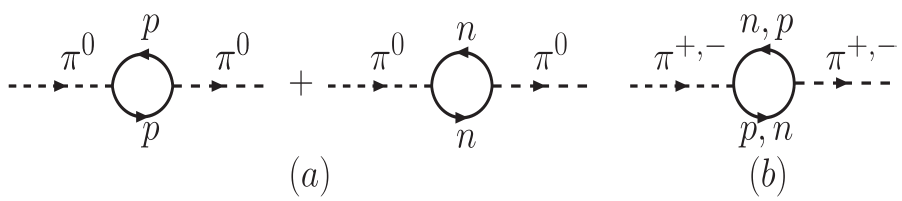

Figure 3.1: *One-loop self-energy diagram for π^0 (a), and (b) represents the same for $\pi^{\pm}$.*

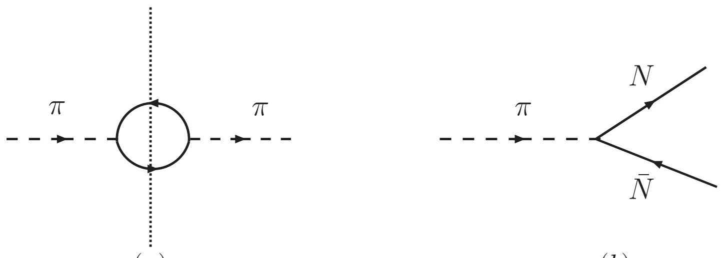

Figure 3.2: *Cutting of nucleon loop implied by the product of two delta functions (a), and the decay of pion into nucleon-antinucleon (b).*

dependent (or medium) part, G_N^{*D} as shown in Eq.(2.44). Now the self-energy given in Eq.(3.9) in terms of G_N^{*F} and G_N^{*D} reads

$$\begin{aligned} i\Pi^{*(N)}_{\pi\pi}(q^2) &= \int \frac{d^4k}{(2\pi)^4}\mathrm{Tr}\left[\Gamma_\pi(q)G_N^{*F}(k)\Gamma_\pi(-q)G_N^{*F}(k+q)\right. \\ &+ \Gamma_\pi(q)G_N^{*F}(k)\Gamma_\pi(-q)G_N^{*D}(k+q) + \Gamma_\pi(q)G_N^{*D}(k)\Gamma_\pi(-q)G_N^{*F}(k+q) \\ &+ \left.\Gamma_\pi(q)G_N^{*D}(k)\Gamma_\pi(-q)G_N^{*D}(k+q)\right]. \end{aligned} \tag{3.10}$$

Here the last term of Eq.(3.10) contains the product of two delta functions ($G_N^{*D}(k)$ $G_N^{*D}(k+q)$) which puts both the loop-nucleons on-shell implying the cut in the loop (Fig.3.2a). This means that pion can decay into nucleon-antinucleon (Fig.3.2b) pair which happens only in the high momentum limit *i.e* $|\mathbf{q}| > 2k_{p,n}$ and also $q_0 > 2E^*_{p,n}$, where $E^*_{p,n} = \sqrt{k^2_{p,n} + M^{*2}_{p,n}}$ is the Fermi energy for proton (or neutron). Under this conditions only last term of Eq.(3.10 contributes to the self-energy. But in the present calculation, we investigate low momentum (of pion) collective excitations only [11]. Thus the total self-energy consists of FF and $(FD+DF)$ parts. The FF part of the self-energy contains the Dirac sea contribution, while $(FD+DF)$ contains the Fermi sea contribution. We denote them by $\Pi^{*(N)}_{\pi\pi,vac}$ and $\Pi^{*(N)}_{\pi\pi,med}$, respectively.

$$i\Pi^{*(N)}_{\pi\pi,vac}(q^2) = \int \frac{d^4k}{(2\pi)^4}\mathrm{Tr}\left[\ \Gamma_\pi(q)G_N^{*F}(k)\Gamma_\pi(-q)G_N^{*F}(k+q)\ \right], \tag{3.11}$$

$$i\Pi^{*(N)}_{\pi\pi,med}(q^2) = \int \frac{d^4k}{(2\pi)^4}\mathrm{Tr}\left[\ \Gamma_\pi(q)G_N^{*F}(k)\Gamma_\pi(-q)G_N^{*D}(k+q)\ \right]$$

$$+ \int \frac{d^4k}{(2\pi)^4} \mathrm{Tr}\left[\, \Gamma_\pi(q) G_N^{*D}(k) \Gamma_\pi(-q) G_N^{*F}(k+q) \,\right] . \tag{3.12}$$

Once the full self-energy $\Pi^*_{\pi\pi}(q^2)$ is calculated, one should use the Dyson-Schwinger equation,

$$\tilde{\Delta}_\pi(q^2) = \Delta_\pi(q^2) + \Delta_\pi(q^2)\Pi^*_{\pi\pi}(q^2)\tilde{\Delta}_\pi(q^2) , \tag{3.13}$$

to find the in-medium dispersion relation. Diagrammatically this has been shown in Fig.3.3. The poles of the dressed (meson) propagator, $\tilde{\Delta}_\pi(q^2)$ of Eq.(3.13) gives the dispersion relations *i.e.*

$$1 - \Delta_\pi(q^2)\Pi^*_{\pi\pi}(q^2) = 0 , \tag{3.14}$$

where $\Delta_\pi(q^2)$ is the bare meson propagator given by

$$\Delta_\pi(q^2) = \frac{1}{q^2 - m_\pi^2} . \tag{3.15}$$

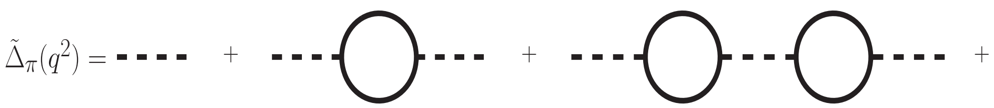

Figure 3.3: *Dressed meson propagator.*

3.2.1 Tachyonic mode of pion

The interaction Lagrangian Eq.(3.1) has a term involving the coupling of pions with the scalar meson (σ meson) given by

$$\mathcal{L}_{\sigma\pi} = \frac{1}{2} \mathrm{g}_{\phi\pi} m_s \Phi_s \vec{\Phi}_\pi^2 \tag{3.16}$$

Here, $\mathrm{g}_{\phi\pi}$ is the coupling constant of the scalar to pion field. The πN scattering amplitude would now involve both nucleon and σ meson in the intermediate state causing sensitive cancellation between the two that gives reasonable value of the s-wave scattering length [124] as mentioned before. At the self-energy level Eqs.(3.3) and (3.16) will generate the exchange and the tadpole diagram as shown in Fig.3.4b

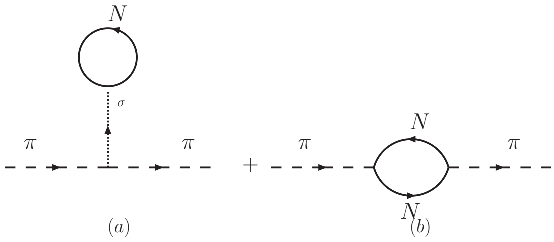

Figure 3.4: *Tadpole contribution to the pion self-energy.*

and 3.4a. First we consider the tadpole diagram whose contribution to the self-energy is given by

$$\Pi_{tad} = -g_{\phi\pi} m_s \phi_0, \tag{3.17}$$

where,

$$\phi_0 = \frac{g_s}{m_s^2}(\rho_{s,p} + \rho_{s,n}). \tag{3.18}$$

Note that $\rho_{s,N}(N = p, n)$ represents the scalar density given in Eq.(2.22). It is to be noted that in the mean field theory (MFT), only the tadpole diagram (*see* Fig.3.4a) contributes, while Fig.3.4b is neglected. The origin of tachyonic mode can now easily be understood. The pion mass in matter due to the tadpole is given by [124]

$$\begin{aligned} m_\pi^{*2} &= m_\pi^2 + \Pi_{tad} \\ &= m_\pi^2 - g_{\phi\pi} m_s \phi_0 \\ &= m_\pi^2 - \frac{g_{\phi\pi} g_s}{m_s}(\rho_{s,p} + \rho_{s,n}) \ . \end{aligned} \tag{3.19}$$

The second term of the last equation is quite large even at densities far below ρ_0 density *viz.* $m_\pi^{*2} < 0$ for $\rho \sim 0.1\rho_0$, where ρ denotes the nuclear matter density.

3.2.2 Self-energy for PS coupling

Now we proceed to calculate the pion self-energies for different charge states of pion. First we calculate the vacuum contribution (Dirac sea contribution) to the pion self-energy using Eq.(3.11). For $\pi^\pm$ the coupling constant g_π gets replaced by $\sqrt{2}g_\pi$. After calculating the trace we obtain

$$\Pi^{*PS}_{\pi\pi,vac}(q^2) = 8ig_\pi^2 \int \frac{d^4k}{(2\pi)^4} \left[\frac{M^{*2} - k\cdot(k+q)}{(k^2 - M^{*2})\,((k+q)^2 - M^{*2})}\right] \ . \tag{3.20}$$

From Eq.(3.20) it is observed that $\Pi^{*PS}_{\pi\pi,vac}(q^2)$ is quadratically divergent. To eliminate these divergences we need to renormalizes $\Pi^{*PS}_{\pi\pi,vac}(q^2)$. Here we adopt the dimensional regularization [130–132] technique to regularize $\Pi^{*PS}_{\pi\pi,vac}(q^2)$ with the following results (details are discussed in **Appendix B**).

$$\begin{aligned}
\tilde{\Pi}^{*PS}_{\pi\pi,vac}(q^2) &= \frac{\mathrm{g}_\pi^2}{2\pi^2}\Bigg[-3(M^2-M^{*2})+(q^2-m_\pi^2)\left(\frac{1}{6}+\frac{M^2}{m_\pi^2}\right) \\
&- 2M^{*2}\ln\left(\frac{M^*}{M}\right)+\frac{8M^2(M-M^*)^2}{(4M^2-m_\pi^2)} \\
&- \frac{2M^{*2}\sqrt{4M^{*2}-q^2}}{q}\tan^{-1}\left(\frac{q}{\sqrt{4M^{*2}-q^2}}\right) \\
&+ \frac{2M^2\sqrt{4M^2-m_\pi^2}}{m_\pi}\tan^{-1}\left(\frac{m_\pi}{\sqrt{4M^2-m_\pi^2}}\right) \\
&+ \left((M^2-M^{*2})+\frac{m_\pi^2(M-M^*)^2}{(4M^2-m_\pi^2)}+\frac{M^2}{m_\pi^2}(q^2-m_\pi^2)\right) \\
&\times \frac{8M^2}{m_\pi\sqrt{4M^2-m_\pi^2}}\tan^{-1}\left(\frac{m_\pi}{\sqrt{4M^2-m_\pi^2}}\right) \\
&+ \int_0^1 dx\; 3x(1-x)q^2\,\ln\left(\frac{M^{*2}-q^2x(1-x)}{M^2-m_\pi^2x(1-x)}\right)\Bigg]. \qquad (3.21)
\end{aligned}$$

It is found that the result given in Eq.(3.21) is finite and no divergences appear further. In the appropriate kinematic regime it might generate imaginary part:

$$\begin{aligned}
\mathrm{Im}\;\Pi^{*PS}_{\pi\pi,vac}(q^2) &= -\frac{\mathrm{g}_\pi^2}{2\pi^2}\int_0^1 dx\;\left(M^{*2}-3q^2x(1-x)\right) \\
&\times\;\mathrm{Im}\left[\ln\left(M^{*2}-q^2x(1-x)-i\xi\right)\right] \\
&= -\frac{\mathrm{g}_\pi^2}{4\pi}\left[q\sqrt{q^2-4M^{*2}}\right]\;\theta\left(q^2-4M^{*2}\right). \qquad (3.22)
\end{aligned}$$

If we consider that (M^*-M) is small enough then the last term of Eq.(3.21) can be approximated to $2\ln(M^*/M)$ and the integral can be easily evaluated to give

$$\tilde{\Pi}^{*PS}_{\pi\pi,vac}(q^2) \simeq -\tilde{c}+\tilde{d}\,q^2, \qquad (3.23)$$

where

$$\tilde{c} = \frac{g_\pi^2}{2\pi^2}\left[3(2M^2 - M^{*2}) + 2M^{*2}\ln\left(\frac{M^*}{M}\right)\right], \tag{3.24a}$$

$$\tilde{d} = \frac{3g_\pi^2}{2\pi^2}\left(\frac{M}{m_\pi}\right)^2. \tag{3.24b}$$

Now we calculate the medium contribution (Fermi sea contribution) to the pion-self energies using Eq.(3.12). After calculating the trace and performing integration over k_0 we obtain

$$\Pi^{*0,PS}_{\pi\pi,med}(q^2) = -8g_\pi^2 \int \frac{d^3k}{(2\pi)^3 E^*}\mathbf{A}_{PS} \tag{3.25}$$

$$\begin{aligned}\Pi^{*\pm,PS}_{\pi\pi,med}(q^2) &= -8g_\pi^2 \int \frac{d^3k}{(2\pi)^3 E^*}[\mathbf{A}_{PS} \mp \mathbf{B}_{PS}] \\ &= \Pi^{*0,PS}_{\pi\pi,med}(q^2) \mp \delta\Pi^{*PS}_{\pi\pi,med}(q^2),\end{aligned} \tag{3.26}$$

where,

$$\delta\Pi^{*PS}_{\pi\pi,med}(q^2) = -8g_\pi^2 \int \frac{d^3k}{(2\pi)^3 E^*}\mathbf{B}_{PS}. \tag{3.27}$$

The self-energies of π^0 and $\pi^\pm$ are denoted by the superscripts 0 and $\pm$ as shown in Eqs.(3.25) and (3.26). The explicit expression for $\mathbf{A}_{PS}$ and $\mathbf{B}_{PS}$ are presented below:

$$\mathbf{A}_{PS} = \left[\frac{(k\cdot q)^2}{q^4 - 4(k\cdot q)^2}\right](\theta_p + \theta_n), \tag{3.28}$$

$$\mathbf{B}_{PS} = \frac{1}{2}\left[\frac{q^2(k\cdot q)}{q^4 - 4(k\cdot q)^2}\right](\theta_p - \theta_n), \tag{3.29}$$

with $\theta_{p,n} = \theta(k_{p,n} - |\mathbf{k}|)$. We restrict ourselves in the long wavelength limit *i.e.* when the pion momentum ($\mathbf{q}$) is small compared to the Fermi momentum ($k_{p,n}$) of the system where the many body effects manifest strongly. In this case particle propagation can be understood in terms of collective excitation [11] of the system which permits analytical solutions of the dispersion relations [11, 133]. But in the short wavelength limit *i.e.* when the pion momentum ($\mathbf{q}$) is much larger than the Fermi momentum ($k_{p,n}$), particle dispersion approaches to that of the free propagation.

Note that for SNM, $\mathbf{B}_{PS} = 0$ implying

$$\Pi^{*\pm,PS}_{\pi\pi,med} = \Pi^{*0,PS}_{\pi\pi,med} \ . \tag{3.30}$$

In the long wavelength limit we neglect the term q^4 compared to the term $4(k\cdot q)^2$ from the denominator of both $\mathbf{A}_{PS}$ and $\mathbf{B}_{PS}$ in Eqs.(3.28) and (3.29). Explicitly, after a straight forward calculation we get,

$$\begin{aligned}
\Pi^{*0,PS}_{\pi\pi,med}(q^2) &= \frac{g_\pi^2}{2\pi^2}\left[k_p\ E_p^* - \frac{1}{2}M^{*2}\ln\left|\frac{1+v_p}{1-v_p}\right|\right] \\
&+ \frac{g_\pi^2}{2\pi^2}\left[k_n\ E_n^* - \frac{1}{2}M^{*2}\ln\left|\frac{1+v_n}{1-v_n}\right|\right] \ ,
\end{aligned} \tag{3.31}$$

and

$$\begin{aligned}
\delta\Pi^{*PS}_{\pi\pi,med}(q^2) &= \frac{g_\pi^2}{2\pi^2}\left[\frac{1}{2}E_p^*\ln\left|\frac{c_0+v_p}{c_0-v_p}\right| - \frac{M^*}{\sqrt{c_0^2-1}}\tan^{-1}\left(\frac{k_p\sqrt{c_0^2-1}}{c_0 M^*}\right)\right]\frac{q^2}{|\mathbf{q}|} \\
&- \frac{g_\pi^2}{2\pi^2}\left[\frac{1}{2}E_n^*\ln\left|\frac{c_0+v_n}{c_0-v_n}\right| - \frac{M^*}{\sqrt{c_0^2-1}}\tan^{-1}\left(\frac{k_n\sqrt{c_0^2-1}}{c_0 M^*}\right)\right]\frac{q^2}{|\mathbf{q}|},
\end{aligned} \tag{3.32}$$

where $v_{p,n} = k_{p,n}/E^*_{p,n}$ and $c_0 = q_0/|\mathbf{q}|$. The approximate results of Eqs.(3.31) and(3.32) are given below:

$$\Pi^{*0,PS}_{\pi\pi,med}(q^2) \simeq \Omega^{PS}_{\pi\pi,med} \ , \tag{3.33a}$$

$$\delta\Pi^{*0,PS}_{\pi\pi,med}(q^2) \simeq = \tilde{e}\ \frac{q^2}{q_0} \ . \tag{3.33b}$$

where

$$\begin{aligned}
\Omega^{PS}_{\pi\pi,med} &= \frac{g_\pi^2}{2\pi^2}\left[\left(k_p\ E_p^* + k_n\ E_n^*\right) - \frac{1}{3}M^{*2}\left(\frac{k_p^3}{E_p^{*3}} + \frac{k_n^3}{E_n^{*3}}\right)\right. \\
&- \left.\frac{1}{5}M^{*2}\left(\frac{k_p^5}{E_p^{*5}} + \frac{k_n^5}{E_n^{*5}}\right) - M^{*2}\left(\frac{k_p}{E_p^*} + \frac{k_n}{E_n^*}\right)\right],
\end{aligned} \tag{3.34a}$$

$$\tilde{e} = \frac{g_\pi^2}{2\pi^2}\left[\frac{1}{3}\left(\frac{k_p^3}{M^{*2}} - \frac{k_n^3}{M^{*2}}\right)\right]. \tag{3.34b}$$

Thus the total pion self-energy with the tadpole contribution reads

$$\Pi^{*(0,\pm)PS}_{\pi\pi,total}(q^2) = \left[\tilde{\Pi}^{*PS}_{\pi\pi,vac}(q^2) + \Pi^{*(0,\pm)PS}_{\pi\pi,med}(q^2)\right] + \Pi_{tad}(q^2)\ . \tag{3.35}$$

3.2.2.1 Dispersion without Dirac sea

In this subsection we use the self-energies of Eq.(3.58) to find the pion dispersion relations. We obtain the dispersion relations solving the Dyson-Schwinger Eq.(3.14) which reads

$$\left(q^2 - m^2_{\pi^{0,\pm}}\right) - \Pi^{*(0,\pm)PS}_{\pi\pi,total}(q^2) = 0 \tag{3.36}$$

Here $m_{\pi^{0,\pm}}$ are the masses of π^0 and $\pi^\pm$. Substituting every thing in Eq.(3.36) and performing algebraic manipulation and after simplification the dispersion relations can be cast into the following form:

$$q_0^2 \simeq m^{*2}_{\pi^{0,\pm}} + \mathbf{q}^2. \tag{3.37}$$

The medium modified masses or effective masses of pions can be presented as

$$m^{*2}_{\pi^0} \simeq m^2_{\pi^0} + \Pi_{tad} + \Omega^{PS}_{\pi\pi,med}\ , \tag{3.38a}$$

$$m^{*2}_{\pi^\pm} \simeq \frac{m^2_{\pi^\pm} + \Pi_{tad} + \Omega^{PS}_{\pi\pi,med}}{1 \mp \delta\Omega^{PS}_{\pi\pi,med}}\ , \tag{3.38b}$$

where,

$$\delta\Omega^{PS}_{\pi\pi,med} = \left[\frac{\tilde{e}}{\sqrt{m^2_{\pi^\pm} + \Pi_{tad} + \Omega^{PS}_{\pi\pi,med}}}\right]\ . \tag{3.39}$$

3.2.2.2 Dispersion with Dirac sea

Solving the Eq.(3.36) and after simplification we obtain the following pion dispersion relation:

$$q_0^2 \simeq m^{*2}_{\pi^{0,\pm}} + \mathbf{q}^2. \tag{3.40}$$

The medium modified masses or effective masses of different charged states of pions in presence of Dirac sea can be presented as

$$m_{\pi^0}^{*2} \simeq \frac{1}{\tilde{d}} \left[\Omega^{PS}_{\pi\pi,total} - m^2_{\pi^0}\right] , \tag{3.41a}$$

$$m_{\pi^\pm}^{*2} \simeq \left[\frac{\Omega^{PS}_{\pi\pi,total} - m^2_{\pi^\pm}}{(1 \mp \delta\Omega^{PS}_{\pi\pi,total})\,\tilde{d}}\right], \tag{3.41b}$$

where,

$$\Omega^{PS}_{\pi\pi,total} = \tilde{c} - \Pi_{tad} - \Omega^{PS}_{\pi\pi,med}, \tag{3.42a}$$

$$\delta\Omega^{PS}_{\pi\pi,total} = \left[\frac{\tilde{e}}{\sqrt{\left(\Omega^{PS}_{\pi\pi,total} - m^2_{\pi^\pm}\right)\tilde{d}}}\right]. \tag{3.42b}$$

In the PS coupling the asymmetry driven mass splitting is of $\mathcal{O}(k^3_{p(n)}/M^{*2})$. The terms $\delta\Omega^{PS}_{\pi\pi,total}$ and $\delta\Omega^{PS}_{\pi\pi,med}$ are non-vanishing in ANM and responsible for the pion mass splitting.

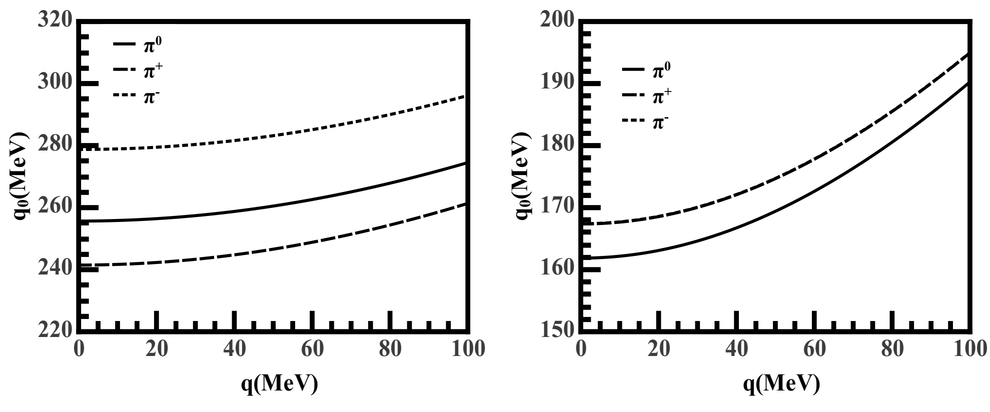

Figure 3.5: *Pion dispersions for PS coupling at $\rho = 0.17 fm^{-3}$ and $\alpha = 0.2$.*

Pion dispersions (for PS coupling) at $\rho = 0.17fm^{-3}$ and $\alpha = 0.2$ are shown in Fig.3.5. The dispersions for various charge states of pion without the effect of Dirac sea are displayed on the left figure and on the right figure the same are displayed with the contribution of Dirac sea. Without the Dirac sea, dispersions are found to be different for different charge states of pion while, with Dirac sea contribution,

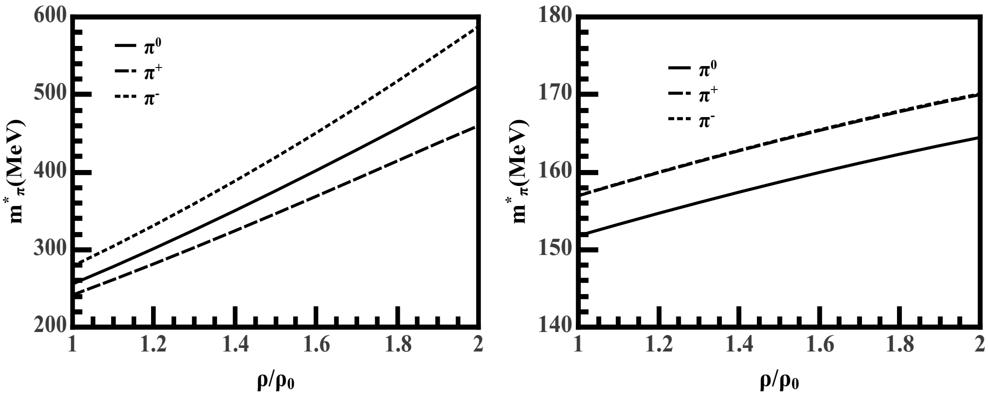

Figure 3.6: *Density dependent effective masses of pion at $\alpha = 0.2$ for PS coupling.*

the π^+ and π^- dispersions are not distinguishable from each other. In Fig.3.6 and Fig.3.7 we present, the density (ρ) and asymmetry parameter (α) dependent medium modified masses for the various charged states of pions. In the left figure we present the results without vacuum correction (Dirac sea). Here we include both the tadpole and NN-loop.

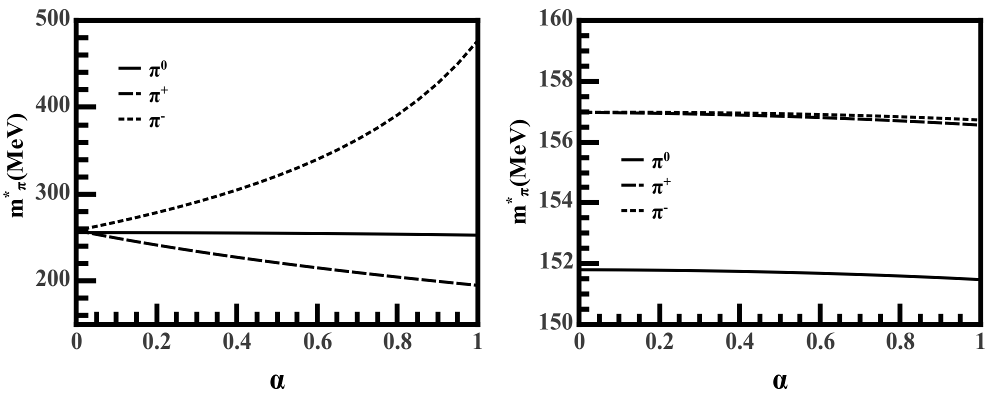

Figure 3.7: *Asymmetry parameter (α) dependent pion masses at normal nuclear matter density for PS coupling.*

It is evident that the inclusion of (3.4b) diagram removes the tachyonic mode but gives rise to effective pion masses unrealistically large as discussed by Kaputa [124]. This is shown in the left figure of Fig.3.6. It is found that with the increase of asymmetry, α, effective mass of π^+ decreases and for π^- it increases rapidly. But in presence of Dirac sea, the in-medium masses of π^+ and π^- are almost degenerate

Table 3.1: *Effective pion masses including the tadpole contribution to the self-energy in PS coupling. Kapusta corresponds to ref. [124] and BDM corresponds to the present calculation.*

	$m^{*2}_{\pi^0}$	$m^{*2}_{\pi^\pm}$
MFT	$m^2_{\pi^0} + \Pi_{tad}$	$m^2_{\pi^\pm} + \Pi_{tad}$
Kapusta	$(m^2_{\pi^0} + \Pi_{tad}) + \Omega^{PS}_{\pi\pi,med}$	$\frac{(m^2_{\pi^\pm} + \Pi_{tad}) + \Omega^{PS}_{\pi\pi,med}}{1 \mp \delta\Omega^{PS}_{\pi\pi,med}}$
BDM	$\frac{1}{\tilde{d}}[\tilde{c} - (m^2_{\pi^0} + \Pi_{tad} + \Omega^{PS}_{\pi\pi,med})]$	$\frac{\tilde{c} - (m^2_{\pi^\pm} + \Pi_{tad} + \Omega^{PS}_{\pi\pi,med})}{(1 \mp \delta\Omega^{PS}_{\pi\pi,total})\ \tilde{d}}$

below $\alpha = 0.4$ as evident from the (right) Fig.3.7.

It is to be noted that the inclusion of the vacuum part reduces the effective pion masses and gives reasonable value for the density dependent pion masses in medium at normal nuclear matter density. The reason for this could be understood from the Table 3.1 which enumerates expressions for the effective pion masses that we obtain in three different cases. The top row represents effective pion masses for the case considered in [121] which gives rise to the tachyonic mode, the second row corresponds to the case discussed by Kapusta [124] and in the last row we present results of the present work as by BDM. The presence of the additional term $\tilde{d}$ somewhat tames the dispersion curve bringing the masses down compared to [124]. This can be noted that at the MFT level Π_{tad} involves sum of the scalar densities $\rho_{s,n}$ and $\rho_{s,p}$. Therefore, in MFT, as expected, the masses are insensitive to asymmetry parameter α.

3.2.3 Self-energy for PV coupling

First we calculate the Dirac sea contribution to the pion self-energy. After calculating trace we obtain from Eq.(3.11),

$$\Pi^{*PV}_{\pi\pi,vac}(q^2) = 8i\left(\frac{f_\pi}{m_\pi}\right)^2 \int \frac{d^4k}{(2\pi)^4} \left[\frac{M^{*2}q^2 + k\cdot(k+q)q^2 - 2(k\cdot q)(k+q)\cdot q}{(k^2 - M^{*2})((k+q)^2 - M^{*2})}\right]. \quad (3.43)$$

Direct power counting shows that the term $\Pi^{*PV}_{\pi\pi,vac}(q^2)$ is divergent. The appropriate renormalization scheme for the present model has been developed in Ref. [122]. We first consider a simple subtraction scheme described in **Appendix B** to obtain

$$\tilde{\Pi}^{*PV}_{\pi\pi,vac}(q^2) = \frac{q^2}{2\pi^2}\left(\frac{f_\pi}{m_\pi}\right)^2\left[2M^{*2}\int_0^1 dx\ \ln\left(\frac{M^{*2}-q^2x(1-x)}{M^{*2}-m_\pi^2x(1-x)}\right)\right]. \tag{3.44}$$

Now $\tilde{\Pi}^{*PV}_{\pi\pi,vac}(q^2)$ can be approximated to

$$\tilde{\Pi}^{*PV}_{\pi\pi,vac}(q^2) \simeq c - d\ q^2\ . \tag{3.45}$$

On the other hand borrowing results from [122] one has,

$$\tilde{\Pi}^{*PV}_{\pi\pi,vac}(q^2) \simeq c' + d'\ q^2\ . \tag{3.46}$$

Here,

$$c = \left(\frac{f_\pi}{\sqrt{6}\ \pi}\right)^2\ , \tag{3.47a}$$

$$d = \left(\frac{f_\pi}{\sqrt{6}\ \pi\ m_\pi}\right)^2\ , \tag{3.47b}$$

$$c' = \left(\frac{f_\pi}{\pi}\right)^2\left[\frac{4}{3}M(M-M^*)\right], \tag{3.47c}$$

$$d' = \left(\frac{f_\pi}{\pi\ m_\pi}\right)^2\left[2M^{*2}\ln\left(\frac{M^*}{M}\right)\ q^2\right]\ . \tag{3.47d}$$

It might be mentioned, although $\tilde{\Pi}^{*PV}_{\pi\pi,vac}(q^2)$ are different their effect on the effective pion masses and corresponding dispersion relations are found to be marginal as we discuss later. $\Pi^{*PV}_{\pi\pi,vac}(q^2)$ develops the following imaginary part:

$$\mathrm{Im}\ \Pi^{*PV}_{\pi\pi,vac}(q^2) = -\left(\frac{f_\pi}{m_\pi}\right)^2\left[\frac{q}{\pi}2M^{*2}\sqrt{q^2-4M^{*2}}\right]\ \theta\left(q^2-4M^{*2}\right)\ . \tag{3.48}$$

It is observed from Eq.(3.48) that Im $\Pi^{*PV}_{\pi\pi,vac}(q^2)$ is non-vanishing only if $q^2 > 4M^{*2}$. Now we proceed to calculate the density dependent (Fermi sea contribution) pion self-energy. After calculating trace and performing the k_0 integration we obtain

$$\Pi^{*0,PV}_{\pi\pi,med}(q^2) = -8\left(\frac{f_\pi}{m_\pi}\right)^2 \int \frac{d^3k}{(2\pi)^3 E^*} \mathbf{A}_{PV} \ , \tag{3.49}$$

$$\begin{aligned}\Pi^{*\pm,PV}_{\pi\pi,med}(q^2) &= -8\left(\frac{f_\pi}{m_\pi}\right)^2 \int \frac{d^3k}{(2\pi)^3 E^*} \left[\mathbf{A}_{PV} \mp \mathbf{B}_{PV}\right] \\ &= \Pi^{*0,PV}_{\pi\pi,med}(q^2) \mp \delta\Pi^{*,PV}_{\pi\pi,med}(q^2) \ ,\end{aligned} \tag{3.50}$$

where,

$$\delta\Pi^{*PV}_{\pi\pi,med}(q^2) = -8\mathrm{g}_\pi^2 \int \frac{d^3k}{(2\pi)^3 E^*} \mathbf{B}_{PV} \ . \tag{3.51}$$

The superscripts 0 and $\pm$ denote the self-energies of π^0 and $\pi^\pm$. The explicit expressions for $\mathbf{A}_{PV}$ and $\mathbf{B}_{PV}$ are presented below:

$$\mathbf{A}_{PV} = \left[\frac{M^{*2}q^4}{q^4 - 4(k\cdot q)^2}\right](\theta_p + \theta_n) \ , \tag{3.52}$$

$$\mathbf{B}_{PV} = \frac{1}{2}\left[1 + \frac{4M^{*2}q^2}{q^4 - 4(k\cdot q)^2}\right](k\cdot q)(\theta_p - \theta_n) \ . \tag{3.53}$$

In the long wavelength limit considering collective excitations near the Fermi surface, Fermi sea contribution to the pion-self energy can be evaluated analytically. In this case we can neglect the term q^4 compared to the term $4(k\cdot q)^2$ from the denominator of $\mathbf{A}_{PV}$ and $\mathbf{B}_{PV}$ in Eqs.(3.52) and (3.53). This is called hard nucleon loop (HNL) approximation [133]. Explicitly, after a straight forward calculation, we get,

$$\begin{aligned}\Pi^{*0,PV}_{\pi\pi,med}(q^2) &= \frac{1}{2}M^{*2}\left(\frac{f_\pi}{\pi m_\pi}\right)^2\left[\left(\ln\left|\frac{1+v_p}{1-v_p}\right| - c_0\ln\left|\frac{c_0+v_p}{c_0-v_p}\right|\right)\right] \\ &+ \frac{1}{2}M^{*2}\left(\frac{f_\pi}{\pi m_\pi}\right)^2\left[\left(\ln\left|\frac{1+v_n}{1-v_n}\right| - c_0\ln\left|\frac{c_0+v_n}{c_0-v_n}\right|\right)\right] ,\end{aligned} \tag{3.54}$$

$$\begin{aligned}\delta\Pi^{*PV}_{\pi\pi,med}(q^2) &= \left(\frac{f_\pi}{\pi m_\pi}\right)^2\left[\frac{2}{3}k_p^3\, q_0 - \frac{M^{*2}q^2}{|\mathbf{q}|}\left(E_p^*\ln\left|\frac{c_0+v_p}{c_0-v_p}\right|\right.\right. \\ &\left.\left. - \frac{2M^*}{\sqrt{c_0^2-1}}\tan^{-1}\frac{k_p\sqrt{c_0^2-1}}{c_0M^*}\right)\right]\end{aligned}$$

$$
\begin{aligned}
& - \left(\frac{f_\pi}{\pi m_\pi}\right)^2 \left[\frac{2}{3} k_n^3 \; q_0 - \frac{M^{*2} q^2}{|\mathbf{q}|} \left(E_n^* \ln \left| \frac{c_0 + v_n}{c_0 - v_n} \right| \right.\right. \\
& \left.\left. - \frac{2M^*}{\sqrt{c_0^2 - 1}} \tan^{-1} \frac{k_n \sqrt{c_0^2 - 1}}{c_0 M^*} \right) \right] . \qquad (3.55)
\end{aligned}
$$

The results of Eqs.(3.54) and (3.55) are approximated to

$$
\Pi^{*0,PV}_{\pi\pi,med}(q^2) \;\simeq\; a \, \frac{q^4}{q_0^2} + b \; q^2 \; , \qquad (3.56a)
$$

$$
\delta \Pi^{*PV}_{\pi\pi,med}(q^2) \;\simeq\; e' \; q_0 \; . \qquad (3.56b)
$$

where,

$$
a \;=\; \left(\frac{f_\pi M^*}{\pi \; m_\pi}\right)^2 \left[\frac{1}{3}\left(\frac{k_P^3}{E_p^{*3}} + \frac{k_n^3}{E_n^{*3}}\right)\right] \; , \qquad (3.57a)
$$

$$
b \;=\; \left(\frac{f_\pi M^*}{\pi \; m_\pi}\right)^2 \left[\frac{1}{5}\left(\frac{k_P^5}{E_p^{*5}} + \frac{k_n^5}{E_n^{*5}}\right)\right] \; , \qquad (3.57b)
$$

$$
e' \;=\; \left(\frac{f_\pi}{\pi \; m_\pi \;\; M^*}\right)^2 \left[\frac{2}{5}\left(k_p^5 - k_n^5\right)\right] \; . \qquad (3.57c)
$$

The total pion self-energy for PV coupling is

$$
\Pi^{*(0,\pm)PV}_{\pi\pi,total}(q^2) = \tilde{\Pi}^{*PV}_{\pi\pi,vac}(q^2) + \Pi^{*(0,\pm)PV}_{\pi\pi,med}(q^2) \; . \qquad (3.58)
$$

3.2.3.1 Dispersion without Dirac sea

Solving the Dyson-Schwinger Eq.(3.36) replacing $\Pi^{*(0,\pm)PS}_{\pi\pi,total}(q^2)$ with $\Pi^{*(0,\pm)PV}_{\pi\pi,med}(q^2)$ and performing some algebraic manipulation we obtain the algebraic dispersion relations for $\pi^{0,\pm}$ without the Dirac sea effect.

$$
q_0^2 \simeq m^{*2}_{\pi^{0,\pm}} + \gamma_{\pi\pi} \mathbf{q}^2 + \left[\frac{\gamma^2_{\pi\pi}}{4} + \alpha_{\pi\pi}\right] \frac{\mathbf{q}^4}{m^{*2}_{\pi^{0,\pm}}} \; , \qquad (3.59)
$$

where

$$
\alpha_{\pi\pi} \;=\; \frac{a}{1 \; - \; \Omega^{PV}_{\pi\pi,med}} \; , \qquad (3.60a)
$$

$$\gamma_{\pi\pi} \;=\; 1 - \frac{\Omega^{PV}_{\pi\pi,med}}{1 \;-\; \Omega^{PV}_{\pi\pi,med}} + \frac{b}{1 \;-\; \Omega^{PV}_{\pi\pi,med}} \;. \tag{3.60b}$$

and $m^{*2}_{\pi^{0,\pm}}$ is the effective pion masses without Dirac sea effect:

$$m^{*2}_{\pi^0} \;\simeq\; \frac{m^2_{\pi^0}}{1 \;-\; \Omega^{PV}_{\pi\pi,med}} \;, \tag{3.61a}$$

$$m^{*2}_{\pi^\pm} \;\simeq\; \frac{m^2_{\pi^\pm}}{1 \;-\; (\Omega^{PV}_{\pi\pi,med} \;\pm\; \delta\Omega^{PV}_{\pi\pi,med})} \;, \tag{3.61b}$$

where,

$$\Omega^{PV}_{\pi\pi,med} \;=\; a + b \;, \qquad \text{and} \qquad \delta\Omega^{PV}_{\pi\pi,med} \;=\; \frac{e'}{m_{\pi^\pm}} \;. \tag{3.62}$$

3.2.3.2 Dispersion with Dirac sea

The dispersion relations including the effect of Dirac sea can be found by solving Eq.(3.36) replacing $\Pi^{*(0,\pm)PS}_{\pi\pi,total}(q^2)$ with $\Pi^{*(0,\pm)PV}_{\pi\pi,total}(q^2)$. The dispersion relations for $\pi^{0,\pm}$ can be written as,

$$q_0^2 \;\simeq\; m^{*2}_{\pi^{0,\pm}} + \left[\gamma'_{\pi\pi} + 2m^{*2}_{\pi^{0,\pm}}\delta_{\pi\pi}\right]\mathbf{q}^2 + \left[\frac{\gamma'^2_{\pi\pi}}{4} + \alpha'_{\pi\pi} - \delta_{\pi\pi}\left(m^{*2}_{\pi^{0,\pm}} - 2\gamma'_{\pi\pi}\right)\right]\frac{\mathbf{q}^4}{m^{*2}_{\pi^{0,\pm}}} \;. \tag{3.63}$$

The effective masses (m^*_π) of different charged states of pion are found from Eq.(3.63) in the limit $|\mathbf{q}| = 0$.

$$m^{*2}_{\pi^0} \;\simeq\; \frac{m^2_{\pi^0}}{1 \;-\; \Omega^{PV}_{\pi\pi,total}} \;, \tag{3.64a}$$

$$m^{*2}_{\pi^\pm} \;\simeq\; \frac{m^2_{\pi^\pm}}{1 \;-\; (\Omega^{PV}_{\pi\pi,total} \;\pm\; \delta\Omega^{PV}_{\pi\pi,med})} \;. \tag{3.64b}$$

where,

$$\Omega^{PV}_{\pi\pi,total} \;=\; \Omega^{PV}_{\pi\pi,med} + c \;, \tag{3.65a}$$

$$\alpha'_{\pi\pi} \;=\; \frac{a}{1 \;-\; \Omega^{PV}_{\pi\pi,total}} \;, \tag{3.65b}$$

$$\delta_{\pi\pi} = \frac{d}{1 - \Omega^{PV}_{\pi\pi,total}} , \tag{3.65c}$$

$$\gamma'_{\pi\pi} = 1 - \frac{\Omega^{PV}_{\pi\pi,total}}{1 - \Omega^{PV}_{\pi\pi,total}} + \frac{b}{1 - \Omega^{PV}_{\pi\pi,total}} + \frac{c}{1 - \Omega^{PV}_{\pi\pi,total}} . \tag{3.65d}$$

This is to be noted that, if one uses Eq.(3.46) instead of Eq.(3.45); $m^2_{\pi^{0,\pm}}$ and d will be replaced by

$$m^2_{\pi^{0,\pm}} \longrightarrow m^2_{\pi^{0,\pm}} + c' , \qquad \text{and} \qquad d \longrightarrow d' . \tag{3.66}$$

and $\delta_{\pi\pi}$ will vanish. Numerically, as mentioned before, Eq.(3.45) and Eq.(3.46) give results very close to each other.

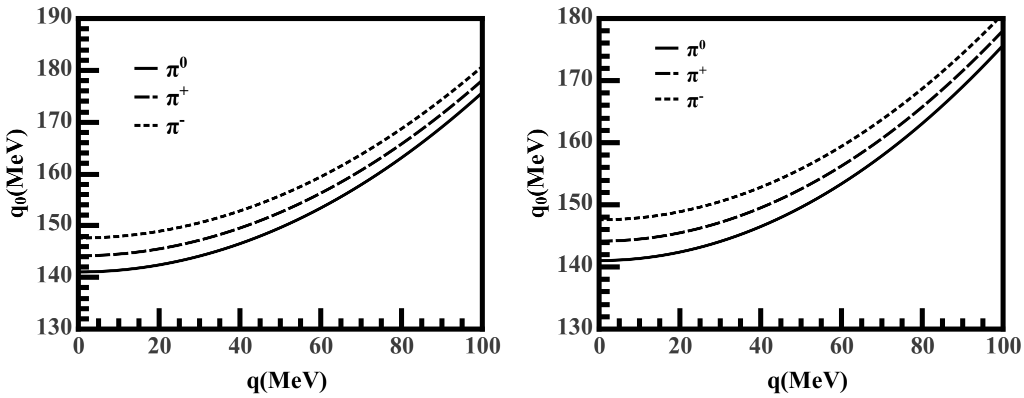

Figure 3.8: *Pion dispersion relations (PV coupling) without (left) and with (right) the effect of Dirac sea at* $\rho = 0.17 fm^{-3}$ *and* $\alpha = 0.2$.

The pion dispersions in ANM for various charge states of pion are presented in Fig.3.8 for PV coupling. Unlike to the PS coupling, the dispersions for π^+ and π^- are found to be clearly distinguishable even with Dirac sea contribution as shown on right figure.

In Fig.3.9 we show results for the density dependence of effective pion masses for various charge states at $\alpha = 0.2$. It is observed that the π^- mass increases in matter while π^+ decreases at higher density. The mass splitting is quite significant even at density $\rho \gtrsim 1.25\rho_0$. The in-medium masses of π^+ and π^0 are found to be equal at

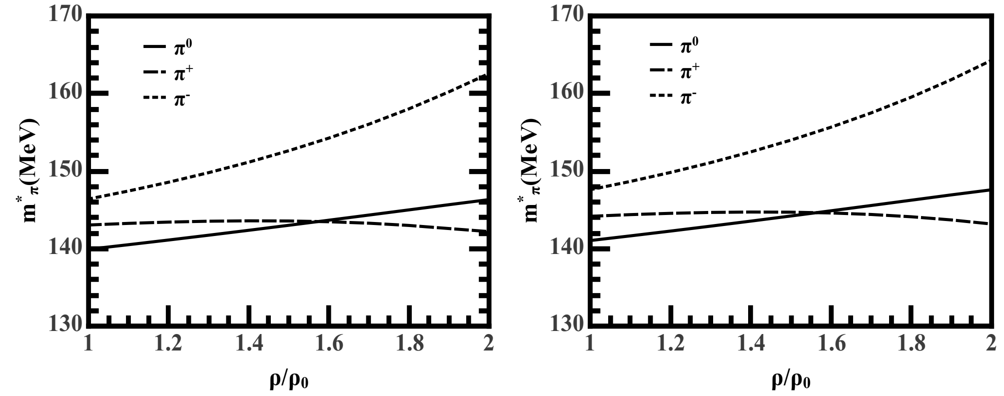

Figure 3.9: *Density dependence of effective masses for PV coupling without Dirac sea (left) and with Dirac sea (right) at* $\alpha = 0.2$.

density $\rho \gtrsim 1.6\rho_0$. In the right figure we present results with vacuum corrections. Evidently the effect of vacuum corrections is found to be small.

We also present results of asymmetry parameter dependence effective masses for different charge states of pion in Fig.3.10 at normal nuclear matter density. The left and right figures present the effective pion masses without and with vacuum correction. It can be observed that the asymmetry parameter dependent pion mass splitting is insensitive to the vacuum correction.

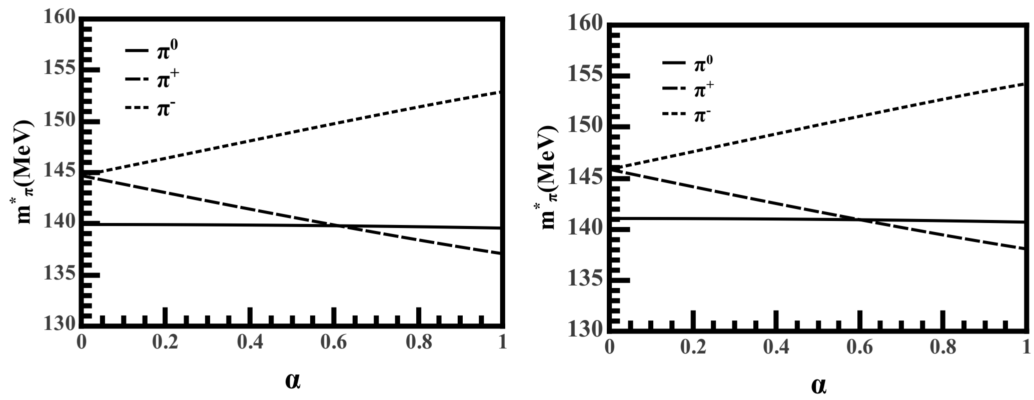

Figure 3.10: *Asymmetry parameter* (α) *dependent effective pion masses (for PV coupling) at* $\rho = 0.17fm^{-3}$, *without (left) and with (right) vacuum correction.*

Table 3.2: Pion mass shifts in Pb-like nuclei.

	Dirac sea	mass shift (MeV) Δm_{π^-}	Δm_{π^0}	Δm_{π^+}
PS	without	139.2	120.7	102.0
	with	17.41	16.8	17.37
PV	without	6.82	4.95	3.47
	with	8.02	6.07	4.6

It should however be mentioned that unlike to the PS coupling, the vacuum correction part for PV coupling is rather small. For loops involving heavy baryons it could be quite high. We refer the readers to [134, 135] for detailed discussion. In present case we have taken only the nucleon-loop in presence of the scalar mean field. Typical values of the pion mass shifts in ANM for PS and PV couplings at $\rho = 0.17 fm^{-3}$ and $\alpha = 0.2$ *i. e.* for Pb-like nuclei are presented in Table3.2.

3.3 Modern Technique

In the previous sections we have discussed pion propagation in ANM using both the PS and PV interaction within the framework of non-chiral model. However, the interactions as represented by Eq.3.1 and Eq.3.6, fail to describe in-medium πN dynamics as shown in [122]. It was also observed that the chirally symmetric model (linear) has also various limitations [122]. For example, as mentioned before, it fails to account for the pion-nucleus dynamics in nuclear matter both in the PS and PV representations. In fact, it gives too strong pion nucleon interaction in matter which cannot be adjusted by fixing the s-wave πN interaction in free space even in PV case. In this context the Dirac vacuum involving baryon loops was found to play a significant role. If one uses the chiral model and breaks the symmetry explicitly, the results are found to be very sensitive to the renormalization scheme [122]. In [136] it was shown that the relativistic chiral models with a light scalar meson appear to provide an economical marriage of successful relativistic MFT and chiral symmetry. It, however, fails to reproduce observed properties of finite nuclei, such as spin-orbit splittings, shell structure, charge densities and surface energies. Since then, there has been series of attempts to construct a model which has the virtue of describing both the properties of nuclear matter and finite nuclei [134, 137–141].

Currently, the non-linear chiral effective field theoretic approach seems to be quite successful in this respect. It might be recalled here, that, in such a framework, the explicit calculation of the Dirac vacuum is not required, rather, on the contrary, here, the short distance dynamics are absorbed into the parameters of the theory adjusted phenomenologically by fitting empirical data [135, 140, 141]. Now we proceed to calculate the effective pion masses in ANM in this approach.

By retaining only the lowest order terms in the pion fields, one obtains the following Lagrangian from the chirally invariant Lagrangian [141]:

$$\begin{aligned}\mathcal{L} &= \bar{\Psi}(i\gamma_\mu\partial^\mu - M)\Psi + \mathrm{g}_s\bar{\Psi}\phi_s\Psi - \mathrm{g}_\omega\bar{\Psi}\gamma_\mu\Phi^\mu_\omega\Psi - \frac{\mathrm{g}_A}{f_\pi}\bar{\Psi}\gamma_5\gamma_\mu\partial^\mu\vec{\tau}\cdot\vec{\Phi}_\pi\Psi \\ &+ \frac{1}{2}\left(\partial_\mu\Phi_s\partial^\mu\Phi_s - m_s^2\Phi_s^2\right) + \frac{1}{2}\left(\partial_\mu\vec{\Phi}_\pi\cdot\partial^\mu\vec{\Phi}_\pi - m_\pi^2\vec{\Phi}^2\right) + \frac{1}{2}m_\omega^2\Phi_{\omega\mu}\Phi^\mu_\omega \\ &- \frac{1}{4}G_{\mu\nu}G^{\mu\nu} + \mathcal{L}_{NL} + \delta\mathcal{L}. \end{aligned} \tag{3.67}$$

The terms $\mathcal{L}_{NL}$ and $\delta\mathcal{L}$ contain, respectively the nonlinear terms of the meson sector and all of the counter terms. The explicit expressions for $\mathcal{L}_{NL}$ and $\delta\mathcal{L}$ can be found in [141]. It is to be noted that the meson self-energy can be found by differentiating the energy density [141] at the two-loop level with respect to the meson propagator as indicated in Fig 3.11. One may therefore, identify the FF, FD and DD parts of the self-energy with the vacuum-fluctuation (VF), Lamb-shift(LS) and exchange (EX) contributions to the self-energy respectively. The VF and LS terms are related to the short-range physics while EX part is related to the long-range physics. The detailed discussion about this short and long distance separation can be found in [135,140,141]. The diverging FF part of the self-energy and LS can be expressed as a sum of terms which already exists in the effective field theoretical Lagrangian and can

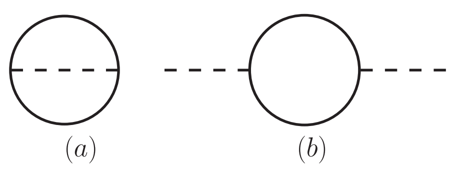

Figure 3.11: *Two-loop self-energy diagram.*

be absorbed into the counter terms. The short distance physics, as shown in [141], while calculating exchange energies, are either removed by field redefinitions or the coefficients are determined by fitting with the empirical data. The long-range part is computed explicitly that produce modest corrections to the nuclear binding energy curve. This can be compensated by a small adjustment of the coupling parameters. Recently in Ref. [141] the exchange energy contributions of pion has been calculated

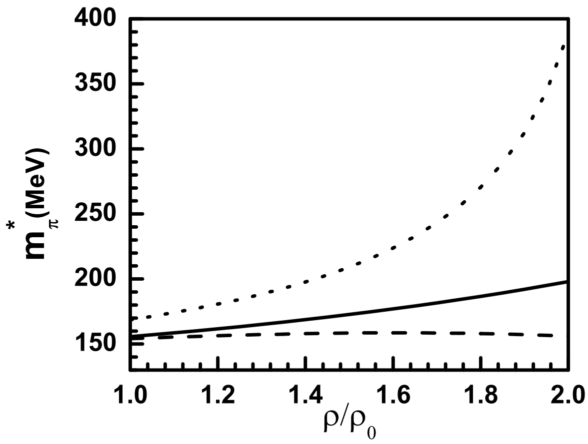

Figure 3.12: *Pion mass in medium at different densities and* $\alpha = 0.2$.

within this theoretical framework. We adopt the same parameter set as designated by **MOA** in [141] to calculate the π self-energy explicitly. The corresponding results are presented in Fig.3.12. Here we simply depict the final results as the expressions, at this order, for the pion self-energy and density dependent masses of π^0 and $\pi^\pm$ remain same as those of Eq.3.64b except for the coupling parameters. Quantitatively, it is found that, for the lower density, *i.e* $\rho \sim \rho_0$, the effective masses for π^- (dotted curve), π^0 (solid curve) and π^+ (dashed curve) states are comparable with that of PV coupling (Fig.3.9), while at higher density the mass splitting is significantly enhanced. The charged states, *i.e.* $\pi^\pm$ show stronger density dependence compared to PV coupling. We also observe that the density dependence of π^0 is rather weak.

Chapter 4

Mixing of Hadrons in ANM

Mixing of hadrons, as we have mentioned in the introduction, is an effect of symmetry violation of the strong interaction. Neutral mesons with the same spin-parity but of different isospins can mix at the fundamental level† due to the finite mass difference between up (u) and (d) quark [142]. At the hadronic level, neutron (n) - proton (p) mass difference *i.e.* $M_n \neq M_p$ causes various isospin pure resonant states like π-η, ρ-ω etc. to mix without violating any conservation principles dictated by other symmetries. On the other hand, if the ground state contains unequal number of neutrons and protons *i.e.* $\rho_n \neq \rho_p$, ground state induced mixing takes place even in the limit $M_n = M_p$ [143].

Such matter induced mixing was first studied in Ref. [143] and was subsequently studied in Refs. [129,144–147]. The calculations are mostly confined to the time-like region where the main motivation is to investigate the role of such matter induced mixing on the dilepton spectrum observed in heavy ion collisions, pion form factor. It is also to be noted that such mixing amplitudes, in asymmetric nuclear matter (ANM), have non-zero contribution even if the quark or nucleon masses are taken to be equal. Interestingly, such mixing, as we shall show in the next chapter, can modify the nucleon-nucleon interaction considerably giving rise to charge symmetry violating (CSV) effects in various observables where medium corrections are relevant.

Here we present the study of π-η and ρ-ω mixing in ANM based on a purely hadronic model. Such hadronic model has some added advantage. All the parameters like masses, coupling constants etc. are well known in the hadronic description. Furthermore, hadronic models are relatively successful for describing various nuclear

† *see* Appendix A

properties. The main assumption of our calculation is that the mixing is generated by the $N\bar{N}$-loops and the mixing amplitude is driven by the difference between proton and neutron loop contributions as shown in Fig.4.1. We, in this chapter, neglect medium modification of the nuclear mass due to scalar and vector mean field (MF) and, consider both pseudoscalar (PS) and pseudovector (PV) representations for π-η mixing.

To understand the origin of relative sign between p and n loops, we invoke the meson-nucleon interaction Lagrangians of one-boson exchange (OBE) model where the NN interaction is generated via the exchange of various mesons. One may write the general form of isovector (i) meson-nucleon interaction and isoscalar (j) meson-nucleon interaction explicitly as

$$\mathcal{L}_{i\ NN} = \bar{\Psi}_p \Gamma_i \Phi_i \Psi_p - \bar{\Psi}_n \Gamma_i \Phi_i \Psi_n, \tag{4.1a}$$

$$\mathcal{L}_{j\ NN} = \bar{\Psi}_p \Gamma_j \Phi_j \Psi_p + \bar{\Psi}_n \Gamma_j \Phi_j \Psi_n, \tag{4.1b}$$

where Ψ_p (Ψ_n) is the proton (neutron) wave function, Φ_i (orΦ_j) represents the meson field and Γ_i (orΓ_j) denotes the meson-nucleon vertex factors. From the above Eqs.(4.1a) and (4.1b), it is clear that the isovector mesons like π or ρ couple to p and n with opposite sign while the isoscalar mesons like η or ω, couple to p and n with the same sign. This brings in a relative sign between the p and n loops.

$$\Pi_{ij,total}(q^2) = \Pi^{(p)}_{ij,total}(q^2) - \Pi^{(n)}_{ij,total}(q^2), \tag{4.2}$$

where $\Pi^{(p)}_{ij,total}(q^2)$ or $\Pi^{(n)}_{ij,total}(q^2)$ is the contribution of total mixing self-energy due to p-loop or n-loop.

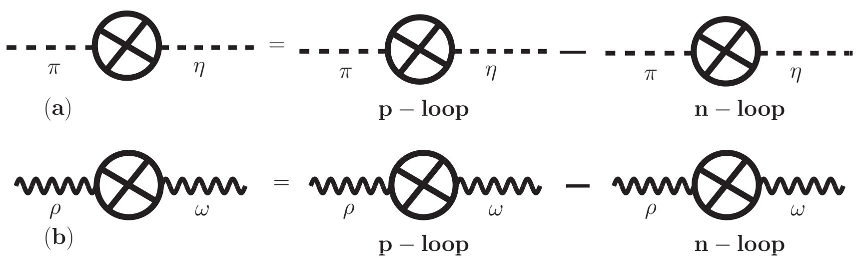

Figure 4.1: *The mixing amplitude is generated by the difference between proton and neutron loops. The crossed blob represents the CSV piece i.e. the mixing of mesons.*

The one-loop contribution to the mixing self-energy reads

$$i\Pi^{(N)}_{ij,total}(q^2) = \int \frac{d^4k}{(2\pi)^4} \mathrm{Tr}\left[\, \Gamma_i(q) G_N(k) \Gamma_j(-q) G_N(k+q) \,\right], \tag{4.3}$$

where the subscript N stands for nucleon index (*i.e.* $N = p$ or n), $k = (k_0, \mathbf{k})$ and $q = (q_0, \mathbf{q})$ denote the four momenta of the nucleon and meson, respectively. Here G_N denotes in-medium nucleon propagator instead of G^*_N as we use the free nucleon mass M_N instead of mean field modified nucleon mass M^*_N. The nucleon propagator G_N consists of a free (or vacuum) part G^F_N and a density dependent (or medium) part G^D_N [45]:

$$G^F_N(k) = \frac{\not{k} + M_N}{k^2 - M_N^2 + i\zeta}, \tag{4.4a}$$

$$G^D_N(k) = \frac{i\pi}{E_N} (\not{k} + M_N)\, \delta(k_0 - E_N) \theta(k_N - |\mathbf{k}|), \tag{4.4b}$$

where $E_N = \sqrt{M_N^2 + k_N^2}$ is the energy of a nucleon with the Fermi momentum k_N. Substituting the full in-medium nucleon propagator like in previous chapter, $G_N = G^F_N + G^D_N$, in Eq.(4.3), one may identify a vacuum part, $\Pi^{(N)}_{ij,vac}(q^2)$ which involves $G^F_N G^F_N$ and a density dependent part, $\Pi^{(N)}_{ij,med}(q^2)$ with the combination of $G^F_N G^D_N + G^D_N G^F_N + G^D_N G^D_N$. In the present study, the term proportional to $G^D_N G^D_N$ does not contribute as it vanishes for low energy excitation [11]. Thus the Eq.(4.3) reduces to

$$\Pi^{(N)}_{ij,total}(q^2) = \Pi^{(N)}_{ij,vac}(q^2) + \Pi^{(N)}_{ij,med}(q^2). \tag{4.5}$$

Now explicitly the vacuum and density dependent parts read, respectively,

$$i\Pi^{(N)}_{ij,vac}(q^2) = \int \frac{d^4k}{(2\pi)^4} \mathrm{Tr}\left[\, \Gamma_i(q) G^F_N(k) \Gamma_j(-q) G^F_N(k+q) \,\right], \tag{4.6}$$

and

$$\begin{aligned} i\Pi^{(N)}_{ij,med}(q^2) &= \int \frac{d^4k}{(2\pi)^4} \mathrm{Tr}\left[\, \Gamma_i(q) G^F_N(k) \Gamma_j(-q) G^D_N(k+q) \,\right] \\ &+ \int \frac{d^4k}{(2\pi)^4} \mathrm{Tr}\left[\, \Gamma_i(q) G^D_N(k) \Gamma_{ij}(-q) G^F_N(k+q) \,\right]. \end{aligned} \tag{4.7}$$

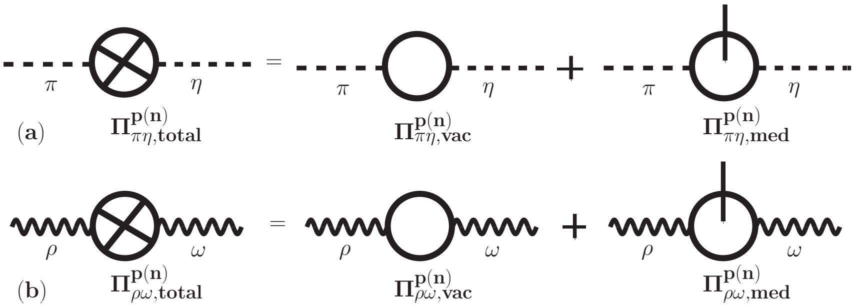

Figure 4.2: Total mixing amplitude contains a vacuum part and a medium part.

4.1 π-η mixing : PS coupling

In this section we discuss π-η mixing considering the pseudo scalar coupling (PS) of mesons to nucleons to describe πNN and ηNN interactions which are represented by the following Lagrangians:

$$\mathcal{L}^{PS}_{\pi NN} = -ig_\pi \bar{\Psi}\gamma_5 \tau \cdot \mathbf{\Phi}_\pi \Psi, \tag{4.8a}$$

$$\mathcal{L}^{PS}_{\eta NN} = -ig_\eta \bar{\Psi}\gamma_5 \Phi_\eta \Psi, \tag{4.8b}$$

where Ψ and Φ represent the nucleon and meson fields, respectively, and g denotes the meson-nucleon coupling constants. For PS coupling the vertex factors are $\Gamma_\pi = -ig_\pi\gamma_5$ and $\Gamma_\eta = -ig_\eta\gamma_5$.

After calculating the trace, one obtains from Eqs.(4.6) and (4.7), the vacuum and density-dependent parts of π-η mixing self-energy given by

$$\Pi^{(N)}_{\pi\eta,vac}(q^2) = 4ig_\pi g_\eta \int \frac{d^4k}{(2\pi)^4}\left[\frac{M_N^2 - k\cdot(k+q)}{(k^2-M_N^2)((k+q)^2-M_N^2)}\right] \tag{4.9}$$

and

$$\Pi^{(N)}_{\pi\eta,med}(q^2) = -8g_\pi g_\eta \int_0^1 \frac{d^3\mathbf{k}}{(2\pi)^3 E_N}\left[\frac{(k\cdot q)^2}{q^4 - 4(k\cdot q)^2}\right]\theta(k_N - |\mathbf{k}|). \tag{4.10}$$

Eq.(4.10) is obtained after the k_0 integration. From the dimensional counting it is found that the integral of Eq.(4.9) is divergent. We use dimensional regularization

[130–132] to isolate the singularities in Eq.(4.9) which reduces to [148]:

$$\begin{aligned}\Pi^{(N)}_{\pi\eta,vac}(q^2) &= \frac{g_\pi g_\eta}{4\pi^2}\left[\frac{q^2}{3}+\left(M_N^2-\frac{q^2}{2}\right)\left(1+\frac{1}{\epsilon}-\gamma_E+\ln(4\pi\mu^2)\right)\right.\\ &- \left.\int_0^1 dx[M_N^2-3q^2x(1-x)]\ln(M_N^2-q^2x(1-x))\right]. \quad (4.11)\end{aligned}$$

In Eq.(4.11) μ is an arbitrary scale parameter, γ_E is the Euler-Mascheroni constant and $\epsilon = 2 - D/2$, where D stands for the dimension of the integral. Notice, ϵ in Eq.(4.11) contains the singularity and it diverges as $D \to 4$. The divergences of Eq.(4.11) can be removed by adding appropriate counter terms [122]. However, in the present calculation we use subtraction method to remove the these divergences.

It is clear from Eq.(4.11) that unlike ρ-ω mixing amplitude, as we shall see in the subsection 4.3, the singularities cannot be removed completely by simply subtracting the neutron loop contribution from the proton loop contribution. This is because of the singular term proportional to the mass term *i.e.* M_N/ϵ. But one can eliminate this singular term by subtracting $\Pi^{(N)}_{\pi\eta,vac}(q^2=0)$ from $\Pi^{(N)}_{\pi\eta,vac}(q^2)$ which yields

$$\begin{aligned}\hat{\Pi}^{(N)}_{\pi\eta,vac}(q^2) &= \Pi^{(N)}_{\pi\eta,vac}(q^2)-\Pi^{(N)}_{\pi\eta,vac}(q^2=0)\\ &= \frac{g_\pi g_\eta}{4\pi^2}\left[\frac{q^2}{3}+M_N^2\ln M_N^2-\frac{q^2}{2}\left(1+\frac{1}{\epsilon}-\gamma_E+\ln(4\pi\mu^2)\right)\right.\\ &- \left.\int_0^1 dx[M_N^2-3q^2x(1-x)]\ln\left(M_N^2-q^2x(1-x)\right)\right]. \quad (4.12)\end{aligned}$$

Note that $\hat{\Pi}^{(N)}_{\pi\eta,vac}(q^2)$, however, is not finite but the divergent part proportional to the mass term has been removed. Now one can easily obtain finite π-η mixing amplitude in vacuum by subtracting $\hat{\Pi}^{(n)}_{\pi\eta,vac}(q^2)$ from $\hat{\Pi}^{(p)}_{\pi\eta,vac}(q^2)$.

$$\begin{aligned}\Pi^{PS}_{\pi\eta,vac}(q^2) &= \frac{g_\pi g_\eta}{4\pi^2}\left[q^2\ln\left(\frac{M_p}{M_n}\right)+q\sqrt{4M_p^2-q^2}\tan^{-1}\left(\frac{q}{\sqrt{4M_p^2-q^2}}\right)\right.\\ &- \left.q\sqrt{4M_n^2-q^2}\tan^{-1}\left(\frac{q}{\sqrt{4M_n^2-q^2}}\right)\right]. \quad (4.13)\end{aligned}$$

Eq.(4.13) represents the q^2 dependent vacuum part of π-η mixing amplitude which has no divergences and is finite. We obtain $\Pi^{PS}_{vac}(q^2=m_\eta^2) = -1197$ MeV^{-2}, while experimentally it is found that $\Pi^{PS}_{\pi\eta,vac}(q^2=m_\eta^2) = -4200$ MeV^{-2} [148].

Substituting $q_0 = 0$ in Eq.(4.13) to obtain three momentum, $\mathbf{q}$, dependent mixing amplitude $\Pi^{PS}_{\pi\eta,vac}(\mathbf{q}^2)$. We have expanded the mixing amplitude $\Pi^{PS}_{\pi\eta,vac}(\mathbf{q}^2)$ in terms of $\mathbf{q}^2/M_N^2$ and keeping the lowest order we obtain

$$\Pi^{PS}_{\pi\eta,vac}(\mathbf{q}^2) \simeq -a_1\mathbf{q}^2, \tag{4.14}$$

where

$$a_1 = \frac{g_\pi g_\eta}{4\pi^2}\ln\left(\frac{M_p}{M_n}\right) . \tag{4.15}$$

If $M_p = M_n$, mixing amplitude in vacuum *i.e.* $\Pi^{PS}_{\pi\eta,vac}(\mathbf{q}^2)$ vanishes. Now we calculate the density dependent part of the π-η mixing self-energy. Substituting $E_N \simeq M_N$ and $q_0 = 0$, and carried out the integration Eq.(4.10) reads

$$\Pi^{(N)}_{\pi\eta,med}(\mathbf{q}^2) = \frac{g_\pi g_\eta}{\pi^2 M_N}\left[\frac{k_N^3}{3} - \frac{\mathbf{q}^2 k_N}{8} - \frac{\mathbf{q}}{8}\left(k_N^2 - \frac{\mathbf{q}^2}{4}\right)\ln\left(\frac{\mathbf{q}+2k_N}{\mathbf{q}-2k_N}\right)\right] . \tag{4.16}$$

The above Eq.(4.16) represents three momentum dependent medium part of the π-η mixing self-energy. After suitable expansion Eq.(4.16)in terms of $\frac{\mathbf{q}}{k_N}$, the mixing amplitude, as mentioned earlier, generated by the difference between contributions from the proton and neutron loops reduces to

$$\Pi^{PS}_{\pi\eta,med}(\mathbf{q}^2) \simeq a_0' - a_1'\mathbf{q}^2, \tag{4.17}$$

where the leading order contribution has been considered and

$$a_0' = \frac{g_\pi g_\eta}{3\pi^2}\left(\frac{k_p^3}{M_p} - \frac{k_n^3}{M_n}\right), \tag{4.18a}$$

$$a_1' = \frac{g_\pi g_\eta}{4\pi^2}\left(\frac{k_p}{M_p} - \frac{k_n}{M_n}\right). \tag{4.18b}$$

From Eq.(4.18), it is clear that the medium part of π-η mixing amplitude given in Eq.(4.17) does not vanish in ANM ($k_p \neq k_n$) even if $M_p = M_n$, while the vacuum part vanishes as evident from Eqs.(4.14) and (4.15).

4.2 π-η mixing : PV coupling

In this section we consider pseudo vector (PV) coupling for meson-nucleon interaction [45, 122]. The pseudo vector representation of πNN and ηNN interactions are given by the following effective Lagrangians:

$$\mathcal{L}^{PV}_{\pi NN} = -\frac{g_\pi}{2M_N}\bar{\Psi}\gamma_5\gamma^\mu\partial_\mu\tau\cdot\mathbf{\Phi}_\pi\Psi, \tag{4.19a}$$

$$\mathcal{L}^{PV}_{\eta NN} = -\frac{g_\eta}{2M_N}\bar{\Psi}\gamma_5\gamma^\mu\partial_\mu\Phi_\eta\Psi, \tag{4.19b}$$

where Ψ, $\mathbf{\Phi}$ and g have been defined in the previous subsection. τ is the isospin vector. The factor $\frac{f_\pi}{m_\pi}$ $(\frac{f_\eta}{m_\eta})$ has been replaced by $\frac{g_\pi}{2M_N}$ $(\frac{g_\eta}{2M_N})$. The vertex factors are $\Gamma_\pi = ig_\pi\gamma_5\gamma^\mu q_\mu/2M_N$ and $\Gamma_\eta = ig_\eta\gamma_5\gamma^\mu q_\mu/2M_N$. The vacuum part and density dependent part of π-η mixing self-energy for PV coupling are given by

$$\begin{aligned}\Pi^{(N)}_{\pi\eta,vac}(q^2) &= 4i\left(\frac{g_\pi}{2M_N}\right)\left(\frac{g_\eta}{2M_N}\right)\int\frac{d^4k}{(2\pi)^4} \\ &\times \left[\frac{q^2(M_N^2-k\cdot(k+q))-2q\cdot(k+q)(k\cdot q)}{(k^2-M_N^2)((k+q)^2-M_N^2)}\right].\end{aligned} \tag{4.20}$$

and

$$\Pi^{(N)}_{\pi\eta,med}(q^2) = -8\left(\frac{g_\pi}{2M_N}\right)\left(\frac{g_\eta}{2M_N}\right)\int\frac{d^3\mathbf{k}}{(2\pi)^3E_N}\left[\frac{q^2\ M_N^2}{q^4-4(k\cdot q)^2}\right]\theta(k_N-|\mathbf{q}|). \tag{4.21}$$

Note that the integral Eq.(4.21) is divergent. We use dimensional regularization, similar to PS coupling, to isolate the singularities.

$$\Pi^{(N)}_{\pi\eta,vac}(q^2) = \frac{g_\pi g_\eta}{8\pi^2}\left[-\frac{1}{\epsilon}+\gamma_E-\ln(4\pi\mu^2)+\int_0^1 dx\ln(M_N^2-q^2x(1-x))\right]q^2, \tag{4.22}$$

where ϵ, μ and γ_E have been discussed earlier. It is important to note that unlike PS coupling, there is no divergent term in Eq.(4.22) proportional to the nuclear mass M_N. Therefore, like ρ-ω mixing [149], simple subtraction of the n-loop contribution from the p-loop contribution, will remove all the divergent parts yielding $\Pi^{(N)}_{\pi\eta,vac}(q^2)$ finite which reads

$$\begin{aligned}\Pi^{PV}_{\pi\eta,vac}(q^2) &= \frac{g_\pi g_\eta}{4\pi^2}\left[q^2\ln\left(\frac{M_p}{M_n}\right)+q\sqrt{4M_p^2-q^2}\tan^{-1}\left(\frac{q}{\sqrt{4M_p^2-q^2}}\right)\right. \\ &- \left. q\sqrt{4M_n^2-q^2}\tan^{-1}\left(\frac{q}{\sqrt{4M_n^2-q^2}}\right)\right].\end{aligned} \tag{4.23}$$

It is to be noted from Eq.(4.23) and Eq.(4.13), the vacuum parts of the mixing amplitude for both PS and PV couplings are identical at the one-loop level. Similar to the PS coupling, the leading order vacuum contribution of π-η mixing amplitude is obtained

$$\Pi^{PV}_{\pi\eta,vac}(\mathbf{q}^2) \simeq -a_1\mathbf{q}^2. \tag{4.24}$$

The three momentum dependent medium part of π-η mixing self-energy can now be obtained from Eq.(4.21) substituting $E_N \simeq M_N$ and $q_0 = 0$.

$$\Pi^{(N)}_{\pi\eta,med}(\mathbf{q}^2) = -\frac{\mathrm{g}_\pi \mathrm{g}_\eta}{8\pi^2 M_N}\left[\mathbf{q}^2 k_N + \mathbf{q}\left(k_N^2 - \frac{\mathbf{q}^2}{4}\right)\ln\left(\frac{\mathbf{q}+2k_N}{\mathbf{q}-2k_N}\right)\right]. \tag{4.25}$$

Similarly, the leading order medium contribution of the mixing amplitude reads

$$\Pi^{PV}_{\pi\eta,med}(\mathbf{q}^2) \simeq -a_1'\mathbf{q}^2\ . \tag{4.26}$$

Notice, the leading order density dependent mixing amplitude in PV coupling differs with that of PS coupling only by the term a_0' given by Eq.(4.18a). Thus

$$\Pi^{PS}_{\pi\eta,total}(\mathbf{q}^2) = a_0' + \Pi^{PV}_{\pi\eta,total}(\mathbf{q}^2)\ . \tag{4.27}$$

4.3 ρ-ω mixing

In this section we revisit the problem of ρ-ω mixing driven by the asymmetry of the nuclear matter. To calculate the ρ-ω mixing amplitude we use the following meson-nucleon interaction Lagrangians:

$$\mathcal{L}_{\omega NN} = \mathrm{g}_\omega \bar{\Psi}\gamma_\mu \Phi^\mu_\omega \Psi \tag{4.28a}$$

$$\mathcal{L}_{\rho NN} = \mathrm{g}_\rho \bar{\Psi}\left[\gamma_\mu + \frac{C_\rho}{2M}\sigma_{\mu\nu}\partial^\mu\right]\tau\cdot\mathbf{\Phi}^\nu_\rho \Psi \tag{4.28b}$$

where Ψ and Φ denote nucleon and meson fields, respectively, and $C_\rho = \mathrm{f}_\rho/\mathrm{g}_\rho$ is the ratio of vector to tensor couplings. The tensor coupling of ω is not included in the present calculation because it is negligible in comparison to the vector coupling. All the parameters used in the present calculation are taken from those given by the Bonn group [80]. In this case the vertex factors are:

$$\Gamma^{\mu}_{\omega} = \mathrm{g}_{\omega}\gamma^{\mu} \quad \text{and} \quad \Gamma^{\mu}_{\rho} = \mathrm{g}_{\rho}\left[\gamma^{\mu} - \frac{C_{\rho}}{2M} i\sigma_{\mu\nu}q^{\nu}\right]. \tag{4.29}$$

Once the interaction Lagrangians are given, one may proceed to to calculate the polarization tensor of ρ-ω mixing. The total polarization tensor,

$$\Pi^{\mu\nu,(N)}_{\rho\omega,total}(q^2) = \Pi^{\mu\nu,(N)}_{\rho\omega,vac}(q^2) + \Pi^{\mu\nu,(N)}_{\rho\omega,med}(q^2) \tag{4.30}$$

where $\Pi^{\mu\nu,(N)}_{\rho\omega,vac}(q^2)$ and $\Pi^{\mu\nu,(N)}_{\rho\omega,med}(q^2)$ represent the vacuum and density dependent parts of the polarization tensor of ρ-ω mixing.

$$i\Pi^{\mu\nu,(N)}_{\rho\omega,vac}(q^2) = \int \frac{d^4k}{(2\pi)^4} \mathrm{Tr}\left[\Gamma^{\mu}_{\omega}(q)G^F_N(k)\Gamma^{\nu}_{\rho}(-q)G^F_N(k+q)\right], \tag{4.31}$$

and

$$\begin{aligned} i\Pi^{\mu\nu(N)}_{\rho\omega,med}(q^2) &= \int \frac{d^4k}{(2\pi)^4} \mathrm{Tr}\left[\Gamma^{\mu}_{\omega}(q)G^F_N(k)\Gamma^{\nu}_{\rho}(-q)G^D_N(k+q)\right] \\ &+ \int \frac{d^4k}{(2\pi)^4} \mathrm{Tr}\left[\Gamma^{\mu}_{\omega}(q)G^D_N(k)\Gamma^{\nu}_{\rho}(-q)G^F_N(k+q)\right]. \end{aligned} \tag{4.32}$$

Since, ρ and ω being the vector mesons, their propagation through matter should have longitudinal (L) and transverse (T) components depending upon whether their spins are parallel or perpendicular to the direction of propagation. However, in the static limit *i.e.* $\mathbf{q} = 0$, both the longitudinal and transverse components coincide. We choose z-axis as the direction of propagation so that one may define the longitudinal and transverse polarization:

$$\Pi^{L,(N)}_{\rho\omega,total} = \Pi^{33,(N)}_{\rho\omega,total} - \Pi^{00,(N)}_{\rho\omega,total} \tag{4.33a}$$

$$\Pi^{T,(N)}_{\rho\omega,total} = \Pi^{11,(N)}_{\rho\omega,total} = \Pi^{22,(N)}_{\rho\omega,total}. \tag{4.33b}$$

Note that the polarization tensor $\Pi^{\mu\nu(N)}_{\rho\omega,total}(q^2)$ can be expressed as the sum of longitudinal component, $\Pi^{L,(N)}_{\rho\omega,total}(q^2)$, and transverse component, $\Pi^{T,(N)}_{\rho\omega,total}(q^2)$:

$$\Pi^{\mu\nu,(N)}_{\rho\omega,total}(q^2) = \Pi^{L,(N)}_{\rho\omega,total}(q^2)A^{\mu\nu} + \Pi^{T,(N)}_{\rho\omega,total}(q^2)B^{\mu\nu}, \tag{4.34}$$

where $A^{\mu\nu}$ and $B^{\mu\nu}$ are the longitudinal and transverse projection operators [150]. We, in the present calculation, use the average of longitudinal and transverse components of the polarization tensor instead of $\Pi^{L,(N)}_{\rho\omega,total}$ and $\Pi^{T,(N)}_{\rho\omega,total}$. The average mixing amplitude is denoted by

$$\begin{aligned}\bar{\Pi}^{(N)}_{\rho,\omega,total}(q^2) &= \frac{1}{3}\left[\Pi^{L,(N)}_{\rho\omega,total}(q^2) + 2\Pi^{T,(N)}_{\rho\omega,total}(q^2)\right] \\ &= \bar{\Pi}^{(N)}_{\rho\omega,vac}(q^2) + \bar{\Pi}^{(N)}_{\rho\omega,med}(q^2).\end{aligned} \tag{4.35}$$

In Eq.(4.35), $\bar{\Pi}^{(N)}_{\rho\omega,vac}(q^2)$ and $\bar{\Pi}^{(N)}_{\rho\omega,med}(q^2)$ denote the average ρ-ω mixing amplitudes of vacuum and density dependent parts, respectively.

Now Eqs.(4.31) and (4.32) can be used to calculate various components of the polarization tensor. The polarization tensor contains two parts one corresponding to vector-vector (vv) and other the tensor-vector (tv) interactions. This is because of the vertex factors shown in Eq.(4.29). Hence the polarization tensor reads

$$\Pi^{\mu\nu,(N)}_{\rho\omega,vac}(q^2) = \left[\Pi^{vv,(N)}_{\rho\omega,vac}(q^2) + \Pi^{tv,(N)}_{\rho\omega,vac}(q^2)\right] Q^{\mu\nu} \ , \tag{4.36a}$$

$$\Pi^{\mu\nu,(N)}_{\rho\omega,med}(q^2) = \left[\Pi^{\mu\nu,vv(N)}_{\rho\omega,med}(q^2) + \Pi^{\mu\nu,tv(N)}_{\rho\omega,med}(q^2)\right] . \tag{4.36b}$$

After evaluating the trace, one may find the vv and tv terms:

$$\Pi^{vv,(N)}_{\rho\omega,vac}(q^2) = 8i\mathrm{g}_\rho \mathrm{g}_\omega \int_0^1 dx \int \frac{d^4k}{(2\pi)^4}\left[\frac{q^2\ x(1-x)}{(k^2 - M_N^2 + q^2\ x(1-x))^2}\right] , \tag{4.37a}$$

$$\Pi^{tv,(N)}_{\rho\omega,vac}(q^2) = 4i\mathrm{g}_\rho \mathrm{g}_\omega \left(\frac{C_\rho}{2M}\right)\int_0^1 dx \int \frac{d^4k}{(2\pi)^4}\left[\frac{q^2 M_N}{(k^2 - M_N^2 + q^2\ x(1-x))^2}\right] , \tag{4.37b}$$

and

$$\Pi^{\mu\nu,vv(N)}_{\rho\omega,med}(q^2) = 16\mathrm{g}_\rho \mathrm{g}_\omega \int \frac{d^3k}{(2\pi)^3 2E_N}\left[\frac{q^2 K^{\mu\nu} - (q\cdot k)^2 Q^{\mu\nu}}{q^4 - 4(q\cdot k)^2}\right]\theta(k_N - |\mathbf{k}|) , \tag{4.38a}$$

$$\Pi^{\mu\nu,tv(N)}_{\rho\omega,med}(q^2) = 4\rho\omega C_\rho \int \frac{d^3k}{(2\pi)^3 2E_N}\left[\frac{q^4 Q^{\mu\nu}}{q^4 - 4(q\cdot k)^2}\right]\theta(k_N - |\mathbf{k}|) , \tag{4.38b}$$

To derive Eqs.(4.37a) and (4.37b) we use Feynman parametrization. Here

$$Q^{\mu\nu} = (-g^{\mu\nu} + \frac{q^\mu q^\nu}{q^2}) , \tag{4.39a}$$

$$K^{\mu\nu} = \left(k^\mu - (q\cdot k)\frac{q^\mu}{q^2}\right)\left(k^\nu - (q\cdot k)\frac{q^\nu}{q^2}\right) . \tag{4.39b}$$

yielding,

$$q_\mu Q^{\mu\nu} = q_\nu Q^{\mu\nu} = 0 \quad \text{and} \quad q_\mu K^{\mu\nu} = q_\nu K^{\mu\nu} = 0 . \tag{4.40}$$

It is clear from Eqs.(4.37)-(4.38), both $\Pi^{\mu\nu,(N)}_{\rho\omega,vac}(q^2)$ and $\Pi^{\mu\nu,(N)}_{\rho\omega,med}(q^2)$ obey the current conservation:

$$q_\mu\, \Pi^{\mu\nu,(N)}_{\rho\omega,vac}(q^2) = q_\nu\, \Pi^{\mu\nu,(N)}_{\rho\omega,vac}(q^2) = 0, \tag{4.41a}$$
$$q_\mu\, \Pi^{\mu\nu,(N)}_{\rho\omega,med}(q^2) = q_\nu\, \Pi^{\mu\nu,(N)}_{\rho\omega,med}(q^2) = 0, \tag{4.41b}$$

The dimensional counting shows that both the integrals given in Eqs.(4.37a) and (4.37b) are ultraviolet divergent and dimensional regularization [130–132] is used to isolate the divergent parts which are found to be

$$\Pi^{vv,(N)}_{\rho\omega,vac}(q^2) = \frac{g_\rho g_\omega}{2\pi^2}\left[\frac{1}{6\epsilon} - \frac{\gamma_E}{6} - \int_0^1 dx(1-x)x\ln\left(\frac{M_N^2 - x(1-x)q^2}{\Lambda^2}\right)\right] q^2, \tag{4.42a}$$
$$\Pi^{tv,(N)}_{\rho\omega,vac}(q^2) = \frac{g_\rho g_\omega}{8\pi^2}C_\rho\left[\frac{1}{\epsilon} - \gamma_E - \int_0^1 dx\ln\left(\frac{M_N^2 - x(1-x)q^2}{\Lambda^2}\right)\right] q^2, \tag{4.42b}$$

where Λ is an arbitrary renormalization constant; γ_E is the Euler-Mascheroni constant. $\epsilon = 2 - D/2$ contains the singularity; $\epsilon \to 0$ as $D \to 4$. Since the mixing amplitude is generated by the difference between the proton and neutron loop contributions, the divergent parts cancel out yielding the vv and tv parts finite.

$$\begin{aligned}\Pi^{vv}_{\rho\omega,vac}(q^2) &= \Pi^{vv(p)}_{\rho\omega,vac}(q^2) - \Pi^{vv(n)}_{\rho\omega,vac}(q^2) \\ &= \frac{g_\rho g_\omega}{2\pi^2}\int_0^1 dx(1-x)x\ln\left(\frac{M_p^2 - x(1-x)q^2}{M_n^2 - x(1-x)q^2}\right) q^2,\end{aligned} \tag{4.43a}$$

$$\begin{aligned}\Pi^{tv}_{\rho\omega,vac}(q^2) &= \Pi^{tv(p)}_{\rho\omega,vac}(q^2) - \Pi^{tv(n)}_{\rho\omega,vac}(q^2) \\ &= \frac{g_\rho g_\omega C_\rho}{8\pi^2}\int_0^1 dx\ln\left(\frac{M_p^2 - x(1-x)q^2}{M_n^2 - x(1-x)q^2}\right) q^2,\end{aligned} \tag{4.43b}$$

Thus the full vacuum part of the polarization tensor reduces to

$$\Pi^{\mu\nu}_{\rho\omega,vac}(q^2) = Q^{\mu\nu}\left[\Pi^{vv}_{\rho\omega,vac}(q^2) + \Pi^{tv}_{\rho\omega,vac}(q^2)\right] = Q^{\mu\nu}\Pi_{\rho\omega,vac}(q^2), \tag{4.44}$$

where

$$\Pi_{\rho\omega,vac}(q^2) = \frac{g_\rho g_\omega}{2\pi^2} q^2 \int_0^1 dx \, \left((1-x)x + \frac{C_\rho}{4}\right) \ln\left(\frac{M_p^2 - x(1-x)q^2}{M_n^2 - x(1-x)q^2}\right). \quad (4.45)$$

From the above Eqs.(4.44) and (4.45), one may now calculate the longitudinal component, $\Pi^L_{\rho\omega,vac}(q^2)$, and the transverse component, $\Pi^T_{\rho\omega,vac}(q^2)$, of the vacuum mixing amplitude. Since, $\Pi^L_{\rho\omega,vac}(q^2) = \Pi^T_{\rho\omega,vac}(q^2)$, the average vacuum mixing amplitude is found to be

$$\bar{\Pi}_{\rho\omega,vac}(q^2) = \frac{1}{3}\left[\Pi^L_{\rho\omega,vac}(q^2) + 2\Pi^T_{\rho\omega,vac}(q^2)\right] = \Pi_{\rho\omega,vac}(q^2). \quad (4.46)$$

Thus, Eq.(4.45) represents the four-momentum dependent vacuum part of the ρ-ω mixing amplitude. We obtain $\Pi_{\rho\omega,vac}(q^2 = m_\omega^2) = -4314$ MeV^2 and $\Pi_{\rho\omega,vac}(q^2 = m_\rho^2) = -4152$ MeV^2. These are within the limit of experimentally extracted values ($\sim -4520 \pm 600$ MeV^2) [151].

The three momentum dependent vacuum part of ρ-ω mixing amplitude can be obtained from Eq.(4.44) substituting $q_0 = 0$. Keeping the lowest order terms in $\mathbf{q}^2$, we find

$$\Pi_{\rho\omega,vac}(\mathbf{q}^2) \simeq -b_1 \, \mathbf{q}^2, \quad (4.47)$$

where

$$b_1 = \frac{g_\rho g_\omega}{12\pi^2}(2 + 3C_\rho) \ln\left(\frac{M_p}{M_n}\right). \quad (4.48)$$

From Eq.(4.48), it is observed that the vacuum mixing amplitude $\Pi_{\rho\omega,vac}(\mathbf{q}^2)$ vanishes if $M_p = M_n$.

To calculate density dependent mixing amplitude from Eq.(4.38a) and (4.38a) we consider $E_N \approx M_N$. In the limit $q_0 \to 0$, one finds following expressions:

$$\begin{aligned}
\Pi^{00,vv(N)}_{\rho\omega,med}(\mathbf{q}^2) &= -\frac{g_\rho g_\omega}{4\pi^2 M_N}\left[\frac{4}{3}k_N^3 - \frac{1}{2}k_N \mathbf{q}^2 + 2k_N M_N^2\right. \\
&- \left.\left(\frac{\mathbf{q}^3}{8} - \frac{\mathbf{q}k_N^2}{2} - \frac{\mathbf{q}M_N^2}{2} + 2\frac{M_N^2 k_N^2}{\mathbf{q}}\right)\ln\left(\frac{\mathbf{q}-2k_N}{\mathbf{q}+2k_N}\right)\right], \quad (4.49a)
\end{aligned}$$

$$\Pi^{00,tv(N)}_{\rho\omega,med}(\mathbf{q}^2) = -\frac{g_\rho g_\omega C_\rho}{8\pi^2 M_N}\left[\mathbf{q}^2 k_N + \left(\frac{\mathbf{q}^3}{4} - \mathbf{q}k_N^2\right)\ln\left(\frac{\mathbf{q}-2k_N}{\mathbf{q}+2k_N}\right)\right], \quad (4.49b)$$

and

$$\Pi^{vv,11(N)}_{\rho\omega,med}(\mathbf{q}^2) = \frac{g_\rho g_\omega}{4\pi^2 M_N}\left[\frac{1}{3}k_N^3 - \frac{3}{8}\mathbf{q}^2 k_N - \left(\frac{3}{32}\mathbf{q}^3 + \frac{k_N^4}{2\mathbf{q}} + \frac{\mathbf{q}^2 k_N}{4}\right)\ln\left(\frac{\mathbf{q}-2k_N}{\mathbf{q}+2k_N}\right)\right], \tag{4.50a}$$

$$\Pi^{tv,11(N)}_{\rho\omega,med}(\mathbf{q}^2) = \frac{g_\rho g_\omega C_\rho}{8\pi^2 M_N}\left[\mathbf{q}^2 k_N + \left(\frac{\mathbf{q}^3}{4} - \mathbf{q}k_N^2\right)\ln\left(\frac{\mathbf{q}-2k_N}{\mathbf{q}+2k_N}\right)\right]. \tag{4.50b}$$

Note that the terms in the Eqs.(4.49a) and (4.50a) arise from the vector-vector interaction while the terms in the Eqs.(4.49b) and (4.50b) arise from tensor-vector interaction. The 33 component of the density dependent polarization tensor vanishes *i.e.* $\Pi^{33,(N)}_{\rho\omega,med}(\mathbf{q}^2) = 0$. Now

$$\bar{\Pi}_{\rho\omega,med}(\mathbf{q}^2) = \frac{1}{3}\left[\Pi^L_{\rho\omega,med}(\mathbf{q}^2) + 2\Pi^T_{\rho\omega,med}(\mathbf{q}^2)\right], \tag{4.51}$$

where

$$\Pi^L_{\rho\omega,med}(\mathbf{q}^2) = -\left[\Pi^{00,(p)}_{\rho\omega,med}(\mathbf{q}^2) - \Pi^{00,(n)}_{\rho\omega,med}(\mathbf{q}^2)\right], \tag{4.52a}$$

$$\Pi^T_{\rho\omega,med}(\mathbf{q}^2) = -\left[\Pi^{11,(p)}_{\rho\omega,med}(\mathbf{q}^2) - \Pi^{11,(n)}_{\rho\omega,med}(\mathbf{q}^2)\right]. \tag{4.52b}$$

With the suitable expansion of Eqs.(4.49) and (4.50) in terms of $|\mathbf{q}|/k_{p(n)}$ and keeping $\mathcal{O}(\mathbf{q}^2/k^2_{p(n)})$ terms we get

$$\bar{\Pi}_{\rho\omega,med}(\mathbf{q}^2) \simeq b_0' - b_1'\ \mathbf{q}^2, \tag{4.53}$$

where

$$b_0' = \frac{g_\rho g_\omega}{12\pi^2}\left[3\left(\frac{k_p^3}{M_P} - \frac{k_n^3}{M_n}\right) + 4(k_p M_p - k_n M_n)\right], \tag{4.54a}$$

$$b_1' = \frac{g_\rho g_\omega}{12\pi^2}\left[3(1-C_\rho)\left(\frac{k_p}{M_p} - \frac{k_n}{M_n}\right) + \frac{1}{3}\left(\frac{M_p}{k_p} - \frac{M_n}{k_n}\right)\right]. \tag{4.54b}$$

Clearly, $\bar{\Pi}_{\rho\omega,med}(\mathbf{q}^2)$ is three momentum dependent medium part of ρ-ω mixing and it vanishes in SNM if $M_n = M_p$, but it is non-vanishing in ANM.

The ratio of vacuum part of ρ-ω mixing amplitude to that of π-η mixing amplitude is found to be

$$\frac{\bar{\Pi}_{\rho\omega,vac}(\mathbf{q}^2)}{\Pi^{PS}_{\pi\eta,vac}(\mathbf{q}^2)} = \left(\frac{\mathrm{g}_\rho \mathrm{g}_\omega}{\mathrm{g}_\pi \mathrm{g}_\eta}\right)\left[\frac{2}{3} + C_\rho\right] = 3.476. \tag{4.55}$$

In Fig.4.3 three momentum dependent mixing amplitudes at normal nuclear matter density are presented. On the left panel π-η mixing amplitudes are shown and ρ-ω mixing amplitude on the right panel. The medium part of the mixing amplitude for PS coupling (solid curve) is found to be negative compared to that of PV coupling (dashed curve) for the momentum $\mathbf{q} \lesssim 500$ MeV and both are positive for $\mathbf{q} > 500$. The magnitude of the medium part for PV coupling is found to be larger compared to that for PS coupling. Clearly, the $\mathbf{q}^2$ dependent medium part of ρ-ω mixing amplitude is negative compared to that of π-η mixing for PV coupling.

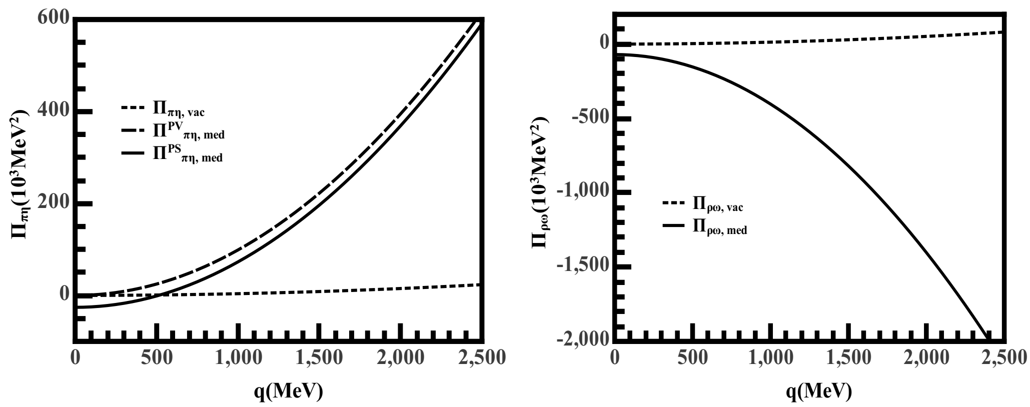

Figure 4.3: *Three momentum dependent mixing amplitudes normal nuclear matter density and at* $\alpha = 0.2$.

Chapter 5

CSV Potential in ANM

The study of charge symmetry violation (CSV) in nucleon-nucleon (NN) interaction is an important area of research in nuclear physics. Because the small but observable effects of CSV, as discussed earlier, might provide significant insight into the dynamics of isospin symmetry breaking in the NN interactions.

Experimentally CSV can be observed at various levels [152–158]. For instance, in NN interaction, the effect of CSV is traditionally inferred from the difference of the pp and nn scattering lengths in the ${}^1S_0$ state. The most recent scattering data [88, 159, 160] observes that the amount of CSV in the ${}^1S_0$ state is $\Delta a_{CSV} = a^N_{pp} - a^N_{nn} = 1.6 \pm 0.6\ fm$, where the superscript N indicates the 'nuclear' effect obtained after the electromagnetic (EM) corrections. Other convincing evidence of CSV NN interaction comes from the binding energy difference of mirror nuclei which is known as Okamoto-Nolen -Schifer (ONS) anomaly [161–163]. The modern manifestation of CSV includes difference of neutron-proton form factors, hadronic correction to $g - 2$ [164] and the observation of the decay of $\Psi'(3686) \to (J/\Psi)\pi^0$ etc. [164].

The charge symmetry phenomena giving rise to neutron-proton mass splitting causes mixing of pure isospin states of various mesons like π-η or ρ-ω as we have discussed in the last chapter. These issues had although been addressed earlier, had some ingredient missing while constructing the vacuum level CSV potentials. Most of the earlier calculations performed to construct CSV potential considered the on-shell [165] or constant ρ-ω mixing amplitude [151], which are claimed to be successful in explaining various CSV observables [151, 166]. This success has been called into question [149, 167] on the ground of the use of on-shell mixing amplitude

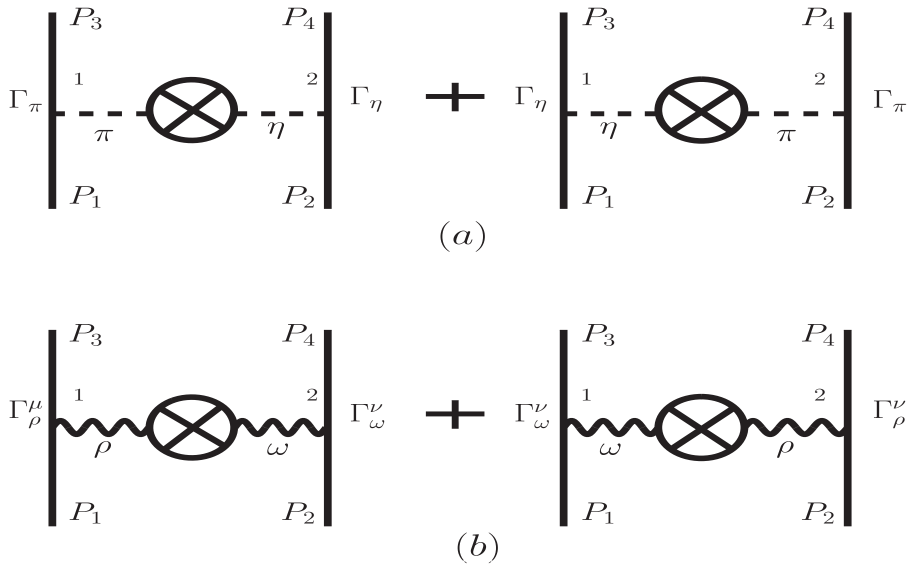

Figure 5.1: *Feynman Diagrams for CSV potential due to π-η mixing (a) and ρ-ω mixing (b). The crossed blobs represent symmetry breaking piece. Nucleons are indicated by the solid lines and dashed and wavy lines represent mesons.*

for the construction of CSV potential.

First in [149] and then in [142, 168–171], it has been shown that the ρ-ω mixing has strong momentum dependence which even changes its sign as one moves away from the ρ (or ω) pole to the space-like region which is relevant for the construction of the CSV potential. Therefore inclusion of off-shell corrections are necessary for the calculation of CSV potential. In this chapter we construct CSV NN potential in ANM which might be important to calculate various CSV observables.

5.1 CSV potential

The construction of CSV potential involves the evaluation of NN scattering diagrams with the intermediate states that include mixing of various isospin states such as π-η and ρ-ω mesons. The relevant Feynman diagrams for the construction of two-body CSV potential have been shown in Fig.5.1 where the crossed blobs represent the CSV pieces in ANM *i.e.* the mixing of isovector-isoscalar mesons in ANM. The mixing is assumed to be generated by the $N\bar{N}$ loops. We will use the three momentum dependent mixing amplitudes constructed in the previous chapter to construct the CSV nucleon-nucleon potential in ANM. We start with the nucleon-nucleon scattering amplitudes obtained from the Feynman diagrams shown in Fig.5.1:

$$\begin{aligned}\mathcal{M}_{ij}^{NN}(q^2) &= [\bar{u}_N(p_3)\tau_3(1)\Gamma_i(q)u_N(p_1)]\ \Delta_i(q^2)\Pi_{ij}(q^2)\Delta_j(q^2)\ [\bar{u}_N(p_4)\Gamma_j(-q)u_N(p_2)] \\ &+ [\bar{u}_N(p_3)\Gamma_j(q)u_N(p_1)]\ \Delta_j(q^2)\Pi_{ij}(q^2)\Delta_i(q^2)\ [\bar{u}_N(p_4)\tau_3(2)\Gamma_i(-q)u_N(p_2)].\end{aligned} \tag{5.1}$$

where i denotes π, ρ mesons and j denotes η, ω mesons. u_N's represent Dirac spinors, p_k, $(k = 1-4)$ and q are the four momenta of nucleons and mesons, respectively. $\tau_3(1)$ and $\tau_3(2)$ are isospin operators at vertices '1' and '2' (*see* Fig.5.1). The vertex factors $\Gamma_i(q)$ (or $\Gamma_j(q)$) can be found in chapter 4 (*see* 4.1, 4.2 and 4.3). The meson propagators $\Delta_i(q^2)$ (or $\Delta_j(q^2)$) are given by

$$\Delta_{\pi(\eta)}(q^2) = \frac{1}{q^2 - m^2_{\pi(\eta)}}\,, \tag{5.2a}$$

$$\Delta^{\mu\nu}_{\rho(\omega)}(q^2) = \frac{g^\mu g^\nu - q^\mu q^\nu/q^2}{q^2 - m^2_{\rho(\omega)}}\,. \tag{5.2b}$$

Eq.(5.1) in the limit $q_0 \longrightarrow 0$ leads to the CSV potential in momentum space $V_{ij}^{NN}(\mathbf{q}^2)$ *i.e*

$$\mathcal{M}_{ij}^{NN}(q_0 = 0) \longrightarrow V_{ij}^{NN}(\mathbf{q}^2). \tag{5.3}$$

Since the mixing amplitudes $\Pi_{ij}(q^2)$ contain a vacuum part and a medium part, the momentum space CSV potentials, therefore, contain a medium contribution, $V_{ij,vac}^{NN}(\mathbf{q}^2)$, together with the usual vacuum contribution, $V_{ij,med}^{NN}(\mathbf{q}^2)$.

$$V_{ij,total}^{NN}(\mathbf{q}^2) = V_{ij,vac}^{NN}(\mathbf{q}^2) + V_{ij,med}^{NN}(\mathbf{q}^2) \tag{5.4}$$

To derive the potential in momentum space, it is customary to expand the relativistic energy E_N of the Dirac spinor's in powers of $\mathbf{q}^2$ and $\mathbf{P}^2$. Here, $\mathbf{P} = \frac{1}{2}(\mathbf{p}_2 + \mathbf{p}_4) = -\frac{1}{2}(\mathbf{p}_1 + \mathbf{p}_3)$ and is the average three momentum of the nucleon and the three momentum transfer is denoted by $\mathbf{q} = (\mathbf{p}_1 - \mathbf{p}_3) = (\mathbf{p}_4 - \mathbf{p}_2)$. Keeping the lowest orders in $\mathbf{q}^2/M_N^2$ and $\mathbf{P}^2/M_N^2$, one obtains $E_N \simeq M_N + \mathbf{P}^2/2M_N + \mathbf{q}^2/8M_N$. Thus the Dirac spinor's reads

$$u_N(\mathbf{p}_1) \simeq \left(1 - \frac{\mathbf{P}^2}{8M_N^2} - \frac{\mathbf{q}^2}{32M_N^2}\right)\left(\begin{array}{c} 1 \\ \frac{\sigma_1\cdot(\mathbf{P}+\mathbf{q}/2)}{2M_N} \end{array}\right), \qquad (5.5)$$

where $\sigma_{1(2)}$ is the nucleon spin. The relevant expressions which will be needed to construct the momentum space potential are the following:

$$\bar{u}_N(\mathbf{p}_3)\gamma^0 u_N(\mathbf{p}_1) \simeq 1 + \left[\frac{\mathbf{P}^2}{4M_N^2} - \frac{\mathbf{q}^2}{16M_N^2} + i\frac{\sigma_1\cdot(\mathbf{q}\times\mathbf{P})}{4M_N^2}\right], \qquad (5.6a)$$

$$\bar{u}_N(\mathbf{p}_3)\gamma u_N(\mathbf{p}_1) \simeq \left[\sigma_1\left(\frac{\sigma_1\cdot\mathbf{p}_1}{2M_N}\right) + \left(\frac{\sigma_1\cdot\mathbf{p}_3}{2M_N}\right)\sigma_1\right], \qquad (5.6b)$$

$$\bar{u}_N(\mathbf{p}_4)\sigma_{l0}q^l u_N(\mathbf{p}_2) \simeq i\left(\frac{\mathbf{q}^2}{2M_N^2}\right), \qquad (5.6c)$$

$$\bar{u}_N(\mathbf{p}_4)\sigma_{lk}q^l u_N(\mathbf{p}_2) \simeq -(\sigma_2\times\mathbf{q})_k\,, \quad \text{where } (l,k) = 1,2,3. \qquad (5.6d)$$

The potential in coordinate space is obtained by Fourier transformation of the momentum space potential.

$$V_{ij,total}^{NN}(r) = \frac{1}{(2\pi)^3}\int V_{ij,total}^{NN}(\mathbf{q}^2)\; e^{-i\mathbf{q}\cdot\mathbf{r}}\; d^3\mathbf{q}. \qquad (5.7)$$

5.1.1 CSV potential due to π-η mixing

First we construct the CSV potential in momentum space for π-η mixing considering pseudo scalar (PS) coupling of πNN and ηNN interactions. The three momentum dependent mixing amplitudes (*see* chapter 4) are

$$\Pi_{\pi\eta,vac}^{PS}(\mathbf{q}^2) = -a_1\mathbf{q}^2, \qquad (5.8a)$$

$$\Pi_{\pi\eta,med}^{PS}(\mathbf{q}^2) = a_0' - a_1'\mathbf{q}^2 \qquad (5.8b)$$

where

$$a_1 = \frac{g_\pi g_\eta}{4\pi^2}\ln\left(\frac{M_p}{M_n}\right), \qquad (5.9a)$$

$$a_0' = \frac{g_\pi g_\eta}{3\pi^2}\left(\frac{k_p^3}{M_p} - \frac{k_n^3}{M_n}\right), \qquad (5.9b)$$

$$a_1' = \frac{g_\pi g_\eta}{4\pi^2}\left(\frac{k_p}{M_p} - \frac{k_n}{M_n}\right). \tag{5.9c}$$

After a straight forward calculation on obtains the momentum space CSV potential given by

$$\begin{aligned} V^{NN,PS}_{\pi\eta,total}(\mathbf{q}^2) &= T_3^+\left(\frac{g_\pi g_\eta}{4M_N^2}\right)\left[\frac{\Pi^{PS}_{\pi\eta,vac}(\mathbf{q}^2)}{(\mathbf{q}^2+m_\pi^2)(\mathbf{q}^2+m_\eta^2)} + \frac{\Pi^{PS}_{\pi\eta,med}(\mathbf{q}^2)}{(\mathbf{q}^2+m_\pi^2)(\mathbf{q}^2+m_\eta^2)}\right] \\ &\times\left[1 - \frac{\mathbf{q}^2}{8M_N^2} - \frac{\mathbf{P}^2}{2M_N^2}\right](\sigma_\mathbf{1}\cdot\mathbf{q})(\sigma_\mathbf{2}\cdot\mathbf{q}), \end{aligned} \tag{5.10}$$

where $T_3^+ = \tau_3(1) + \tau_3(2)$. It is evident from Eq.(5.10) presents CSV class (III) potential in momentum space [148,149,164]. Note that the terms within the square bracket are the contributions coming from the external nucleon legs because of the expansion of relativistic nucleon energy E_N in the Dirac spinors as discussed in section 5.1.1. This expansion is important as it contains nucleon mass M_N, which is also a source of CSV.

$$\begin{aligned} V^{NN,PS}_{\pi\eta,vac}(\mathbf{q}^2) &= -\,T_3^+\left(\frac{g_\pi g_\eta}{4M_N^2}\right)\frac{a_1\ \mathbf{q}^2}{(\mathbf{q}^2+m_\pi^2)(\mathbf{q}^2+m_\eta^2)}(\sigma_\mathbf{1}\cdot\mathbf{q})(\sigma_\mathbf{2}\cdot\mathbf{q}) \\ &-\ T_3^+\left(\frac{g_\pi g_\eta}{4M_N^2}\right)\frac{a_1\ \mathbf{q}^2}{(\mathbf{q}^2+m_\pi^2)(\mathbf{q}^2+m_\eta^2)}\left(-\frac{\mathbf{q}^2}{8M_N^2}\right)(\sigma_\mathbf{1}\cdot\mathbf{q})(\sigma_\mathbf{2}\cdot\mathbf{q}). \end{aligned} \tag{5.11}$$

In Eq.(5.11) the $-\frac{\mathbf{q}^2}{8M_N^2}$ dependent term is the correction over the central part due to the contribution of the external nucleon legs. Notice that we drop the term $3\mathbf{P}^2/2M_N^2$ from Eq.(5.11) as this term is not important in the present context. However, it should be noted that to fit the $^1S_0$ and $^3P_2$ phase shifts simultaneously this term is necessary as $\mathbf{P}^2$ gives the operator ∇_R^2 in coordinate space. The usual vacuum CSV potential in momentum space reads

$$\begin{aligned} V^{NN,PS}_{\pi\eta,med}(\mathbf{q}^2) &= T_3^+\left(\frac{g_\pi g_\eta}{4M_N^2}\right)\frac{a_0' - a_1'\ \mathbf{q}^2}{(\mathbf{q}^2+m_\pi^2)(\mathbf{q}^2+m_\eta^2)}(\sigma_\mathbf{1}\cdot\mathbf{q})(\sigma_\mathbf{2}\cdot\mathbf{q}) \\ &+\ T_3^+\left(\frac{g_\pi g_\eta}{4M_N^2}\right)\frac{a_0' - a_1'\ \mathbf{q}^2}{(\mathbf{q}^2+m_\pi^2)(\mathbf{q}^2+m_\eta^2)}\left(-\frac{\mathbf{q}^2}{8M_N^2}\right)(\sigma_\mathbf{1}\cdot\mathbf{q})(\sigma_\mathbf{2}\cdot\mathbf{q}). \end{aligned} \tag{5.12}$$

Eq.(5.12) represents the purely density dependent CSV potential in momentum space. It is important to note that in the limit $M_p = M_n$ vacuum CSV potential does not exists as $a_1 = 0$, but the density dependent part does not vanish in ANM.

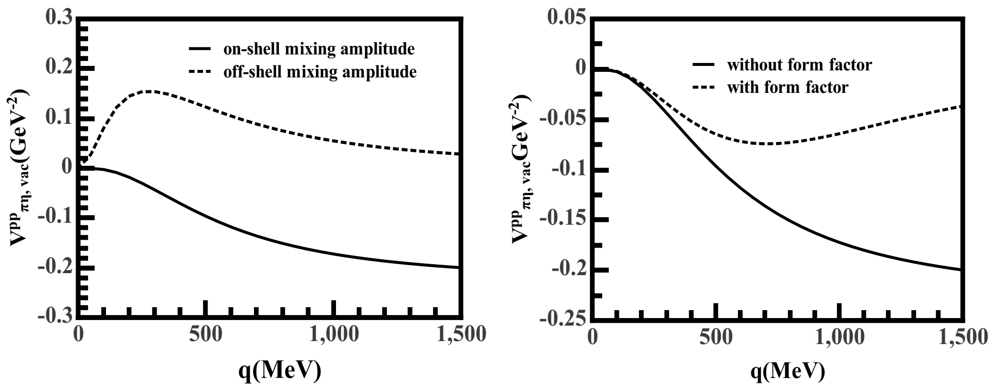

Figure 5.2: *CSV potential in momentum space for π-η mixing.*

Fig.5.2 shows the vacuum CSV potential (for $^1S_0$ state) in momentum space. It is observed that the potential is positive for on-shell mixing amplitude and is negative for off-shell mixing amplitude (left). The magnitude of the potential is found to be large for on-shell mixing amplitude compared to that for off-shell mixing amplitude in the long range region. The figure in the right panel shows the effect of form factor.

Now the potential in coordinate space can be easily obtained following Eq.(5.7). First we present the potential in coordinate space with the on-shell mixing amplitude given by

$$V^{NN,PS}_{\pi\eta,vac}(r) = -\, T_3^+ \left(\frac{g_\pi g_\eta}{48\pi\ M_N^2}\right) \Pi^{PS}_{\pi\eta,vac}(q^2 = m_\eta^2) \\ \times \left[\left(\frac{m_\pi^3\ U(x_\pi) - m_\eta^3\ U(x_\eta)}{m_\eta^2 - m_\pi^2}\right) + \frac{1}{8M_N^2}\left(\frac{m_\pi^5\ U(x_\pi) - m_\eta^5\ U(x_\eta)}{m_\eta^2 - m_\pi^2}\right)\right] \quad (5.13)$$

Clearly the second term within the square bracket of Eq.(5.13) is the correction term due external nucleon legs and the first term is the central part of the potential. Here

$$U(x_i) = Y_0(x_i)(\sigma_\mathbf{1}\cdot\sigma_\mathbf{2}) + S_{12}(\hat{\mathbf{r}})Y_2(x_i)\ , \quad (5.14a)$$

$$Y_2(x_i) = \left(1 + \frac{3}{x_i} + \frac{3}{x_i^2}\right) Y_0(x_i)\ , \quad (5.14b)$$

$$S_{12}(\hat{\mathbf{r}}) = 3(\sigma_\mathbf{1}\cdot\hat{\mathbf{r}})(\sigma_\mathbf{2}\cdot\hat{\mathbf{r}}) - (\sigma_\mathbf{1}\cdot\sigma_\mathbf{2})\ , \quad (5.14c)$$

with $x_i = m_i r$, $i = \pi, \eta$ and $Y_0(x_i) = e^{-x_i}/x_i$. Now the CSV potential in coordinate space with the three momentum dependent mixing amplitude reads

$$V^{NN,PS}_{\pi\eta,vac}(r) = -T_3^+\left(\frac{g_\pi g_\eta}{48\pi M_N^2}\right)\left[a_1\left(\frac{m_\pi^5 U(x_\pi) - m_\eta^5 U(x_\eta)}{m_\eta^2 - m_\pi^2}\right)\right], \tag{5.15a}$$

$$\begin{aligned} V^{NN,PS}_{\pi\eta,med}(r) &= -T_3^+\left(\frac{g_\pi g_\eta}{48\pi M_N^2}\right)\left[a_0'\left(\frac{m_\pi^3 U(x_\pi) - m_\eta^3 U(x_\eta)}{m_\eta^2 - m_\pi^2}\right)\right. \\ &+ \left.\left(\frac{a_0'}{8M_N^2} + a_1'\right)\left(\frac{m_\pi^5 U(x_\pi) - m_\eta^5 U(x_\eta)}{m_\eta^2 - m_\pi^2}\right)\right]. \end{aligned} \tag{5.15b}$$

Since mesons and nucleons are not point particles and they have internal structures one needs to incorporate vertex corrections which, in principle, can be calculated using renormalizable models based on hadronic degrees of freedom. In the present calculation following phenomenological form factors have been used to incorporate the vertex corrections,

$$g_i(\mathbf{q^2}) \to g_i\left(\frac{\Lambda_i^2 - m_i^2}{\Lambda_i^2 + \mathbf{q}^2}\right), \quad i = \pi, \eta. \tag{5.16}$$

Here Λ_i is the cut-off parameter. In fact, form factors were originally introduced in the meson theory in a purely *ad hoc* manner. Now it is a theoretically well-established concept [172]. With the inclusion of form factors Eq.(5.13) reduces to

$$\begin{aligned} V^{NN,PS}_{\pi\eta,vac}(r) &= -T_3^+\left(\frac{g_\pi g_\eta}{48\pi\ M_N^2}\right)\Pi^{PS}_{\pi\eta,vac}(q^2 = m_\eta^2) \\ &\times \left[\left\{\left(\frac{a_\pi\ m_\pi^3\ U(x_\pi) - a_\eta\ m_\eta^3\ U(x_\eta)}{m_\eta^2 - m_\pi^2}\right)\right.\right. \\ &+ \left.\frac{1}{8M_N^2}\left(\frac{a_\pi\ m_\pi^5\ U(x_\pi) - a_\eta\ m_\eta^5\ U(x_\eta)}{m_\eta^2 - m_\pi^2}\right)\right\} \\ &- \lambda_{\pi\eta}\left\{\left(\frac{b_\pi\ m_\pi^3\ U(X_\pi) - b_\eta\ m_\eta^3\ U(X_\eta)}{m_\eta^2 - m_\pi^2}\right)\right. \\ &+ \left.\left.\frac{1}{8M_N^2}\left(\frac{b_\pi\ m_\pi^5\ U(X_\pi) - b_\eta\ m_\eta^5\ U(X_\eta)}{m_\eta^2 - m_\pi^2}\right)\right\}\right], \end{aligned} \tag{5.17}$$

where

$$a_\pi = \left(\frac{\Lambda_\eta^2 - m_\eta^2}{\Lambda_\eta^2 - m_\pi^2}\right), \tag{5.18a}$$

$$b_\pi = \left(\frac{\Lambda_\eta^2 - m_\eta^2}{m_\eta^2 - \Lambda_\pi^2}\right), \tag{5.18b}$$

$$\lambda_{\pi\eta} = \left(\frac{m_\pi^2 - m_\eta^2}{\Lambda_\pi^2 - \Lambda_\eta^2}\right). \tag{5.18c}$$

and $X_i = \Lambda_i r$. Note that a_η and b_η can be found by replacing $\Lambda_\eta \to \Lambda_\pi$, $m_\eta \to m_\pi$ and $m_\pi \to m_\eta$ in Eq.(5.18a) and Eq.(5.18b), respectively.

The CSV potential with three momentum dependent mixing amplitude and form factors reads

$$\begin{aligned} V^{NN,PS}_{\pi\eta,vac}(r) &= -\, T_3^+ \left(\frac{g_\pi g_\eta}{48\pi M_N^2}\right)\left[a_1\left\{\left(\frac{a_\pi m_\pi^5 U(x_\pi) - a_\eta m_\eta^5 U(x_\eta)}{m_\eta^2 - m_\pi^2}\right)\right.\right. \\ &- \left.\left.\lambda_{\pi\eta}\left(\frac{b_\pi m_\pi^5 U(X_\pi) - b_\eta m_\eta^5 U(X_\eta)}{m_\eta^2 - m_\pi^2}\right)\right\}\right], \end{aligned} \tag{5.19}$$

and

$$\begin{aligned} V^{NN,PS}_{\pi\eta,med}(r) &= -\, T_3^+ \left(\frac{g_\pi g_\eta}{48\pi M_N^2}\right)\left[\left\{a_0'\left(\frac{a_\pi m_\pi^3 U(x_\pi) - a_\eta m_\eta^3 U(x_\eta)}{m_\eta^2 - m_\pi^2}\right)\right.\right. \\ &+ \left.\left(\frac{a_0'}{8M_N^2} + a_1'\right)\left(\frac{a_\pi m_\pi^5 U(x_\pi) - a_\eta m_\eta^5 U(x_\eta)}{m_\eta^2 - m_\pi^2}\right)\right\} \\ &- \lambda_{\pi\eta}\left\{a_0'\left(\frac{b_\pi m_\pi^3 U(X_\pi) - b_\eta m_\eta^3 U(X_\eta)}{m_\eta^2 - m_\pi^2}\right)\right. \\ &+ \left.\left.\left(\frac{a_0'}{8M_N^2} + a_1'\right)\left(\frac{b_\pi m_\pi^5 U(X_\pi) - b_\eta m_\eta^5 U(X_\eta)}{m_\eta^2 - m_\pi^2}\right)\right\}\right]. \end{aligned} \tag{5.20}$$

It is to be mentioned that the vacuum CSV potential for PV coupling is the same as found in Eqs.(5.15a) and (5.19). The density dependent part of for PV coupling can be obtained by substituting $a_0' = 0$ in Eqs.(5.15b) and (5.20). In Fig.5.3 we present the difference between CSV nn and pp potentials at $^1\mathrm{S}_0$ state without form factors (left) and with form factors (right). To obtain density dependent CSV potential we consider nuclear matter density $\rho = 0.148$ fm^{-3} and asymmetry parameter $\alpha = 1/3$. The dotted and dashed curves represent density dependent contributions of PS and PV couplings, respectively. The difference in the contributions of density dependent part of CSV potential for these two types of coupling arises because of the term a_0'. The vacuum contribution (solid curve) of CSV potentials for both PS and PV couplings are same.

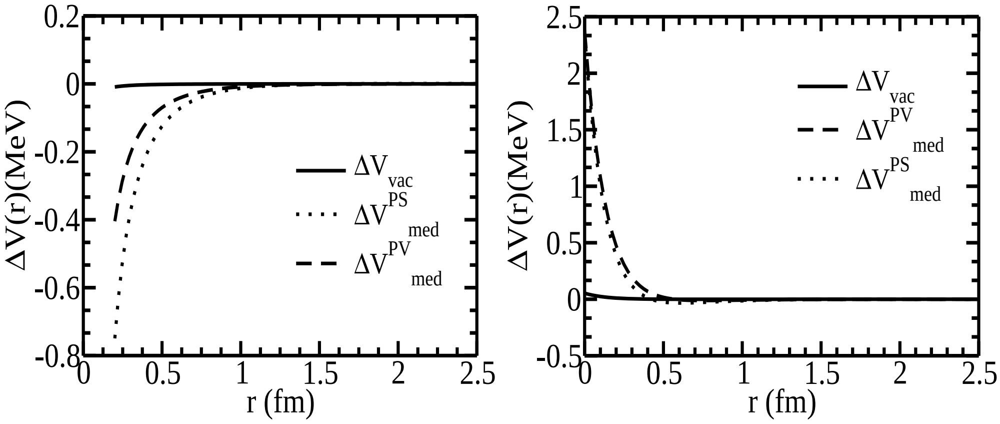

Figure 5.3: *Difference between CSV nn and pp potentials at* $^1S_0$ *state.*

Notice, both the vacuum and medium parts contribute with the same sign. Note that CSV potentials change sign with the inclusion of form factors. The medium contribution near the core region is found to be much larger than the vacuum contribution.

5.1.2 CSV potential due to ρ-ω mixing

In this section we will use the three momentum dependent ρ-ω mixing amplitudes calculated in section 4.3 of chapter 4 to construct the CSV two-body potentials in ANM. We will use average mixing amplitudes which read

$$\bar{\Pi}_{\rho\omega,vac}(\mathbf{q}^2) = -\,b_1\,\mathbf{q}^2, \tag{5.21a}$$

$$\bar{\Pi}_{\rho\omega,med}(\mathbf{q}^2) = b_0' - b_1'\,\mathbf{q}^2, \tag{5.21b}$$

where

$$b_1 = \frac{g_\rho g_\omega}{12\pi^2}\ln\left(\frac{M_p}{M_n}\right)(2+3C_\rho), \tag{5.22a}$$

$$b_0' = \frac{g_\rho g_\omega}{12\pi^2}\left[3\left(\frac{k_p^3}{M_P}-\frac{k_n^3}{M_n}\right)+4(k_pM_p-k_nM_n)\right], \tag{5.22b}$$

$$b_1' = \frac{g_\rho g_\omega}{12\pi^2}\left[3(1-C_\rho)\left(\frac{k_p}{M_p}-\frac{k_n}{M_n}\right)+\frac{1}{3}\left(\frac{M_p}{k_p}-\frac{M_n}{k_n}\right)\right]. \tag{5.22c}$$

After calculation of the amplitude in Eq.(5.1) and taking the limit $q_0 \longrightarrow 0$ one arrive at the CSV potential in momentum space given by

$$
\begin{aligned}
V^{NN}_{\rho\omega,total}(\mathbf{q}^2) &= -\, g_\rho g_\omega \left[\frac{\bar{\Pi}_{\rho\omega,vac}(\mathbf{q}^2)}{(\mathbf{q}^2+m_\rho^2)(\mathbf{q}^2+m_\omega^2)} + \frac{\bar{\Pi}_{\rho\omega,med}(\mathbf{q}^2)}{(\mathbf{q}^2+m_\rho^2)(\mathbf{q}^2+m_\omega^2)}\right] \\
&\times \Bigg[T_3^+ \Bigg\{\Bigg(1 + \frac{3\mathbf{P}^2}{2M_N^2} - \frac{\mathbf{q}^2}{8M_N^2} - \frac{\mathbf{q}^2}{4M_N^2}(\sigma_1\cdot\sigma_2) \\
&+ \frac{3i}{2M_N^2}\mathbf{S}\cdot(\mathbf{q}\times\mathbf{P}) + \frac{1}{4M_N^2}(\sigma_1\cdot\mathbf{q})(\sigma_2\cdot\mathbf{q}) + \frac{1}{M_N^2}(\hat{\mathbf{q}}\cdot\mathbf{P})^2\Bigg) \\
&- \frac{C_\rho}{2M}\Bigg(\frac{\mathbf{q}^2}{2M_N} + \frac{\mathbf{q}^2}{2M_N}(\sigma_1\cdot\sigma_2) - \frac{2i}{M_N}\mathbf{S}\cdot(\mathbf{q}\times\mathbf{P}) \\
&- \frac{1}{2M_N}(\sigma_1\cdot\mathbf{q})(\sigma_2\cdot\mathbf{q})\Bigg)\Bigg\} - T_3^- \frac{C_\rho}{2M}\Bigg\{\Bigg(\frac{\mathbf{q}^2}{2M} - \frac{\mathbf{q}^2}{2M}(\sigma_1\cdot\sigma_2) \\
&+ \frac{1}{2M}(\sigma_1\cdot\mathbf{q})(\sigma_2\cdot\mathbf{q})\Bigg)\frac{\Delta M(1,2)}{M} - \frac{i}{M}(\sigma_1-\sigma_2)\cdot(\mathbf{q}\times\mathbf{P})\Bigg\}\Bigg]\,. \qquad (5.23)
\end{aligned}
$$

Here $T_3^- = \tau_3(1) - \tau_3(2)$ and $\mathbf{S} = \frac{1}{2}(\sigma_1 + \sigma_2)$ is the total spin of the interacting nucleon pair. The spin dependent terms in Eq.(5.23) appear from the contribution of the external nucleon legs. On the other hand, $3\mathbf{P}^2/2M_N^2$ and $-\mathbf{q}^2/8M_N^2$ arise due to expansion of the relativistic energy E_N of the Dirac spinors. We define average nucleon mass and neutron-proton mass difference as

$$
\begin{aligned}
M &= (M_n + M_p)/2, & (5.24a)\\
\Delta M &= (M_n - M_p)/2, & (5.24b)\\
\Delta M(1,2) &= -\,\Delta M(2,1) = \Delta M. & (5.24c)
\end{aligned}
$$

Note that unlike the π-η mixing, ρ-ω mixing generates both class (III) and class (IV) potentials as found in Eq.(5.23), and both these class (III) and class (IV) potentials break the charge symmetry of NN interactions. The class (III) NN interaction differentiates between nn and pp systems but vanishes for np system. On the other hand, class (IV) interaction exists for np system only. In the present thesis we focus on the class (III) NN potential only.

Now we present the spin independent central part of the CSV potential considering the on-shell ρ-ω mixing amplitude:

$$
V^{NN}_{\rho\omega,vac}(\mathbf{q}^2) = -\,T_3^+\; g_\rho g_\omega \frac{\Pi_{\rho\omega,vac}(q^2 = m_\omega^2)}{(\mathbf{q}^2+m_\rho^2)(\mathbf{q}^2+m_\omega^2)}, \qquad (5.25)
$$

and in the coordinate space it becomes

$$V^{NN}_{\rho\omega,vac}(r) = -T_3^+ \left(\frac{g_\rho g_\omega}{4\pi}\right) \Pi_{\rho\omega,vac}(q^2 = m_\omega^2) \left[\frac{m_\rho Y_0(x_\rho) - m_\omega Y_0(x_\omega)}{m_\omega^2 - m_\rho^2}\right], \quad (5.26)$$

where $Y_0(x_i)$ is already defined in 5.1.1 and $x_i = m_i r$, $(i = \rho, \omega)$. The potential in Eq.(5.26) diverges near the core. This can be avoided by the inclusion of form factors. The potential with the form factors of the type given in Eq.(5.16) with $i = \rho, \omega$:

$$\begin{aligned} V^{NN}_{\rho\omega,vac}(r) &= -T_3^+ \left(\frac{g_\rho g_\omega}{4\pi}\right) \Pi_{\rho\omega,vac}(q^2 = m_\omega^2) \left[\left(\frac{a_\rho m_\rho Y_0(x_\rho) - a_\omega m_\omega Y_0(x_\omega)}{m_\omega^2 - m_\rho^2}\right)\right. \\ &- \left.\lambda_{\rho\omega} \left(\frac{b_\rho \Lambda_\rho Y_0(X_\rho) - b_\omega \Lambda_\omega Y_0(X_\omega)}{m_\omega^2 - m_\rho^2}\right)\right], \end{aligned} \quad (5.27)$$

where

$$a_\rho = \left(\frac{\Lambda_\omega^2 - m_\omega^2}{\Lambda_\omega^2 - m_\rho^2}\right), \quad (5.28a)$$

$$b_\rho = \left(\frac{\Lambda_\omega^2 - m_\omega^2}{m_\omega^2 - \Lambda_\rho^2}\right), \quad (5.28b)$$

$$\lambda_{\rho\omega} = \left(\frac{m_\rho^2 - m_\omega^2}{\Lambda_\rho^2 - \Lambda_\omega^2}\right). \quad (5.28c)$$

where $X_i = \Lambda_i r$. One can find a_ω and b_ω replacing $\Lambda_\omega \to \Lambda_\rho$, $m_\omega \to m_\rho$ and $m_\rho \to m_\omega$ in Eq.(5.28a) and Eq.(5.28b), respectively. It is to be noted that in the limit $\Lambda_{\rho(\omega)} \to \infty$, Eq.(5.27) reduces to Eq.(5.26).

From Eq.(5.23) we extract a piece which, in coordinate space, gives rise to δ-function potential. This is known as contact term. The appearance of such term can be avoided by inclusion of form factors. In momentum space it is given by

$$\delta V^{NN}_{\rho\omega,vac} = T_3^+ \, g_\rho g_\omega b_1 \left[\left(\frac{1 + 2C_\rho}{8M_N^2}\right) + \left(\frac{1 + C_\rho}{4M_N^2}\right)(\sigma_1 \cdot \sigma_2)\right], \quad (5.29a)$$

$$\delta V^{NN}_{\rho\omega,med} = T_3^+ \, g_\rho g_\omega b_1' \left[\left(\frac{1 + 2C_\rho}{8M_N^2}\right) + \left(\frac{1 + C_\rho}{4M_N^2}\right)(\sigma_1 \cdot \sigma_2)\right]. \quad (5.29b)$$

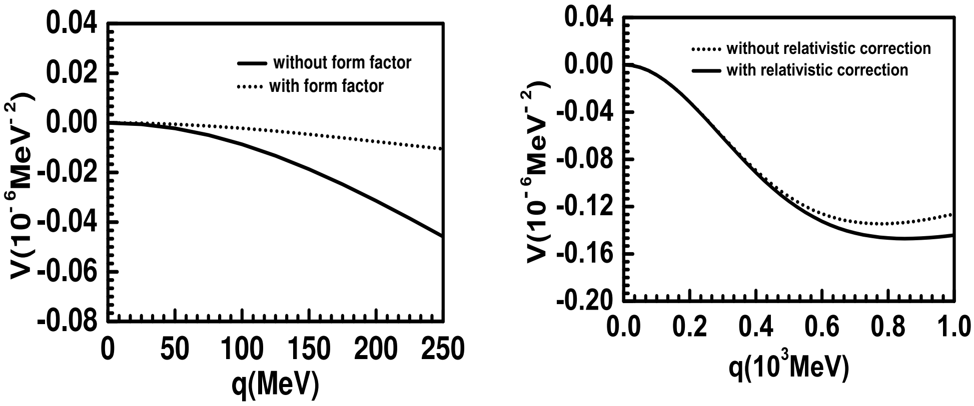

Figure 5.4: *Central part of CSV potential in momentum space. The mixing amplitude is taken to be three momentum dependent as found in Eq.(5.30).*

The potentials with three momentum dependent ρ-ω mixing amplitudes are presented below. The spin independent central part neglecting the contributions due to external nucleon legs and the ρNN tensor coupling, reduces to

$$V^{NN,0}_{\rho\omega,vac}(\mathbf{q}^2) = -T_3^+ \; \mathrm{g}_\rho \mathrm{g}_\omega \frac{-b_1 \; \mathbf{q}^2}{(\mathbf{q}^2 + m_\rho^2)(\mathbf{q}^2 + m_\omega^2)}. \tag{5.30}$$

and in the coordinate space without form factor

$$V^{NN}_{\rho\omega,vac}(r) \;\; = \;\; - \; T_3^+ \left(\frac{\mathrm{g}_\rho \mathrm{g}_\omega}{4\pi}\right) \left[b_1 \left(\frac{m_\rho^3 Y_0(x_\rho) - m_\omega^3 Y_0(x_\omega)}{m_\omega^2 - m_\rho^2} \right) \right]. \tag{5.31}$$

The importance of the relativistic correction (left figure) and the effect of form factor (right figure) to the central part of the CSV potential are shown in Fig.5.4. The three momentum dependent ρ-ω mixing amplitude is considered. It is found that the relativistic correction, as expected, is marginal at low momentum (below $|\mathbf{q}| \sim 500$ MeV). In the short distance regime *i.e.* near the core region, this correction becomes significant which is clearly seen in Fig.5.4.

If one includes the contribution of the external legs and ρNN tensor coupling, then the central part simplifies to

$$V^{NN}_{\rho\omega,vac}(r) \;\; = \;\; -T_3^+ \left(\frac{\mathrm{g}_\rho \mathrm{g}_\omega}{4\pi}\right) \Bigg[b_1 \Bigg\{ \left(\frac{m_\rho^3 Y_0(x_\rho) - m_\omega^3 Y_0(x_\omega)}{m_\omega^2 - m_\rho^2} \right)$$

$$+ \quad \frac{1+2C_\rho}{8M_N^2} \left(\frac{m_\rho^5 Y_0(x_\rho) - m_\omega^5 Y_0(x_\omega)}{m_\omega^2 - m_\rho^2} \right) \Bigg\} \Bigg] . \tag{5.32}$$

In the above equation the first term in the bracket is same as one would have obtained from Eq.(5.30) by taking the momentum dependent mixing amplitude, while the second term contains the contribution coming from the Dirac spinors of the external nucleon legs. The latter, clearly involves ρNN vector and tensor interactions, and, as we shall see, the term containing the tensor coupling (C_ρ) is significantly larger compared to the vector interaction at distances below $0.75 fm$ or so.

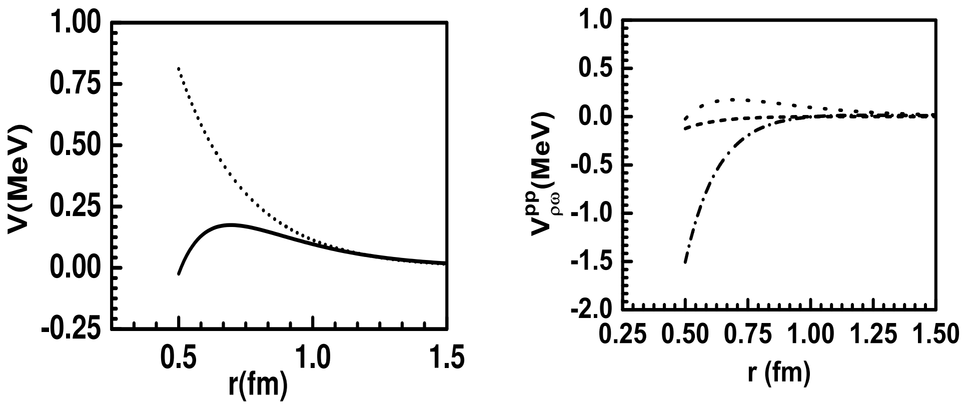

Figure 5.5: *Central part in the coordinate space (left) considering the constant on-shell mixing amplitude (dotted curve) and three momentum dependent mixing amplitude (solid curve). On the right side, the central part (dotted curve), the contribution of external nucleon legs (dashed curve) and the ρNN tensor coupling (dot-dashed curve) are shown. Form factors are not included.*

It is to be noted that ρNN tensor contribution is present only when the external legs are taken into account. We leave out the coordinate space contact terms from Eq.(5.32). In Fig.5.5 we show the central part of CSV potential in coordinate space due to both on-shell and off-shell mixing amplitudes (left figure). It is seen that the contribution of the off-shell ρ^0-ω mixing amplitude to the NN potential is opposite in sign relative to the contribution obtained from using the on-shell value. This, again, is consistent with the observation made in Ref. [149].

The individual contribution of different parts of the central potential given in Eq.(5.32) are presented in Fig.5.5 (right figure). Clearly the contribution of ρNN tensor coupling to the CSV potential is found to be much larger than the contribution of the first part (*i.e.* the central part without external legs and ρNN tensor contribution). Now we use the $\mathbf{q}^2$ dependent mixing amplitude instead of constant on-shell value and for this we consider terms up to $\mathcal{O}(\mathbf{q}^2/M_N^2)$. We drop the $\mathbf{q}^2/2M_N^2$ term as it is not important in the present context. Taking all this into consideration we obtain, after some algebraic manipulations, the coordinate space CSV potential as

$$\begin{aligned}
V^{NN}_{\rho\omega,vac}(r) &= -\,T_3^{+}\left(\frac{g_\rho g_\omega}{4\pi}\right)\left[b_1\left\{\left(\frac{m_\rho^3 Y_0(x_\rho)-m_\omega^3 Y_0(x_\omega)}{m_\omega^2-m_\rho^2}\right)\right.\right.\\
&+\frac{1}{M_N^2}\left(\frac{m_\rho^5 V_{vv}(x_\rho)-m_\omega^5 V_{vv}(x_\omega)}{m_\omega^2-m_\rho^2}\right)\\
&+\left.\left.\frac{C_\rho}{2M_N^2}\left(\frac{m_\rho^5 V_{tv}(x_\rho)-m_\omega^5 V_{tv}(x_\omega)}{m_\rho^2-m_\omega^2}\right)\right\}\right]. \qquad (5.33)
\end{aligned}$$

and

$$\begin{aligned}
V^{NN}_{\rho\omega,med}(r) &= -\,T_3^{+}\left(\frac{g_\rho g_\omega}{4\pi}\right)\left[b_0'\left\{\left(\frac{m_\rho Y_0(x_\rho)-m_\omega Y_0(x_\omega)}{m_\omega^2-m_\rho^2}\right)\right.\right.\\
&+\frac{1}{M_N^2}\left(\frac{m_\rho^3 V_{vv}(x_\rho)-m_\omega^3 V_{vv}(x_\omega)}{m_\omega^2-m_\rho^2}\right)\\
&+\left.\frac{C_\rho}{2M_N^2}\left(\frac{m_\rho^3 V_{tv}(x_\rho)-m_\omega^3 V_{tv}(x_\omega)}{m_\omega^2-m_\rho^2}\right)\right\}\\
&+b_1'\left\{\left(\frac{m_\rho^3 Y_0(x_\rho)-m_\omega^3 Y_0(x_\omega)}{m_\omega^2-m_\rho^2}\right)\right.\\
&+\frac{1}{M_N^2}\left(\frac{m_\rho^5 V_{vv}(x_\rho)-m_\omega^5 V_{vv}(x_\omega)}{m_\omega^2-m_\rho^2}\right)\\
&+\left.\left.\frac{C_\rho}{2M_N^2}\left(\frac{m_\rho^5 V_{tv}(x_\rho)-m_\omega^5 V_{tv}(x_\omega)}{m_\omega^2-m_\rho^2}\right)\right\}\right], \qquad (5.34)
\end{aligned}$$

The spin-spin, tensor and spin-orbit interaction terms are explicitly contained in $V_{vv}(x)$ and $V_{tv}(x)$ which are as follows:

$$V_{vv}(x) = \frac{1}{8}Y_0(x)+\frac{1}{6}Y_0(x)(\sigma_1\cdot\sigma_2)-\frac{1}{12}Y_1(x)S_{12}(\hat{\mathbf{r}})-\frac{3}{2}Y_2(x)\mathbf{L}\cdot\mathbf{S}, \qquad (5.35a)$$

$$V_{tv}(x) = \frac{1}{2}Y_0(x)+\frac{1}{3}Y_0(x)(\sigma_1\cdot\sigma_2)-\frac{1}{6}Y_1(x)S_{12}(\hat{\mathbf{r}})-2Y_2(x)\mathbf{L}\cdot\mathbf{S}. \qquad (5.35b)$$

with,

$$Y_1(x) = \left(1 + \frac{3}{x} + \frac{3}{x^2}\right) Y_0(x) \tag{5.36a}$$

$$Y_2(x) = \left(\frac{1}{x} + \frac{1}{x^2}\right) Y_0(x) \tag{5.36b}$$

$$S_{12}(\hat{\mathbf{r}}) = 3(\sigma_1 \cdot \hat{\mathbf{r}})(\sigma_2 \cdot \hat{\mathbf{r}}) - (\sigma_1 \cdot \sigma_2) \tag{5.36c}$$

In deriving both Eqs.(5.33) and (5.34) we have neglected the contact terms. The first part of Eq.(5.33) represents the central part without contributions from external legs. In addition, the last two terms of Eq.(5.33) are the contributions coming from the external nucleon legs as discussed earlier. It is also to be noted that the central part also receives contributions due to the presence of the first terms in Eq.(5.35a) and Eq.(5.35b). The tensor contribution (C_ρ) of ρ meson is contained in the third term of Eq.(5.33).

Notice both Eqs.(5.33) and (5.34)does not include form factors. It diverges near the core. This divergence can be removed by incorporating form factors. Thus the complete CSV potentials with form factors reduces to

$$\begin{aligned}
V^{NN}_{\rho\omega,vac}(r) &= -\, T_3^+ \left(\frac{g_\rho g_\omega}{4\pi}\right) \left[b_1 \left\{ \left(\frac{a_\rho m_\rho^3 Y_0(x_\rho) - a_\omega m_\omega^3 Y_0(x_\omega)}{m_\omega^2 - m_\rho^2} \right) \right.\right. \\
&+ \frac{1}{M_N^2} \left(\frac{a_\rho m_\rho^5 V_{vv}(x_\rho) - a_\omega m_\omega^5 V_{vv}(x_\omega)}{m_\omega^2 - m_\rho^2} \right) \\
&+ \left.\frac{C_\rho}{2M_N^2} \left(\frac{a_\rho m_\rho^5 V_{tv}(x_\rho) - a_\omega m_\omega^5 V_{tv}(x_\omega)}{m_\omega^2 - m_\rho^2} \right) \right\} \\
&- \lambda_{\rho\omega} b_1 \left\{ \left(\frac{b_\rho \Lambda_\rho^3 Y_0(X_\rho) - b_\omega \Lambda_\omega^3 Y_0(X_\omega)}{m_\omega^2 - m_\rho^2} \right) \right. \\
&+ \frac{1}{M_N^2} \left(\frac{b_\rho \Lambda_\rho^5 V_{vv}(X_\rho) - b_\omega \Lambda_\omega^5 V_{vv}(X_\omega)}{m_\omega^2 - m_\rho^2} \right) \\
&+ \left.\left. \frac{C_\rho}{2M_N^2} \left(\frac{b_\rho \Lambda_\rho^5 V_{tv}(X_\rho) - b_\omega \Lambda_\omega^5 V_{tv}(X_\omega)}{m_\omega^2 - m_\rho^2} \right) \right\} \right],
\end{aligned} \tag{5.37}$$

and

$$V^{NN}_{\rho\omega,med}(r) = -\, T_3^+ \left(\frac{g_\rho g_\omega}{4\pi}\right) \left[b_0' \left\{ \left(\frac{a_\rho m_\rho Y_0(x_\rho) - a_\omega m_\omega Y_0(x_\omega)}{m_\omega^2 - m_\rho^2} \right) \right.\right.$$

$$
\begin{aligned}
&+ \quad \frac{1}{M_N^2}\left(\frac{a_\rho m_\rho^3 V_{vv}(x_\rho) - a_\omega m_\omega^3 V_{vv}(x_\omega)}{m_\omega^2 - m_\rho^2}\right) \\
&+ \quad \frac{C_\rho}{2M_N^2}\left(\frac{a_\rho m_\rho^3 V_{tv}(x_\rho) - a_\omega m_\omega^3 V_{tv}(x_\omega)}{m_\omega^2 - m_\rho^2}\right)\Bigg\} \\
&+ \quad b_1' \left\{\left(\frac{a_\rho m_\rho^3 Y_0(x_\rho) - a_\omega^3 m_\omega Y_0(x_\omega)}{m_\omega^2 - m_\rho^2}\right)\right. \\
&+ \quad \frac{1}{M_N^2}\left(\frac{a_\rho m_\rho^5 V_{vv}(x_\rho) - a_\omega m_\omega^5 V_{vv}(x_\omega)}{m_\omega^2 - m_\rho^2}\right) \\
&+ \quad \frac{C_\rho}{2M_N^2}\left(\frac{a_\rho m_\rho^5 V_{tv}(x_\rho) - a_\omega m_\omega^5 V_{tv}(x_\omega)}{m_\omega^2 - m_\rho^2}\right)\Bigg\} \\
&- \quad \lambda_{\rho\omega} b_0' \left\{\left(\frac{b_\rho \Lambda_\rho Y_0(X_\rho) - b_\omega \Lambda_\omega Y_0(X_\omega)}{m_\omega^2 - m_\rho^2}\right)\right. \\
&+ \quad \frac{1}{M_N^2}\left(\frac{b_\rho \Lambda_\rho^3 V_{vv}(X_\rho) - b_\omega \Lambda_\omega^3 V_{vv}(X_\omega)}{m_\omega^2 - m_\rho^2}\right) \\
&+ \quad \frac{C_\rho}{2M_N^2}\left(\frac{b_\rho \Lambda_\rho^3 V_{tv}(X_\rho) - b_\omega \Lambda_\omega^3 V_{tv}(X_\omega)}{m_\omega^2 - m_\rho^2}\right)\Bigg\} \\
&- \quad \lambda_{\rho\omega} b_1' \left\{\left(\frac{b_\rho \Lambda_\rho^3 Y_0(X_\rho) - b_\omega \Lambda_\omega^3 Y_0(X_\omega)}{m_\omega^2 - m_\rho^2}\right)\right. \\
&+ \quad \frac{1}{M_N^2}\left(\frac{b_\rho \Lambda_\rho^5 V_{vv}(X_\rho) - b_\omega \Lambda_\omega^5 V_{vv}(X_\omega)}{m_\omega^2 - m_\rho^2}\right) \\
&+ \quad \frac{C_\rho}{2M_N^2}\left(\frac{b_\rho \Lambda_\rho^5 V_{tv}(X_\rho) - b_\omega \Lambda_\omega^5 V_{tv}(X_\omega)}{m_\omega^2 - m_\rho^2}\right)\Bigg\}\Bigg] .
\end{aligned}
\tag{5.38}
$$

Note that Eqs.(5.37) and (5.38) contain the contribution of contact terms. Thus potentials with form factors take care of the diverging behavior near the core region.

The $^1S_0$ state CSV potential for *pp* system due to ρ^0-ω mixing is shown in Fig.5.6 (left figure). The importance of the central part with relativistic correction (dashed curve) and tensor contribution (dashed-dotted curve) are clearly revealed. The magnitude of the contribution of tensor coupling is comparable with that of the central part with relativistic correction in the core region. On the other hand, magnitude of the contribution of tensor coupling is found to be much larger than the contribution of the central part (dotted curve) without relativistic correction in the core region. In the dynamical region, it is seen that all the contributions are comparable. The solid curve in this figure represents the total contribution together with the relativistic correction.

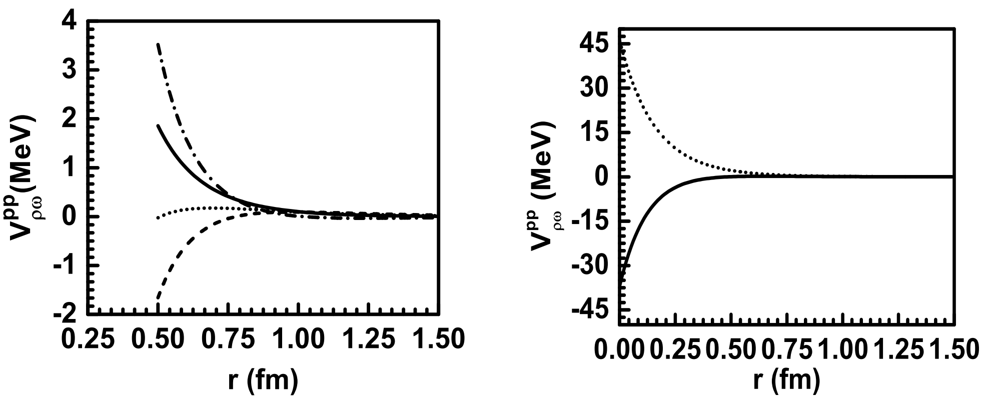

Figure 5.6: *Different parts of CSV potential in coordinate space (without form factors) i.e. the central (dotted), central with external legs plus the ρNN tensor contribution (dashed) and the spin dependent (dashed-dotted) parts at $^1S_0$ state are presented (left). On the right panel, total CSV potential with form factors for pp system is presented by the solid curve and dotted curve shows the same without $\delta \mathrm{V}^{\mathrm{pp}}_{\rho\omega}$.*

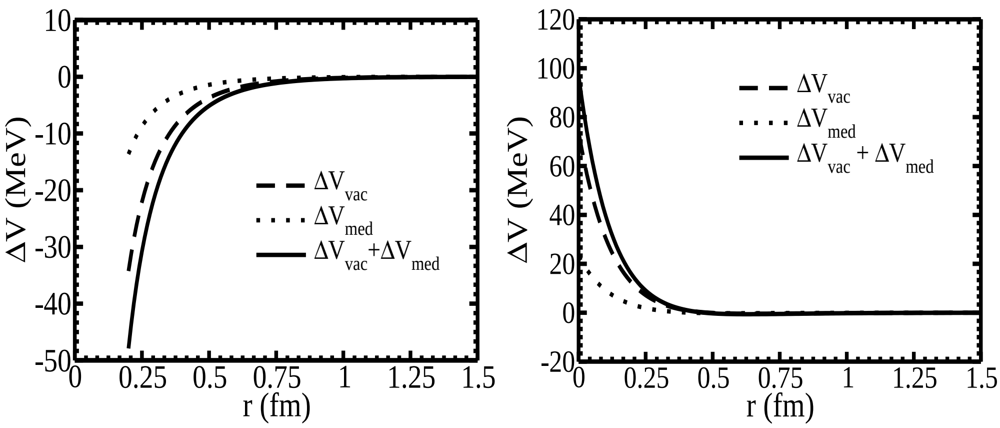

Figure 5.7: *Difference between CSV nn and pp potentials at $^1S_0$ state without (left panel) and with (right panel) formfactors.*

The $^1S_0$ CSV potential with form factors is displayed in on the right panel of the Fig.5.6. It is seen that the inclusion of $\delta \mathrm{V}^{\mathrm{NN}}_{\rho\omega}$ modifies the CSV potential dramatically. It is to be noted that, with its inclusion, the CSV potential changes sign. We show the difference of CSV potentials between nn and pp systems in Fig.5.7 for $^1\mathrm{S}_0$ state without form factor (left) and with form factor (right). To draw the density dependent part we consider nuclear matter density $\rho = 0.148$ fm^{-3} with $\alpha = 1/3$.

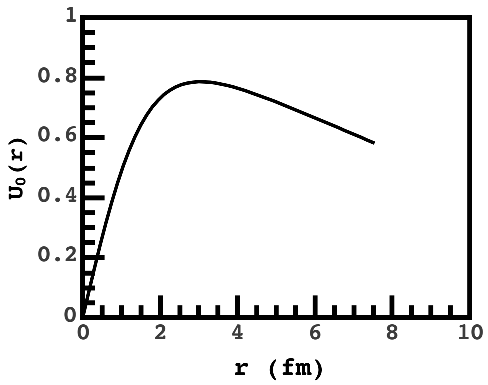

Figure 5.8: *Zero energy wave function.*

5.2 Contribution to Δa

The vacuum part of the CSV potential given in Eqs.(5.33) and (5.33)can be now used to calculate the difference between nn and pp scattering lengths at $^1S_0$ state. The difference between scattering lengths, $\Delta a = a_{pp} - a_{nn}$. The difference between CSV nn and pp potential, $\Delta V_{ij,vac} = V^{nn}_{ij,vac} - V^{pp}_{ij,vac}$, are related by

$$\Delta a = -a^2 M \int_0^\infty \Delta V_{ij,vac}\, u_0^2(r)\, dr \tag{5.39}$$

where $a^2 = a_{nn}a_{pp}$ and $u_0(r)$ is the zero energy wave function, normalized to approach $1 - r/a$ as $r \to \infty$ and $u(0) = 0$. To calculate Δa we use the following zero energy wave function [173]:

$$u_0(r) \;=\; \left[1 - \frac{r}{a}\right] - \left[\gamma(1-\lambda)\frac{r}{2} + (1+\lambda)\right] \frac{e^{-\gamma r}}{1+\lambda e^{-\gamma r}}, \tag{5.40}$$

where $\lambda = (1 - 2r_0/a)^{-1/2}$, $\gamma = 2(1+\lambda)/(r_0\lambda)$ and r_0 is the effective range.

In the present calculation we take $r_0 = 2.8$ fm to calculate the Δa. The difference in scattering length Δa, was computed using the vacuum CSV potentials constructed using $\mathbf{q}^2$ dependent π-η and ρ-ω mixing amplitudes. The results are presented in Table 5.1. It is found that the contribution of π-η mixing to Δa is negligible compared to that of ρ-ω mixing. Δa changes sign with the inclusion of form factors. The value of Δa when calculated using the potential of Eq.(5.37) is markedly different from that calculated ignoring the term $\delta \mathrm{V}^{\mathrm{NN}}_{\rho\omega}$. It would be

Table 5.1: *Difference between pp and nn scattering lengths at* $^1S_0$.

		Δa fm	
		without form factor	with form factor
π-η mixing		0.00082	-0.0001
ρ-ω mixing	$C_\rho = 0$	0.31	-0.06
	$C_\rho = 6.1$	2.14	-0.08

interesting to apply the potential presented here to calculate various other CSV observables to delineate the role of tensor interaction further.

Chapter 6

Effective Hadron Mass with Mixing

In this chapter we shall discuss the effect of isovector-isoscalar meson mixing on the mass and dispersion of hadrons in ANM. Such mixing of isospin pure states like π-η, ρ-ω is observed in vacuum due to n-p mass difference and has been studied in Ref. [148, 149]. But the mechanism we propose here for mixing is generically different. Here, as we shall see, it is driven by the difference of the proton and neutron Fermi momentum *i.e.* $k_p \neq k_n$ and thus it is a purely density dependent effect. We show that how the mixing modifies the π and η meson masses. This above phenomenon, to the best of our knowledge, has not been addressed before.

To focus exclusively on the density dependent effect we neglect explicit symmetry breaking and take $M_p = M_n$. Moreover, we consider the modification of in-medium nuclear mass, M^*, due to scalar mean field while neglecting the contribution of vector mean field. We consider the PV coupling for πNN and ηNN interactions. In this representation, the density dependent part of the self-energy is given by

$$\Pi^{*PV,(N)}_{ij,med}(q^2) = -8\left(\frac{g_i}{2M}\right)\left(\frac{g_j}{2M}\right)\int_0^1 \frac{d^3\mathbf{k}}{(2\pi)^3 E^*_N}\left[\frac{q^2\ M^{*2}}{q^4 - 4(k\cdot q)^2}\right]\theta(k_N - |\mathbf{k}|). \quad (6.1)$$

Here, $i(j) = \pi, \eta$ and N denotes the particle index and $E^*_N = \sqrt{k_N^2 + M_N^{*2}}$. We restrict ourselves in the long wave length limit *i.e.* when the pion or eta momentum ($|\mathbf{q}|$) is small compared to the Fermi momentum($k_{p,n}$) of the system. In this situation the concept of individual scattering breaks and the many body effects manifest strongly. In this condition we may neglect the q^4 term compared to $4(k \cdot q)^2$ from the denominator of Eq.(6.1) as we have seen before in [129]. In effect this captures the spirit of hard nucleon loop approximation [133].

$$\Pi^{*PV,(N)}_{ij,med}(q^2) = \frac{1}{2}\left(\frac{\mathrm{g}_i}{2\pi\ M}\right)\left(\frac{\mathrm{g}_j}{2\pi\ M}\right)\left[\ln\left|\frac{1+v_N}{1-v_N}\right| - c_0 \ln\left|\frac{1+\frac{v_N}{c_0}}{1-\frac{v_N}{c_0}}\right|\right]. \tag{6.2}$$

where $c_0 = \frac{q_0}{|\mathbf{q}|}$ and $v_N = \frac{k_N}{E^*_N}$. To find the in-medium meson mass, we substitute $\mathbf{q} = 0$ in Eq.(6.2) and making suitable density expansion we obtain the total π and η self-energy, and π-η mixing amplitude in ANM.

$$\Pi^{*PV}_{\pi\pi,med}(q_0^2) = \Omega^{PV}_{\pi\pi,med}\ q_0^2\ , \tag{6.3a}$$

$$\Pi^{*PV}_{\eta\eta,med}(q_0^2) = \Omega^{PV}_{\eta\eta,med}\ q_0^2\ , \tag{6.3b}$$

$$\Pi^{*PV}_{\pi\eta,med}(q_0^2) = \Omega^{PV}_{\pi\eta,med}\ q_0^2\ , \tag{6.3c}$$

where,

$$\Omega^{PV}_{\pi\pi,med} = \left(\frac{\mathrm{g}_\pi\ M^*}{2\pi\ M}\right)\left(\frac{\mathrm{g}_\pi\ M^*}{2\pi\ M}\right)\left[\frac{1}{3}\left(\frac{k_p^3}{E_p^{*3}} + \frac{k_n^3}{E_n^{*3}}\right) + \frac{1}{5}\left(\frac{k_p^5}{E_p^{*5}} + \frac{k_n^5}{E_n^{*5}}\right)\right], \tag{6.4a}$$

$$\Omega^{PV}_{\eta\eta,med} = \left(\frac{\mathrm{g}_\eta\ M^*}{2\pi\ M}\right)\left(\frac{\mathrm{g}_\eta\ M^*}{2\pi\ M}\right)\left[\frac{1}{3}\left(\frac{k_p^3}{E_p^{*3}} + \frac{k_n^3}{E_n^{*3}}\right) + \frac{1}{5}\left(\frac{k_p^5}{E_p^{*5}} + \frac{k_n^5}{E_n^{*5}}\right)\right], \tag{6.4b}$$

$$\Omega^{PV}_{\pi\eta,med} = \left(\frac{\mathrm{g}_\pi\ M^*}{2\pi\ M}\right)\left(\frac{\mathrm{g}_\eta\ M^*}{2\pi\ M}\right)\left[\frac{1}{3}\left(\frac{k_p^3}{E_p^{*3}} - \frac{k_n^3}{E_n^{*3}}\right) + \frac{1}{5}\left(\frac{k_p^5}{E_p^{*5}} - \frac{k_n^5}{E_n^{*5}}\right)\right]. \tag{6.4c}$$

Note the difference of sign in Eq.(6.4c) and Eq.(6.4a) or (6.4b). Clearly $\Omega^{PV}_{\pi\eta,med}$ is non-zero in ANM and vanishes for $E^*_p = E^*_n$.

In presence of mixing the pion and eta propagation gets coupled with each other and can be represented by 2×2 matrix [45, 143]

$$\begin{pmatrix} 1 - \frac{\Pi^{*PV}_{\pi\pi,med}}{q_0^2\ -\ m_\pi^2} & \frac{\Pi^{*PV}_{\pi\eta,med}}{q_0^2\ -\ m_\pi^2} \\ \\ \frac{\Pi^{*PV}_{\pi\eta,med}}{q_0^2\ -\ m_\eta^2} & 1 - \frac{\Pi^{*PV}_{\eta\eta,med}}{q_0^2\ -\ m_\eta^2} \end{pmatrix}. \tag{6.5}$$

Shifted masses are obtained by solving the following equation.

$$\left(q_0^2 - m_\pi^2 - \Pi^{*PV}_{\pi\pi,med}(q_0^2)\right)\left(q_0^2 - m_\eta^2 - \Pi^{*PV}_{\eta\eta,med}(q_0^2)\right) - \left(\Pi^{*PV}_{\pi\eta,med}(q_0^2)\right)^2 = 0\ . \tag{6.6}$$

The above equation Eq.6.6 can be simplified to

$$q_0^4(1-\Delta_{\pi\eta}) - q_0^2(m_{\pi^0}^{*2} + m_\eta^{*2}) + m_{\pi^0}^{*2} m_\eta^{*2} = 0\ , \tag{6.7}$$

where,

$$\Delta_{\pi\eta} = \left(\frac{\Omega^{PV}_{\pi\eta,med}}{1\ -\ \Omega^{PV}_{\pi\pi,med}}\right)\ \left(\frac{\Omega^{PV}_{\pi\eta,med}}{1\ -\ \Omega^{PV}_{\eta\eta,med}}\right)\ , \tag{6.8}$$

and $m^*_{\pi^0}$ and m^*_η are the effective masses of π^0 and η given by

$$m_\pi^{*2} = \frac{m_\pi^2}{1\ -\ \Omega^{PV}_{\pi\pi,med}}\ , \qquad m_\eta^{*2} = \frac{m_\eta^2}{1\ -\ \Omega^{PV}_{\eta\eta,med}}\ . \tag{6.9}$$

These in-medium masses, $m^*_{\pi^0}$ and m^*_η are further modified by π-η mixing and the mixing modified effective masses can be found by solving Eq.6.7 which read

$$\tilde{m}_{\pi^0} \simeq m^*_{\pi^0}(1+\frac{1}{2}\Delta_{\pi\eta}) - \frac{m^*_\eta}{2}\left[\frac{m^*_{\pi^0} m^*_\eta}{m_\eta^{*2} - m_\pi^{*2}}\right]\Delta_{\pi\eta}, \tag{6.10a}$$

$$\tilde{m}_{\eta} \simeq m^*_{\eta}(1+\frac{1}{2}\Delta_{\pi\eta}) + \frac{m^*_{\pi^0}}{2}\left[\frac{m^*_{\pi^0} m^*_\eta}{m_\eta^{*2} - m_\pi^{*2}}\right]\Delta_{\pi\eta}. \tag{6.10b}$$

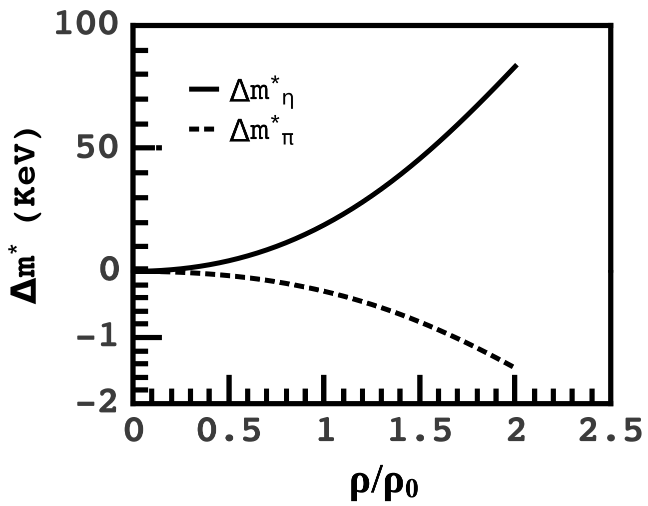

Figure 6.1: *Mixing modified mass shift in ANM.*

Here, $\tilde{m}_{\pi^0}$ ($\tilde{m}_{\eta^0}$) denotes the mixing modified pion (eta) mass. Note that in SNM, mixing does not further modify the in-medium masses as $\Delta_{\pi\eta} = 0$ or $\Omega^{PV}_{\pi\eta,med} = 0$. From Eq.(6.10a) and Eq.(6.10b), it is clear that, in ANM, due to mixing the effective masses of π increases and that of η decreases.In Fig.6.1 we show the mixing modified mass shift, $\Delta m^* = \tilde{m} - m^*$ at $\alpha = 0.2$ as a function of density.

Finally we present pionic dispersion relation along with the dispersion relation of eta in ANM with the possible π-η mixing:

$$(q_0^2)_{\pi^0} \simeq \tilde{m}^2_{\pi^0} - \left[\frac{m^{*2}_{\pi^0}(\gamma_{\pi\pi} + \gamma_{\eta\eta} - \delta_{\pi\eta})}{(1-\Delta_{\pi\eta})(m^{*2}_{\eta} - m^{*2}_{\pi^0})} - \frac{(\gamma_{\pi\pi} m^{*2}_{\eta} + \gamma_{\eta\eta} m^{*2}_{\pi^0})}{(m^{*2}_{\eta} - m^{*2}_{\pi^0})}\right]\mathbf{q}^2, \tag{6.11a}$$

$$(q_0^2)_{\eta} \simeq \tilde{m}^2_{\eta} + \left[\frac{m^{*2}_{\eta}(\gamma_{\pi\pi} + \gamma_{\eta\eta} - \delta_{\pi\eta})}{(1-\Delta_{\pi\eta})(m^{*2}_{\eta} - m^{*2}_{\pi^0})} - \frac{(\gamma_{\pi\pi} m^{*2}_{\eta} + \gamma_{\eta\eta} m^{*2}_{\pi^0})}{(m^{*2}_{\eta} - m^{*2}_{\pi^0})}\right]\mathbf{q}^2, \tag{6.11b}$$

Where,

$$\delta_{\pi\eta} = 4\,\Omega^{PV}_{\pi\eta,med}\left[\frac{\Omega^{PV}_{\pi\eta,med} - \beta_{\pi\eta,med}}{\left(1 - \Omega^{PV}_{\pi\pi,med}\right)\left(1 - \Omega^{PV}_{\eta\eta,med}\right)}\right], \tag{6.12}$$

$$\beta_{\pi\eta,med} = \left(\frac{\mathrm{g}_\pi}{2\pi}\frac{M^*}{M}\right)\left(\frac{\mathrm{g}_\eta}{2\pi}\frac{M^*}{M}\right)\left[\frac{k_p^5/E_p^{*5} - k_n^5/E_n^{*5}}{10\left(1 - \Omega^{PV}_{\pi\eta,med}\right)}\right]. \tag{6.13}$$

The pure density dependent mixing at the $\eta-$pole is estimated to be $\Pi^{*PV}_{\pi\eta,med} = -1217.475$ MeV^2, $\Pi^{*PV}_{\pi\eta,med} = -1661.11$ MeV^2, at $\alpha = 0.2$ and $\alpha = 0.3$, respectively at normal nuclear matter density with coupling parameters same as those of [148]. It is seen that even at normal nuclear matter density the mixing amplitudes are of the same order as that of the vacuum mixing amplitude, $\Pi^{*PV}_{\pi\eta,med} = -4200$ MeV^2 [148].

Chapter 7

Summary and Conclusion

In this thesis we have investigated the hadronic properties in nuclear matter (NM), in particular we focus on the asymmetric nuclear matter (ANM) where the results for symmetric nuclear matter (SNM) appear as a limiting case. First we have examined the properties of pion in ANM, in particular the mass splitting of different charge states of pion is clearly revealed along with their full dispersion characteristics.

The in-medium modifications of pion properties in ANM has been studied in chapter 3 within the framework of relativistic hadrodynamics in presence of the scalar mean field. We start with the model developed in [122] and present analytical results for the pion dispersion relations by making HNL approximation and suitable density expansion of the pion self-energy calculated at the one-loop level. We also discussed the contribution of Dirac vacuum to the dispersion relations as well as its contribution to the in-medium pion masses. Subsequently, we invoke the chirally invariant Lagrangian [174,175] by retaining only the lowest order terms in pion field and compare the results with non-chiral model calculations.

The splitting of various isospin modes of pion in ANM is found to be quite significant even at normal nuclear matter density. Such mass splitting is important as it is related to the pion-nucleus optical potential [105,129]. It is found that the π^- in neutron rich matter experiences more repulsion than π^0 and π^+ in agreement with the chiral perturbation theory calculation [105]. Such mode splittings in ANM is, in fact, a generic feature of all the isovector mesons. Therefore, it would be interesting to estimate similar splitting for the ρ meson and other isovector states.

In addition to the isospin mode splitting of pion, we have studied the mixing of hadrons in chapter 4 which is an isospin symmetry breaking effect resulting from the asymmetry in the number of protons and neutrons in the ground state. We have concentrated on π-η and ρ-ω mixing via nucleon-nucleon excitations in ANM. In principle such mixing should be derived from Quantum Chromodynamics (QCD). We, in the present work, restrict ourselves to the hadronic model which has reasonable phenomenological success. It would be interesting to compare the present estimates of the mixing amplitude with calculations from other models, for example, QCD in large N_c limit or QCD sum rule etc.

The mixing amplitude in ANM is found to be non-vanishing even if $M_p = M_n$. In SNM, with degenerate nucleon mass the proton and neutron loop contributions exactly cancel. It is found that the estimated values of on-shell vacuum mixing amplitudes for both π-η and ρ-ω mixing are in well agreement with the experimental values. We have studied the effect of density dependent π-η mixing on π^0 and η meson masses in chapter 6, considering the scalar mean field to understand the effect of interacting ground state. It is shown that the mixing further modifies the masses of pion and eta mesons. The effective pion mass is found to decrease by the π-η mixing while eta mass increases. Though the mixing effect in this case is not large.

In chapter 5, we constructed various charge symmetry violating (CSV) potentials with corrections due to n-p mass difference coming from the external legs. This modifies the existing potential and contribution is found to be significant. Then we incorporate the medium effect with the density dependent mixing amplitudes calculated in chapter 4 to determine CSV potential in ANM. It is to be noted that here we use three momentum dependent mixing amplitudes to construct CSV potentials within the framework of one boson exchange (OBE) model. It is observed that density dependent contribution of π-η mixing is larger than the vacuum contribution near the core region. In case of ρ-ω mixing it is found that the vacuum mixing amplitude and the density dependent mixing amplitude are of similar order of magnitude and both contribute with the same sign. We have shown that the contribution of density dependent CSV potential is not negligible in comparison to the vacuum CSV potential. Various CSV observables will be able to probe such effects.

It is observed in this work that the contributions coming from the external legs are important, particularly in the isovector sector, because of the strength of the ρNN tensor interactions. The charge symmetry violation at the external legs were ignored in the previous work [149]. The strength of the CSV interaction could be significantly larger even when the off-shell amplitude for the ρ^0 -ω mixing is considered. It is important to note that contribution from the spinors also modifies the central part of the two-body potential. It is observed that both for the density dependent and vacuum parts, the role of π-η mixing is smaller than that of ρ-ω mixing. We have estimated the contribution of π-η and ρ-ω mixing to the difference of pp and nn scattering lengths at $^1S_0$ state, where only the vacuum part of the CSV potential contributes. The π-η contribution is found negligible compared to that of ρ-ω mixing. We have shown explicitly the contribution of $\delta \mathrm{V}_{\rho\omega}^{\mathrm{NN}}$ and it is found that Δa changes sign with the inclusion of $\delta \mathrm{V}_{\rho\omega}^{\mathrm{NN}}$.

As a future outlook, it might be noted that in-medium properties of pion in asymmetric nuclear matter find major applications in astrophysics where there are enough scope to extend the present investigation. In particular, the inclusion of Δ resonance might be an important step forward in this direction. On the other hand the two-body CSV potential as presented here might be applied to see its consequences on experimental observables and on existing calculations. Furthermore, the mixing phenomena, particular the ρ-ω mixing can have important contribution to the dilepton spectra in experiments with high baryon density. Therefore this might be relevant for the compressed baryonic matter studies - an area which remains relatively unexplored.

Appendix A

Mechanism of mixing

Mixing at QCD level

The mixing of hadrons can be understood at the QCD level. In the presence of charge independence, the neutral mesons of u-d flavor are pure isospin states *viz.*

$$|T=1\,\rangle = \frac{1}{\sqrt{2}}(|u\bar{u}\,\rangle - |d\bar{d}\,\rangle)\ , \quad \text{and} \quad |T=0\,\rangle = \frac{1}{\sqrt{2}}(|u\bar{u}\,\rangle + |d\bar{d}\,\rangle)\ . \tag{A.1}$$

Now consider the interaction Hamiltonian

$$H = m_d\ \bar{d}d + m_u\ \bar{u}u\ . \tag{A.2}$$

The mixing matrix element

$$\langle\, T=1|H_m|T=0\,\rangle = m_u - m_d \neq 0\ . \tag{A.3}$$

It is clear from the above equation that the mixing of $|T=1\,\rangle$ and $|T=0\,\rangle$ states yields non-vanishing mixing matrix element as $m_u \neq m_d$. The neutral mesons are mixtures of $|T=0\,\rangle$ and $|T=1\,\rangle$ states, for example

$$|\rho^0\,\rangle = a_1|T=0\,\rangle + a_2|T=1\,\rangle \quad \text{and} \quad |\omega\,\rangle = b_1|T=0\,\rangle + b_2|T=1\,\rangle\,, \tag{A.4}$$

Thus the matrix element of ρ^0-ω mixing at the QCD level is found to be

$$\langle\, \rho^0|H_m|\omega\,\rangle \sim m_u - m_d. \tag{A.5}$$

which is non vanishing.

Appendix **B**

Dimensional regularization

★ PS coupling

After using Feynman parametrization, the term $\Pi^{*PS}_{\pi\pi,vac}(q^2)$ in Eq.(3.20) can be written as

$$\begin{aligned}
\Pi^{*PS}_{\pi\pi,vac}(q^2) &= 8i\mathrm{g}_\pi^2\mu^{2\epsilon}\int_0^1 dx\int\frac{d^Nk}{(2\pi)^N}\left[\frac{M^{*2}-k\cdot(k+q)}{((k+qx)^2+q^2x(1-x)-M^{*2})^2}\right]\\
&= \frac{\mathrm{g}_\pi^2}{2\pi^2}\int_0^1 dx\,(4\pi\mu^2)^\epsilon\,\frac{\Gamma(\epsilon)}{1-\epsilon}\left[\frac{M^{*2}-3q^2x(1-x)+2\epsilon q^2x(1-x)}{(M^{*2}-q^2x(1-x))^\epsilon}\right]\\
&= \frac{\mathrm{g}_\pi^2}{2\pi^2}\frac{q^2}{3}+\frac{g_\pi^2}{2\pi^2}\frac{1}{\epsilon}\left(M^{*2}-\frac{q^2}{2}\right)\\
&- \frac{\mathrm{g}_\pi^2}{2\pi^2}\left(M^{*2}-\frac{q^2}{2}\right)\left(\gamma_E'-\ln\left(4\pi\mu^2\right)\right)\\
&- \frac{\mathrm{g}_\pi^2}{2\pi^2}\int_0^1 dx\left(M^{*2}-3q^2x(1-x)\right)\ln\left(M^{*2}-q^2x(1-x)\right)\ . \qquad \text{(B.1)}
\end{aligned}$$

Here $\epsilon = 2-\frac{N}{2}$ and μ is an arbitrary scaling parameter. γ_E is the Euler-Mascheroni constant and $\gamma_E' = (\gamma_E - 1)$. The imaginary part of $\Pi^{*PS}_{\pi\pi,vac}(q^2)$ can easily be found by simply replacing $\ln(M^{*2}-q^2x(1-x))$ with $\ln(M^{*2}-q^2x(1-x)\ \ -i\xi)$ where ξ is an arbitrarily small parameter and the term $i\xi$ comes from the denominator of G_N^{*F} when Feynman parametrization is performed considering $i\zeta$ in the denominator of the propagator.

Here the term $\ln(M^{*2}-q^2x(1-x))$ has branch cut only for $M^{*2}-q^2x(1-x)<0$ and it begins at $q^2=4M^{*2}$ *i.e.* the threshold condition for nucleon-antinucleon pair production. So the limit of x-integration changes from $(0,1)$ to $(\frac{1}{2}-\frac{1}{2}\alpha,\frac{1}{2}+\frac{1}{2}\alpha)$

where $\alpha = \sqrt{1 - \frac{4M^{*2}}{q^2}}$ and we used $\mathrm{Im}\ln\left(Z - i\xi\right) = -\pi$.Now,

$$\int_{\frac{1}{2}-\frac{1}{2}\alpha}^{\frac{1}{2}+\frac{1}{2}\alpha} dx\ \theta\left(q^2 - 4M^{*2}\right) \ = \ \sqrt{1 - \frac{4M^{*2}}{q^2}}\ \theta\left(q^2 - 4M^{*2}\right)\ . \tag{B.2}$$

The imaginary part of $\Pi^{*PS}_{\pi\pi,vac}(q^2)$ is,

$$\begin{aligned} \mathrm{Im}\ \Pi^{*PS}_{\pi\pi,Vac}(q^2) &= -\frac{\mathrm{g}_\pi^2}{2\pi^2}\int_0^1 dx\ \left(M^{*2} - 3q^2x(1-x)\right) \\ &\times\ \mathrm{Im}\left[\ln\left(M^{*2} - q^2x(1-x) - i\xi\right)\right] \\ &= -\frac{\mathrm{g}_\pi^2}{4\pi}\left[q\sqrt{q^2 - 4M^{*2}}\right]\ \theta\left(q^2 - 4M^{*2}\right)\ . \end{aligned} \tag{B.3}$$

It is clear from the expression of Eq.(B.1) that the second term is divergent in the limit $\epsilon\ \to\ 0$ (as $N\ \to\ 4$). To remove the divergences we need to add the counterterms [122] in the original Lagrangian interaction . The diverging part of Eq.(B.1) is

$$\begin{aligned} \mathcal{D}_{PS} &= \frac{\mathrm{g}_\pi^2}{2\pi^2}\frac{1}{\epsilon}\left(M^{*2} - \frac{q^2}{2}\right) \\ &= \frac{\mathrm{g}_\pi^2}{2\pi^2}\left[\frac{M^2}{\epsilon} - \frac{2}{\epsilon}M\mathrm{g}_s\phi_0 + \frac{1}{\epsilon}\mathrm{g}_s^2\phi_0^2 - \frac{q^2}{2\epsilon}\right]\ . \end{aligned} \tag{B.4}$$

In Eq.(B.4) we substitute the effective nucleon mass $M^* = (M - \mathrm{g}_s\phi_0)$ where M is the nucleon mass and ϕ_0 is the vacuum expectation value of the scalar field ϕ_s. The expression given in Eq.(B.4) tells us that we need to be added four counter terms [122] with the original interaction Lagrangian to remove the divergences from $\Pi^{*PS}_{\pi\pi,vac}(q^2)$. Therefore the counter term Lagrangian [122] is denoted as

$$\mathcal{L}_{CT} = -\ \frac{1}{2!}\beta_1\Phi_\pi\cdot\left(\partial^2 + m_\pi^2\right)\cdot\Phi_\pi + \frac{1}{2!}\beta_2\Phi^2 + \frac{1}{2!}\beta_3\phi_s\Phi_\pi^2 + \frac{1}{2!2!}\beta_4\phi^2\Phi_\pi^2\ . \tag{B.5}$$

The value of the counterterms β_1, β_2, β_3 and β_4 are determined by imposing the appropriate renormalization conditions.

$$\beta_1 = \left(\frac{\partial\Pi^{*PS}_{\pi\pi,vac}(q^2)}{\partial q^2}\right)_{q^2=m_\pi^2} \tag{B.6}$$

$$\beta_2 = \left(\Pi^{*PS}_{\pi\pi,vac}\right)_{q^2=m_\pi^2} \tag{B.7}$$

$$\beta_3 = -g_s \left(\frac{\partial \Pi^{*PS}_{\pi\pi,vac}(q^2)}{\partial M} \right)_{q^2=m_\pi^2} \tag{B.8}$$

$$\beta_4 = -\delta\lambda + g_s^2 \left(\frac{\partial^2 \Pi^{*PS}_{\pi\pi,vac}(q^2)}{\partial M^2} \right)_{q^2=m_\pi^2} \tag{B.9}$$

Here β_1 and β_2 are the wave function and pion mass renormalization counterterms respectively while β_3 and β_4 are the vertex renormalizaton counterterms for the $\phi_s\Phi_\pi^2$ vertex and $\phi_s^2\Phi_\pi^2$ vertex respectively. The conditions of Eq.(B.6)-(B.7) implies that the pion propagator $\tilde{\Delta}_\pi = [q^2 - m_\pi^2 - \tilde{\Pi}^{*PS}_{\pi\pi,vac}(q^2)]^{-1}$ reproduces the physical mass of pions in free space. The counterterm β_4 determines the strength of coupling of the $\phi_s^2\Phi_\pi^2$ vertex. In fact $\Pi^{*PS}_{\pi\pi,vac}(q^2)$ is found by simply replacing M^* with M in Eq.(B.1). We can set $\delta\lambda = 0$ to minimize the effects of many-body forces in the nuclear medium [122] which is consistent with the renormalization scheme for scalar meson. Using the onditions given in Eqs.(B.6)-(B.9) the following results are found:

$$\begin{aligned}
\beta_1 &= \frac{g_\pi^2}{2\pi^2}\left[\frac{1}{3} - \frac{1}{2}\left(\frac{1}{\epsilon} - \gamma_E' + \ln(4\pi\mu^2)\right)\right] \\
&+ \frac{g_\pi^2}{2\pi^2}\left[\int_0^1 dx\; 3x(1-x)\ln\left(M^2 - m_\pi^2 x(1-x)\right)\right] \\
&+ \frac{g_\pi^2}{2\pi^2}\left[\int_0^1 dx \frac{M^2 x(1-x) - 3m_\pi^2 x^2(1-x)^2}{M^2 - m_\pi^2 x(1-x)}\right] ,
\end{aligned} \tag{B.10}$$

$$\begin{aligned}
\beta_2 &= \frac{g_\pi^2}{2\pi^2}\left[\frac{m_\pi^2}{2} + \left(M^2 - \frac{m_\pi^2}{3}\right)\left(\frac{1}{\epsilon} - \gamma_E' + \ln(4\pi\mu^2)\right)\right] \\
&- \frac{g_\pi^2}{2\pi^2}\int_0^1 dx\; \left(M^2 - 3m_\pi^2 x(1-x)\right) \\
&\times \ln(M^2 - m_\pi^2 x(1-x)) ,
\end{aligned} \tag{B.11}$$

$$\begin{aligned}
\beta_3 &= \frac{g_\pi^2}{2\pi^2}\left[-g_s(2M)\left(\frac{1}{\epsilon} - \gamma_E' + \ln(4\pi\mu^2)\right)\right] \\
&+ \frac{g_\pi^2}{2\pi^2}\left[g_s(2M)\int_0^1 dx \ln(M^2 - m_\pi^2 x(1-x)\right] \\
&+ \frac{g_\pi^2}{2\pi^2}\left[g_s(2M)\int_0^1 dx \left(\frac{M^2 - 3m_\pi^2 x(1-x)}{M^2 - m_\pi^2 x(1-x)}\right)\right] ,
\end{aligned} \tag{B.12}$$

$$
\begin{aligned}
\beta_4 &= -\frac{\mathrm{g}_\pi^2}{2\pi^2}6\mathrm{g}_s^2 + \frac{\mathrm{g}_\pi^2}{2\pi^2}\left[2\mathrm{g}_s\left(\frac{1}{\epsilon} - \gamma_E' + \ln(4\pi\mu^2)\right)\right] \\
&- \frac{\mathrm{g}_\pi^2}{2\pi^2}\left[2\mathrm{g}_s^2\int_0^1 dx \ln(M^2 - m_\pi^2 x(1-x))\right] \\
&- \frac{\mathrm{g}_\pi^2}{2\pi^2}\left[2\mathrm{g}_s^2\int_0^1 dx\frac{4M^2 m_\pi^2 x(1-x)}{(M^2 - m_\pi^2 x(1-x))^2}\right] . \qquad \text{(B.13)}
\end{aligned}
$$

The renormalized $\Pi^{*PS}_{\pi\pi,vac}(q^2)$ is

$$
\tilde{\Pi}^{*PS}_{\pi\pi,vac}(q^2) = \Pi^{*PS}_{\pi\pi,vac}(q^2) - \beta_1(q^2 - m_\pi^2) - \beta_2 - \beta_3\phi_0 - \frac{1}{2}\beta_4\phi_0^2 . \qquad \text{(B.14)}
$$

Substituting $\Pi^{*PS}_{\pi\pi,vac}(q^2)$ from Eq.(B.1) and β_1, β_2, β_3, β_4 from Eqs.(B.10)- (B.13) in Eq.(B.14) it is found that divergences in $\Pi^{*PS}_{\pi\pi,vac}(q^2)$ are completely eliminated by the counterterms. After simplification $\tilde{\Pi}^{*PS}_{\pi\pi,vac}(q^2)$ reduces to

$$
\begin{aligned}
\tilde{\Pi}^{*PS}_{\pi\pi,vac}(q^2) &= \frac{g_\pi^2}{2\pi^2}\left[-3(M^2 - M^{*2}) + (q^2 - m_\pi^2)\left(\frac{1}{6} + \frac{M^2}{m_\pi^2}\right) - 2M^{*2}\ln\left(\frac{M^*}{M}\right)\right. \\
&+ \frac{8M^2(M - M^*)^2}{(4M^2 - m_\pi^2)} - \frac{2M^{*2}\sqrt{4M^{*2} - q^2}}{q}\tan^{-1}\left(\frac{q}{\sqrt{4M^{*2} - q^2}}\right) \\
&+ \frac{2M^2\sqrt{4M^2 - m_\pi^2}}{m_\pi}\tan^{-1}\left(\frac{m_\pi}{\sqrt{4M^2 - m_\pi^2}}\right) \\
&+ \left((M^2 - M^{*2}) + \frac{m_\pi^2(M - M^*)^2}{(4M^2 - m_\pi^2)} + \frac{M^2}{m_\pi^2}(q^2 - m_\pi^2)\right) \\
&\times \frac{8M^2}{m_\pi\sqrt{4M^2 - m_\pi^2}}\tan^{-1}\left(\frac{m_\pi}{\sqrt{4M^2 - m_\pi^2}}\right) \\
&+ \left.\int_0^1 dx\ 3x(1-x)q^2\ln\left(\frac{M^{*2} - q^2 x(1-x)}{M^2 - m_\pi^2 x(1-x)}\right)\right] . \qquad \text{(B.15)}
\end{aligned}
$$

★ PV coupling

After Feynman parametrization Eq.(3.43) reduces to

$$
\begin{aligned}
\Pi^{*PV}_{\pi\pi,vac}(q^2) &= 8i\left(\frac{f_\pi}{m_\pi}\right)^2\mu^{2\epsilon}\int_0^1 dx \\
&\times \int\frac{d^N k}{(2\pi)^N}\left[\frac{(M^{*2} + q^2 x(1-x) + k^2)\,q^2 - 2(k\cdot q)^2}{((k + qx)^2 + q^2 x(1-x) - M^{*2})^2}\right]
\end{aligned}
$$

$$
\begin{aligned}
&= -q^2 \left(\frac{f_\pi}{\pi\ m_\pi}\right)^2 \int_0^1 dx\, \left(4\pi\mu^2\right)^\epsilon \Gamma(\epsilon) \left[\frac{2M^{*2}}{\left(M^{*2}-q^2x(1-x)\right)^\epsilon}\right] \\
&= q^2\ M^{*2} \left(\frac{f_\pi}{\pi\ m_\pi}\right)^2 \left[-\frac{1}{\epsilon} + \left(\gamma_E - \ln\left(4\pi\mu^2\right)\right)\right. \\
&+ \left.\int_0^1 dx\ \ln\left(M^{*2} - q^2 x(1-x)\right)\right] . \qquad \text{(B.16)}
\end{aligned}
$$

The imaginary part of $\Pi^{*PV}_{\pi\pi,vac}(q^2)$ can be found as

$$
\mathrm{Im}\ \Pi^{*PV}_{\pi\pi,vac}(q^2) = -2q\ M^{*2} \left(\frac{f_\pi}{\pi\ m_\pi}\right)^2 \sqrt{q^2-4M^{*2}}\ \theta\left(q^2-4M^{*2}\right) . \qquad \text{(B.17)}
$$

It is clear from Eq.(B.17) that $\Pi^{*PV}_{\pi\pi,vac}(q^2)$ vanishes for $q^2 < 4M^{*2}$. With the same argument as stated for PS coupling, we excluded the imaginary part. The diverging part of $\Pi^{*PV}_{\pi\pi,vac}(q^2)$ is

$$
\mathcal{D}_{PV} = -\ q^2\ M^{*2} \left(\frac{f_\pi}{\pi\ m_\pi}\right)^2 \frac{1}{\epsilon} \qquad \text{(B.18)}
$$

Here we use simple subtraction method to remove the divergence. So, the finite FF part of the self-energy is

$$
\begin{aligned}
\tilde{\Pi}^{*PV}_{\pi\pi,vac}(q^2) &= \Pi^{*PV}_{\pi\pi,vac}(q^2) - \Pi^{*PV}_{\pi\pi,vac}(q^2 = m_\pi^2) \\
&= q^2\ M^{*2} \left(\frac{f_\pi}{\pi m_\pi}\right)^2 \int_0^1 dx\ \ln\left(\frac{M^{*2}-q^2x(1-x)}{M^{*2}-m_\pi^2x(1-x)}\right) \qquad \text{(B.19)}
\end{aligned}
$$

Subhrajyoti Biswas
25/04/13

References

[1] H. C. Jean and J. Piekarewicz and A. G. Williams, Phys. Rev. **C 49**, 1981 (1994).

[2] H. Shiomi, T. Hatsuda, Phys. Lett. **B 334**, 281 (1994).

[3] X-Jin and D. B. Leinweber, Phys. Rev. **C 52**, 3344 (1995).

[4] R. Rapp, G. Chanfray and J. Wambach, Nucl. Phys. **A 617**, 472 (1997).

[5] M. C. Ruivo, C. A. De Sousa, B. Hiller and A. H. Blin, Nucl. Phys. **A 575**, 460 (1994).

[6] R. J. Furnstahl and B. D. Serot, Phys. Rev. **C 41**, 262 (1990).

[7] L. H. Xia, C. M. Ko, L. Xiong and J. Q. Wu, Nucl. Phys. **A 485**, 721 (1988).

[8] G. E. Brown and W. Weise, Phys. Rep. **C 22**, 279 (1975).

[9] S. A. Chin and J. D. Walecka, Phys. Lett. **B 52**, 24 (1974)

[10] J. D. Walecka, Ann. Phys. (N.Y.) **83**, 491 (1974).

[11] S. A. Chin, Ann. of Phys. **108**, 301 (1977).

[12] J. D. walecka, Phys. Lett. **B 59**, 109 (1975).

[13] S. A. Chin, Phys. Lett. **B 62**, 263 (1976).

[14] A. L. Fetter and J. D. Walecka, *Quantum Theory of Many Particle Systems*, McGraw-Hill, New York (1971).

[15] M. Gyulassy and L. McLerran, Nucl. Phys. **A 750**, 30 (2005).

[16] CBM Collaboration, Nucl. Phys. **A 749**, 141 (2005).

[17] A. Balanda, Heavy Ion Phys. **7**, 119 (1998).

[18] G. Q. Li, C. M. Ko and G. E. Brown, Phys. Rev. Lett. **75**, 4007 (1995).

[19] W. K. Wilson *et al.*, Nucl. Phys. **A 566**, 387c (1994).

[20] C. Nandet, Phys. Rev. Lett. **62**, 2652 (1989).

[21] G. Roche, Phys. Lett. **B226**, 228 (1989).

[22] R. A. Broglia, P. Kienle and P. F. Bartignon, *Probing the Nuclear Paradigm with Heavy Ion Reactions*, World Scientific, Singapore, (1994), p. 463.

[23] T. Ericson and W. Weise, *Pions and Nuclei*, Oxford University Press (1988).

[24] B. D. Day, Rev. Mod. Phys. **50**, 495 (1978).

[25] V. R. Pandharipande and R. B. Wiringa, Rev. Mod. Phys. **51**, 821 (1979).

[26] J. W. Zabolitzky, *Advances in Nuclear Physics*, Vol. **12**, 1, Plenum Press, New York (1981).

[27] J. W. Negele, Rev. Mod. Phys. **54**, 913 (1982).

[28] J. P. Svenne, *Advances in Nuclear Physics*, Vol. **11**, 179, Plenum Press, New York (1979).

[29] T. H. R. Skyrme, Phil. Mag. **1**, 1043 (1956).

[30] T. H. R. Skyrme, Nucl. Phys. **9**, 615 (1959).

[31] D. Gongy, *Nuclear Physics with Electromagnetic Interaction*, Vol. **108**, 88, Springer, Belin (1979).

[32] C. B. Dover and R. H. Lemmer, Phys. Rev. **165**, 1105 (1968).

[33] C. B. Dover, Ann. Phys. (N.Y.) **50**, 449 (1968).

[34] W. D. Brown, R. D. Puff and L. Wilets, Phys. Rev. **C 2**, 331 (1970).

[35] R. L. Bowers and R. L. Zimmerman, Phys. Rev. **D 7**, 296 (1973).

[36] R. L. Bowers, J. A. Campbell and R. L. Zimmerman, Phys. Rev. **D 7**, 2278 (1973).

[37] R. L. Bowers, J. A. Campbell and R. L. Zimmerman, Phys. Rev. **D 7**, 2289 (1973).

[38] L. D. Miller and A. E. S. Green, Phys. Rev. **C 5**, 241 (1972)

[39] L. D. Miller, Phys. Rev. **C 9** , 537 (1974).

[40] L. D. Miller, Phys. Rev. **C 12** , 710 (1975).

[41] R. Brockmann and W. Weise, Phys. Rev. **C 16**, 1282 (1977).

[42] R. Brockmann, Phys. Rev. **C 18**, 1510 (1978).

[43] E. E. Salpeter and H. A. Bethe, Phys. Rev. **84**, 1232 (1951).

[44] J. D. Bjorken and S. D. Drell, *Relativistic Quantum Fields*, McGraw-Hill, New York, (1965).

[45] B. D. Serot, J. D. Walecka, Adv. Nucl. Phys. **16**, 1 (1986).

[46] K. Erkelenz, Phys. Rep. **C 13** , 191 (1974).

[47] K. Holinde, Phys. Rep. **C 68**, 121 (1981).

[48] H. Yukawa, Proc. Phys. Math. Soc. Japan. **17**, 48 (1935).

[49] H. Yukawa, Proc. Phys. Math. Soc. Japan. **19**, 712 (1937).

[50] H. Yukawa and S. Sakata, Proc. Phys. Math. Soc. Japan. **19**, 1048 (1937).

[51] H. Yukawa, S. Sakata and M. Taketani, Proc. Phys. Math. Soc. Japan. **20**, 319 (1938).

[52] H. Yukawa, S. Sakata, M. Kobayasi and M. Taketani, Proc. Phys. Math. Soc. Japan. **20**, 720 (1938).

[53] M. Conversi, E. Panchini and O. Piccioni, Phys. Rev. **71**, 209, 557 (1947).

[54] A. Proca, J. Phys. Radium **7**, 347 (1936).

[55] N. Kemmer, Proc. Roy. Soc. (London) **A 166**, 127 (1938).

[56] C. Moller and L. Rosenfeld, Kgl. Danske Vid. Selskab, Math-fys. Medd. **17**, No. 8 (1940).

[57] M. Taketani, S. Nakamura and M. Sasaki, Prog. Theor. Phys. (Kyoto) **6**, 581 (1951).

[58] J. Iwadare, S. Otsuki, R. tamagaki and W. Watari, Prog. Theor. Phys. (Kyoto) **15**, 86 (1956).

[59] J. Iwadare, S. Otsuki, R. tamagaki and W. Watari, Prog. Theor. Phys. (Kyoto) **16**, 455 (1956).

[60] D. Y. Wong, Phys. Rev. Lett. **2**, 406 (1959).

[61] P. Cziffra, M. H. MacGregor, M. J. Moravcsik and H. P. Stapp, Phys. Rev. **114**, 880 (1959).

[62] G. Breit, M. H. Hull, K. E. Lassila and K. D. Pyatt, Phys. Rev. **120**, 2227 (1960).

[63] G. Breit, Rev. Mod. Phys. **34**, 766 (1962).

[64] N. K. Glendenning and G. Krammer, Phys. Rev. **126**, 2159 (1962).

[65] M. Taketani, S. Machida and S. Onuma, Prog. Theor. Phys. (Kyoto) **7**, 45 (1952).

[66] K. A. Brueckner K. M. Watson, Phys. Rev. **90**, 699 (1953).

[67] K. A. Brueckner K. M. Watson, Phys. Rev. **92**, 1023 (1953).

[68] N. Hoshizaki and S. Machida, Prog. Theor. Phys. **22**, 562 (1959).

[69] R. J. N. Phillips, Rep. Prog. Phys. **22**, 562 (1959)

[70] M. J. Moravcsik, *The Two-Nucleon Interaction*, Clarendon Press, Oxford (1963).

[71] P. Signell, Adv. Nucl. Phys. **2**, 223 (1969).

[72] R. De. Tourreil, B. Rouben and D. W. L. Sprung, Nucl. Phys. **A 242**, 445 (1975).

[73] M. M. Nagels, T. A. Rijken and J. D. de Swart, Phys. Rev. **D 17**, 768 (1978).

[74] M. M. Nagels, T. A. Rijken and J. D. de Swart, Phys. Rev. **D 20**, 1633 (1979).

[75] K. Holinde and R. Machleidt, Nucl. Phys. **A 247**, 495 (1975).

[76] K. Holinde and R. Machleidt, Nucl. Phys. **A 256**, 497 (1976).

[77] J. Fleischer and J. A. Tjon, Phys. Rev. **D 21**, 87 (1980).

[78] M. J. Zuilhof J. A. Tjon, Phys. Rev. **C 22**, 2369 (1980).

[79] J. W. Durso, A. D. Jackson and B. J. Verwest, Nucl. Phys. **A 345**, 471 (1980).

[80] R. Machleidt, K. Holinde, and Ch. Elster, Phys. Rep. **149**, 1 (1987).

[81] E. M. Henley, G. A. Miller, *Mesons in nuclei* edited by M. Rho and D. Wilkerson, North-Holland (1979).

[82] C. Y. Cheung, E. M. Henley and G. A. Miller, Phys. Rev. Lett. **43**, 1215 (1979).

[83] C. Y. Cheung, E. M. Henley and G. A. Miller, Nucl. Phys. **A 305**, 342 (1978).

[84] C. Y. Cheung, E. M. Henley and G. A. Miller, Nucl. Phys.

[85] M. St. Stevens, Phys. Lett. **19**, 499 (1965).

[86] E. M. Henley and T. E. Keliher, Nucl. Phys. **A189**, 632 (1972).

[87] B. W. Downs and Y. Nogami, Nucl. Phys. **B 2**, 459 (1967).

[88] G. A. Miller, M. K. Nefkens and I. Slaus, Phys. Rep. **194**, 1 (1990).

[89] A. B. Migdal, Rev. Mod. Phys. **50**, 107 (1978).

[90] I. M. Mishustin, F. Myhrer and P. J. Siemens, Phys. Lett. **B 95**, 361 (1980).

[91] M. Gyulassy and W. Greiner, Ann. Phys. **109**, 485 (1977).

[92] G. E. Brown, E. Oset, M. Vicente Vacas and W. Weise, Nucl. Phys. **A 505**, 823 (1989).

[93] C. Gale and J. I. Kapusta, Phys. Rev. **C 35**, 2107 (1987).

[94] E. Oset, H. Toki and W. Weise, Phys. Rep. **83**, 281 (1982).

[95] A. B. Migdal, E. E. Saperstein, M. A. Troitsky and D. N. Voskresensky, Phys. Rep. **192**, 179 (1990).

[96] V. F. Dmitriev, T. Suzuki, Nucl. Phys. **A 438**, 697 (1985).

[97] P. A. Henning, H. Umezawa, Nucl. Phys. **A 571**, 617 (1994).

[98] C. L. Korpa and R. Malfliet, Phys. Rev. **C 52**, 2756 (1995).

[99] J. Helgesson and J. Randrup, Phys. Rev. **C 52**, 427 (1995).

[100] L. Liu and M. Nakano, Nucl. Phys. **A 618**, 337 (1997).

[101] T. Herbert, K. Wehrberger and F. Beck, Nucl. Phys. **A 541**, 699 (1992).

[102] R. Rapp and J. Wambach, Adv. Nucl. Phys. **25**, 1 (2000).

[103] C. Y. Wong, *Introduction to High-Energy Heavy-Ion Collisions*, World Scientific, Singapore (1994).

[104] G. Chanfray and P. Schuck, Nucl. Phys. **A 555**, 329 (1993).

[105] N. Kaiser and W. Weise, Phys. Lett. **B 512**, 283 (2001).

[106] P. Costa, M. C. Ruivo and Yu. L. Kalinovsky, Phys. Lett. **B 560**, 171 (2003).

[107] P. Costa, M. C. Ruivo, C. A. de Sousa and Yu. L. Kalinovsky, Phys. Rev. **C 70**, 025204 (2004).

[108] G. Wolf, B. Friman and M. Soyeur, Nucl. Phys. **A 640**, 129 (1998).

[109] O. Teodorescu, A. K. Dutt-Mazumder, and C. Gale, Phys. Rev. **C 61**, 051901 (2000).

[110] K. Saito, K. Tsushima, A. W. Thomas and A. G. Williams, Phys. Lett. **B 433**, 243 (1998).

[111] J. D. Walecka, *Theoretical Nuclear Physics*, Oxford University Press, New York (1995).

[112] C. J. Horowitz and B. D. Serot, Nucl. Phys. **A 368**, 503 (1981).

[113] C. J. Horowitz and B. D. Serot, Phys. Lett. **140**, 181 (1984).

[114] M. A. Preston and R. K. Bhaduri, *Structure of the Nucleus*, Addison-Wesley, Reading, Massachusetts, 1975.

[115] C. J. Batty, E. Friedman, A. Gal, Phys. Rep. **287**, 385 (1997).

[116] L. S. Kisslinger, Phys. Rev. **98**, 761 (1955).

[117] M. Ericson and T. E. O. Ericson, Ann. Phys. (N. Y.) **36**, 323 (1966).

[118] M. Krell and T. E. O. Ericson, Nucl. Phys. **B 11**, 521 (1969).

[119] K. Stricker, J. A. Carr and H. McManus, Phys. Rev. **C 22**, 2034 (1980).

[120] R. Seki, L. Masutani, M. Oka and K. Yasaki, Phys. Lett. **B 97**, 200 (1980).

[121] B. D. Serot, Phys. Lett. **B 86** (1979) 146; Erratum, Phys. Lett. **B 87**, 403 (1979).

[122] T. Matsui and B. D. Serot, Ann. Phy. (N.Y.) **144**, 107 (1982).

[123] M. Schäfer, H. C. Döngs, A. Engel and U. Mosel, Nucl. Phys. **A 575**, 429 (1994).

[124] J. I. Kapusta, Phys. Rev. **C 23**, 1648 (1981).

[125] S. Weinberg, Phys. Rev. Lett. **18**, 188 (1967).

[126] S. Weinberg, Phys. Rev. **166**, 1568 (1968).

[127] S. Weinberg, Physica **A 96**, 327 (1979).

[128] J. Schwinger, Phys. Lett. **B 24**, 473 (1967).

[129] S. Biswas and A. K. Dutt-Mazumder, Phys. Rev. **C 74**, 065205 (2006).

[130] G. 't Hooft and M.T. Veltmann, Nucl. Phys. **B 44**, 189 (1973).

[131] M. E. Peskin and D. V. Schroeder, *An Introduction to Quantum Field Theory*, Addison-Wesley Publishing Company (1995).

[132] T. P. Cheng and L. F. Li, *Gauge theory of elementary particles*, Clarendon Press, Oxford, New York (2006).

[133] A. K. Dutt-Mazumder, Nucl. Phys. **A 713**, 119 (2003).

[134] R. J. Furnstahl, H. B. Tang and B. D. Serot, Phys. Rev. **C 52**, 1368 (1995).

[135] R. J. Furnstahl, R. J. Perry and B. D. Serot, Phys. Rev. **C 40**, 321 (1989).

[136] R. J. Furnstahl, B. D. Serot, Phys. Rev. **C 47**, 2338 (1993).

[137] R. J. Furnstahl, C. E. Price, G. E. Walker, Phys. Rev. **C 36**, 2590 (1987).

[138] R. J. Furnstahl, B. D. Serot, Phys. Lett. **B 316**, 12 (1993).

[139] R. J. Furnstahl, B. D. Serot, H. B. Tang, Nucl. Phys. **A 598**, 539 (1996).

[140] B. D. Serot and J. D. Walecka, Int. J. Mod. Phys. **E 6**, (1997) 515.

[141] Y. Hu, J. McIntire, B. D. Serot, Nucl. Phys. **A 794**, 187 (2007).

[142] T. Goldman, J. A. Henderson and A. W. Thomas, Few-Body Syst. **12**, 123 (1992).

[143] A. K. Dutt-Mazumder, B. Dutta-Roy, A. Kundu Phys. Lett. **B 399**, 196 (1997).

[144] W. Broniowski and W. Florkowski, Phys. Lett. **B 440**, 7 (1998).

[145] A. K. Dutt-Mazumder, R. Hofmann and M. Pospelov, Phys. Rev. **C 63**, 015204 (2001).

[146] S. Zschocke and B. Kampfer, Phys. Rev. **C 70**, 035207 (2004).

[147] P. Roy, A. K. Dutt-Mazumder, S. Sarkar and J. Alam, J. Phys. **G 35**, 065106 (2008).

[148] J. Piekarewicz, Phys. Rev. **C 48**, 1555 (1993).

[149] J. Piekarewicz and A. G. Williams, Phys. Rev. **C 47**, R2462 (1993).

[150] J. I. Kapusta, *Finite-Temperature Field Theory*, Cambridge University Press, New York (1989).

[151] S. A. Coon and R. C. Barrett, Phys. Rev. **C 36**, 2189 (1987).

[152] C. Y. Cheung, E. M. Henley and G. A. Miller, Phys. Rev. Lett. **43**, 1215 (1979).

[153] C. Y. Cheung, E. M. Henley and G. A. Miller, Nucl. Phys. **A 305**, 342 (1978).

[154] C. Y. Cheung, E. M. Henley and G. A. Miller, Nucl. Phys. **A 348**, 365 (1980).

[155] A. Gersten, Phys. Rev. **C 18**, 2252 (1978).

[156] R. Abegg *et al.* Phys. Rev. Lett. **56**, 2571 (1998).

[157] R. Abegg *et al.* Phys. Rev. **D 39**, 2464 (1989).

[158] R. Abegg *et al.* Phys. Rev. **C 57**, 2126 (1998).

[159] C. R. Howell *et. at.*, Phys. Lett. **B 444**, 252 (1998).

[160] D. E. Gonzalez Trotter *et. al.*, Phys. Rev. Lett. **83**, 3788 (1999).

[161] J. A. Nolen and J. P. Schiffer, Annu. Rev. Nucl. Sci. **19**, 471 (1969).

[162] K. Okamoto, Phys. Lett. **11**, 150 (1964).

[163] L. N Epele, H. Fanchlottl, C. A. Garcia Canal and G. A. Gonzfilez Sprlnberg, Phys. Lett. **B 277**, 33 (1992).

[164] G. A. Miller, A. K. Opper and E. J. Stephenson, *nucl-ex / 0602021*

[165] P. G. Blunden and M. J. Iqbal, Phys. Lett. **B 198**, 14 (1987).

[166] R. Machleidt and H. Müther, Phys. Rev. **C 63**, 034005 (2001).

[167] T. D. Cohen and G. A. Miller, Phys. Rev. **C 52**, 3428 (1995).

[168] G. Krein, A. W. Thomas and A. G. Williams, Phys. Lett. **B 317**, 293 (1993).

[169] H. B. O'Connell, B. C. Pearce, A. W. Thomas and A. G. Williams, Phys. Lett. **B 336**, 1 (1994).

[170] S. A. Coon, B. H. J. McKellar and A. A. Rawlinson, *Intersections Between Particle and Nuclear Physics*, edited by T. W. Donelly, AIP Conf. Proc. No. **412**, p368 (AIP, Woodbury, NY, 1997).

[171] T. Hatsuda, E. M. Henley, Th. Meissner and G. Krein, Phys. Rev. **C 49**, 452 (1994).

[172] R. Machleidt, *Proceedings of the Relativistic Dynamics and Quark-Nuclear Physics*, Wiley, New York (1986).

[173] M. W. Kermode and W. V. Dijk, Phys. Rev. **C 42**, 1891 (1990).

[174] R. J. Furnstahl, B. D. Serot, H. B. Tang, Nucl. Phys. **A 615**, 441 (1997).

[175] R. J. Furnstahl, B. D. Serot, H. B. Tang, Nucl. Phys. **A 640**, 505, Erratum (1998).